2013 Aguadilla Puerto Rico

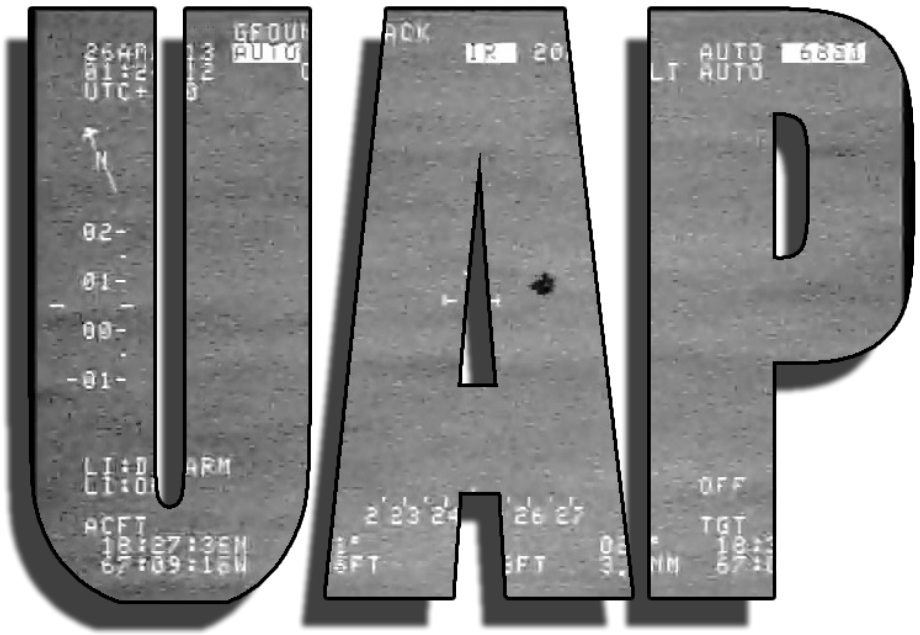

The detailed analysis of an Unidentified Anomalous Phenomenon captured by the Department of Homeland Security.

This report is a detailed analysis of a Homeland Security thermal video taken from an aircraft as it tracked an unidentified object. What you will see in the infra-red is an object that seems capable of traveling at night without lights, at times below tree-top altitude, at speeds approaching 100 mph, and apparently without risk of impacting objects as it passes by.

The report was written under the auspices of the Scientific Coalition of UFOlogy (SCU). The SCU is a think tank of scientists and researchers stretching across organizations, governments and industries to scientifically and publicly explore unknown anomalous phenomenon known around the world as Unidentified Flying Objects (UFOs), Unidentified Aerial Phenomenon (UAPs), the French, Spanish, and Italian equivalent to UFOs (OVNIs), and Unidentified Submersed Objects (USOs).

Scientific Coalition for UFOlogy is open to all scientific based analyses of this report and are willing to provide all the information that we have on this phenomenon to any other serious researchers.

TABLE OF CONTENTS

Executive Summary

On April 25, 2013, at about 9:20 pm local time, an unknown object at low altitude flew directly across the Rafael Hernandez airport runway at Aguadilla, Puerto Rico, causing a delayed departure of a commercial aircraft. There was no squawking transponder signal to alert the aircraft tower, nor was there any communication with the tower to prevent a dangerous situation with departing and arriving aircraft. Fortunately an airborne U.S. Customs and Border Protection aircraft captured the object on infrared video. This report is an analytical evaluation of that video as well as witness statements and radar data of the area.

An original copy of a thermal video was obtained from an official source on October 20th of 2013. The source of this video evidence was vetted and identified. The source wishes to remain completely anonymous to ensure no issues arise with the source's employers. The individual's occupation, address, and background history were verified by the authors of this report as legitimate. Extensive efforts were made to ensure that this video did not contain any classified information and none was found. The three minute video detailed the flight of an unknown object that crossed into northwestern Puerto Rico from the Atlantic Ocean, traversed the Rafael Hernandez airport airspace two times, and returned into the Atlantic Ocean where it appeared to repetitively submerge.

The thermal video imaging system is a standard reconnaissance video system typically used in military, law enforcement and civilian applications. The thermal video was taken from a De Havilland Canada (DHC)-8 DHC-8 Turboprop aircraft that was controlled by the U.S. Customs and Border Protection (CBP). The authenticity of the video used in this report was corroborated using radar data obtained from the U.S. Air Force (USAF) 84th RADar Evaluation Squadron (RADES) group. The radar data displayed the tracking aircraft that took the thermal video. All times and locations of the tracking aircraft were consistent with the thermal imaging video on screen data and the USAF 84th RADES group radar information. Details are available on pages 10-12 of this report.

DHC-8 Turboprop.Courtesy of Homeland Security

An in-person interview with the source indicated that the pilots of the DHC-8 Turboprop took off on a routine mission and as they veered to the northwest saw a pinkish to reddish light over the ocean that was in their vicinity and approaching toward the south. Concerned that the control tower had not alerted them to incoming traffic they contacted the tower. The tower confirmed that they had a visual sighting of the light but did not know its identity. According to the source, once the object came close to shore, the light on the object went out. At about that same time the thermal imaging system was engaged to follow the object.

Thermal Imaging Video

Analysis of the thermal imaging video revealed irregular characteristics of an unknown object not similar to any known natural or man-made objects. The video was split into 7027 individual frames so that careful analysis could be made. Evaluation of the video frame by frame enabled detailed characterizations of the object. The object's size, speed, location, infrared (IR) emissions, directional movement, and other properties were compared against all known possible explanations including state-of-the-art drone capabilities as well as the possibility of a hoax.

Radar Data

In order to support the validity of the thermal video and to look for unknown targets in the area, a Freedom of Information Act (FOIA) request was made to the USAF 84th RADES group to obtain all FAA originated radar in the area during the time frame in question. This request was granted. A second FOIA request for radar data from military radar sources in the area was denied. Using the radar data that was provided, it was possible to validate that the times and locations displayed on the thermal imaging equipment of the CBP aircraft matched a government aircraft that was detected by radar. Additionally, unknown target(s) over the ocean and two to three miles to the north and northwest of the Rafael Hernandez airport were detected. None of these targets had transponders. This information supports the witness's claim that the Border Protection aircraft and the control tower sighted an unknown aircraft moving from the ocean to the south.

Size, Speed, and Location

The size and speed of the object were determined at points in the video when the locations of the object could be accurately determined. This allowed for an exact calculation of distance and angular size of the object. With that information, basic trigonometry was used to calculate the object's size. The object was between three to five feet in length and its speed varied between approximately 40 mph to 120 mph. Its median speed was roughly 80 mph. One of the object's flight characteristics the authors found to be significant was the object's speed through the water which did not vary as it impacted the water. Its speed through the water reached a high of 95 mph and averaged 82.8 mph. Details as to how these parameters were calculated are on pages 16-24.

Interaction with Water

There was very limited interaction with the water, visible within the infrared video, when the object impacted the ocean. Its speed immediately prior to impact was 109.7 mph. Frame by frame analysis indicated that there might be a slight wave or movement of the water as the object entered the ocean. It is unknown at the time of this report if the U.S. or another nation has developed the ability to diminish water displacement caused on impact. It is more difficult to explain the lack of **significant**[1] deceleration as it entered the water despite the absence of an identifiable power supply. See pages 25-30 for additional information.

[1] Significant deceleration as an unpowered object, such as bullet, striking the water.

Splitting Into Two Parts

As can be seen in the video, the object splits into two parts shortly after entering the ocean and then briefly re-emerging. Frame by frame analysis ruled out the possibility of a reflection or of a second object emerging from the water. The object's thermal image actually grew in size momentarily before it split into two parts. Both parts moved through the air and water at the same speed as the original object. There exists no aircraft, projectiles, or other technology known to the authors of this report to have these characteristics or capabilities. The authors discuss this unusual characteristic in detail on pages 31 to 39 of this paper.

Power Source

The unknown in the video displayed qualities that require some type of power source. Over the course of more than four miles the object reached speeds of almost 120 mph, made multiple changes in direction, reduced and increased its speed, entered and exited the ocean at speeds of over 100 mph, and finally split into two parts. In this thermal video, black represents the hotter objects in a given frame and white the cooler objects. The unknown in the video emits more heat than the ambient air and even after submerging in the ocean it continues to emit heat after it exits. However the heat generated is generally less than what is seen from jet engines and automobiles in the video. There is no exhaust plume or any other indication of an aircraft. This is not characteristic of objects with ordinary power sources. The object's speed, maintenance of momentum, directional changes, and its ability to sustain high velocities in water eliminates all aircraft, blimps, balloons, wind-blown objects, any species of bird, mammal, or other natural/man-made phenomenon. See pages 40 to 41.

Maneuverability

The object's ability to maneuver at speeds of 80-100 miles per hour (mph) though residential and commercial at low altitude is of interest. A notable characteristic of the object is its apparent tumbling[2] as it moves through the air, which gives it a very non-aerodynamic appearance. This tumbling action ends prior to the object's entry into the water and as it moves through the water. The object also apparently accelerated while underwater. At 01:23:37 hours in the video the object can be seen to disappear behind a tree momentarily, which places its altitude at below 40 feet. The ability to fly at that altitude at night and between trees requires precise control of movement and a highly responsive propulsion system particularly given the lack of control by aerodynamic devices (like wings). In terms of our technology, advanced sensors or GPS satellites in communications with an on board microprocessor might partially explain such maneuvers. Even more difficult to explain would be the willingness of any government or organization to advertise this capability through a residential area where malfunctions during flight could result in harm to the civilian population and expose an advanced military technology.

The Authors

The six authors of this report all have scientific backgrounds including degrees in chemistry, physics, mathematics, and environmental science. Their work backgrounds are also scientific with experience in the air defense industries, semiconductors–as well as various patents.

[2] The exact nature of the IR emissions from the unknown object is unknown. Tumbling could be an appearance due to the variable nature of the IR emission from that object.

Together they have 86 years combined experience studying the UFO phenomenon. A copy of their backgrounds is listed in Appendix A.

A minimum of 1000 man hours were spent in the analysis of this video over the course of one and a half years. Every effort was made to objectively evaluate the data obtained and ensure the protection of the source's identity, according to his wishes. Non-Disclosure Agreements were signed by all parties which stipulated details would remain secure.

Conclusion

The object witnessed by CBP and tower personnel and recorded on the CBP DHC-8 aircraft's thermal imaging system is of unknown origin. There is no explanation for an object capable of traveling under water at over 90 mph with minimal impact as it enters the water, through the air at 120 mph at low altitude through a residential area without navigational lights, and finally to be capable of splitting into two separate objects. No bird, no balloon, no aircraft, and no known drones have that capability.

The authors are open to any reasonable explanation that addresses the various characteristics displayed by this object. The full analysis and associated appendices can be read for the detailed analysis that contributed to the above summary conclusions.

I. PURPOSE

The purpose of this report is to analyze the characteristics of an unknown flying object, recorded by a thermal camera system, in an effort to determine if the object in the video can be explained.

II. BACKGROUND

Thermal Imaging Video A special investigator known to the authors of this report received information from a personal contact about a sighting of an unknown aerial object by a pilot who was employed with the U.S. Customs and Border Protection (CBP), a branch of the Department of Homeland Security (DHS), in Aguadilla, Puerto Rico. The special investigator's contact was not a direct witness but rather an acquaintance of the direct witness(s). The source is considered the secondary witness. The pilot and crew of the DHC-8 Turboprop aircraft are considered the primary witness(s). On October 21, 2013, the secondary witness provided the special investigator an original copy of the AVI[3] video file depicting the unknown object over Aguadilla, Puerto Rico. According to the secondary witness, the encounter occurred when the pilot was beginning a routine mission and saw a pinkish to reddish light approach from the ocean towards the south. The local time of this event was 9:20 pm on April 25, 2013. The object was visually detected and then tracked using the plane's on board thermal imaging video system. The secondary witness indicated that the pilot could not discern a defined shape of the object but the object did possess a reddish/pink colored light source. The light source turned off as the object entered the Rafael

[3] AVI is Audio Video Interleave; a multimedia format introduced by Microsoft in 1992.

Hernandez airport airspace. From this point the object was exclusively observed through the thermal imaging system of the DHC-8 Turboprop aircraft until the object entered the water and was observed to split into two equal parts and gradually disappear under the water. There were a total of four witnesses to the event on the aircraft and an unknown number of airfield and Federal Aviation Authority (FAA) tower personnel.

Forward Looking InfraRed Systems, Inc. (FLIR) was initially contacted to determine if the thermal imaging system was manufactured by their company. A photo obtained of the thermal camera system was shown to a FLIR representative. The FLIR employee indicated that it was not their thermal system but it belonged to L-3 Wescam, a Canadian company. Wescam Inc. is a subsidiary of L-3 Communications Holdings, Inc. A Wescam representative confirmed that it was their state of the art Wescam MX-15D thermal imaging system. This system uses a InSb sensor with sensitivity in the 3-5 micron range.[4] A specification manual of that system is included in the Appendix B. The capabilities of the system and its output parameters can be seen on a Wescam video located on YouTube[5].

The camera's video output parameters include the latitude/longitude coordinates of the aircraft, date, time, azimuth heading of the aircraft, azimuth bearing to the target, and the altitude above sea level of the tracking aircraft. The imaging system also provides the latitude/longitude of any object within the cross-hair reticle of the camera, the altitude above sea level, and the distance in nautical miles.

The video of the unknown consists of 3 minutes and 54 seconds of video imagery of which 2 minutes and 56 seconds displays the object arriving from over the ocean, traversing land, and then disappearing back into the ocean. The entire video was broken into individual frames for analysis of the unknown object. There were a total of 7027 frames with each frame equating to approximately 1/30 of a second exposure. Breaking the video into individual frames allowed for detailed evaluation of the object's characteristics. Each individual frame is comprised of a set of 345,600 (720 x 480) picture elements (pixels) whose individual values can range from 0 to 255. A given pixel value corresponds to some relative intensity of infrared radiation which formed the image of the object. Low pixel values reflect warmer temperatures (shown in black) while high pixel values correspond to cooler temperatures (shown in white). It is important to understand that the image formed via these wavelengths of infrared is not visible to the human eye but this does not mean the object could not have been seen within visible wavelengths. It does mean, however, all the video image provides as evidence can only be found within the infrared wavelengths given.

Radar Data Radar data was requested through the Freedom of Information Act (FOIA) in November of 2013 from the U.S. Air Force's 84 RADES group as a means to both verify the validity of the thermal imaging video and to look for any unknown targets in the area of operation of the CBP aircraft. Radar data was obtained from three FAA sites in the area of Puerto Rico. The primary radar site was QJQ, which is a long range radar located at 3417 feet elevation. Its coordinates are 18º16'07"N and 65º45'31"W. Radar data was also obtained from SJU located near San Juan, Puerto Rico. This radar site only receives secondary radar,

[4] "NATIBO Collaborative Point Paper on Border Surveillance Technology," December 2007, p.14

[5] https://www.youtube.com/watch?v=eZcFUYMAWBY

also known as transponder signals. It was only useful in verifying the location of the CBP aircraft. The third radar site information was obtained from radar on St. Thomas Island. It is 120 miles to the east of Puerto Rico and was too distant to provide meaningful information. A copy of the FOIA request and the Air Force reply is included in Appendix C along with an example of the data received from the Air Force. The entire file consists of 20 columns by 33,113 rows and is in a Microsoft Excel format.

The radar data from the QJQ site provided both primary and secondary radar (transponder code of the aircraft and its altitude), date, time, latitude/longitude coordinates of the target, distance to the target and the azimuth bearing of the target from the radar site. The radar revolution rate was one sweep every ten seconds.

There is also a military radar installation located on the premises of Rafael Hernandez airport. It is on the west end of the runway and is known as the Punta Borinquen radar site. A FOIA request was made in May of 2014, again to the USAF 84 RADES group. This radar site is the closest to the unknown object in the thermal video and would have been very useful information. Unfortunately, the Air Force denied the request for that information. A copy of the Air Force response is in Appendix C.

Control Tower Logs A FOIA request was made in March of 2014 for the airport's control tower logs, known as the Daily Record of Facility Operation, on the night of April 25, 2013. The tower at the Rafael Hernandez airport is known as the Aguadilla Tower. The FAA responded that their logs are maintained by a private company, Robinson Aviation, which is not required to respond to FOIA requests. A copy of the FOIA request and the denial from the FAA is in Appendix C. Robinson Aviation was contacted for information regarding the control tower logs and did not reply to requests. According to the conversation between an investigator and the Aguadilla Tower manager, the records (logs and recordings) from the tower were destroyed 90 days from the date of any event. The tower manager also indicated they were aware of the events of April 25, 2013, and were not willing to participate further in the investigation.

Weather and Astronomical Conditions At 9:50 pm the surface temperature was 79ºF, the humidity was 74%, barometric pressure at 30.05", scattered clouds, visibility of 10 miles, and the wind was out of the east at 8-13 mph.[6] Upper wind speeds were measured out of San Juan, which is 50 miles to the east of Aguadilla. At 8 pm local time the upper wind speeds from 400 feet to 3200 feet were similar and were out of the east northeast at 12 to 18 mph.[7]

Sunset was at 6:48 pm and astronomical twilight was at 8:04 pm. There was a full moon that night that rose at 6:53 pm. By 9:20 pm the moon was ESE at an elevation of 30 degrees.

Geography and Geology The area geology near the event location is that of Tertiary limestone making up the majority of the nearby coast lines and visible topography. The object traversed areas of steep and gradual inclines from the Atlantic Ocean. Much of the

[6] http://www.wunderground.com/about/data.asp

[7] University of Wyoming, Department of Atmospheric Science. http://weather.uwyo.edu/upperair/sounding.html

coastline in this specific area consists of a combination of erosional beaches and steep cliff faces. The regional geologic structure is considered karst as well as the topography characteristics. Puerto Rico sits near the strike-slip fault of the North American Plate a Caribbean plate which is located sub parallel to the Puerto Rico trench. This area off the coast where the unknown object entered the ocean consists of many geologic transition areas, fault system and deep trench passageways.[8]

Limitations There were various factors that limited either the amount of information for analysis or the quality of that information. Those limitations are listed as follows:

1. A FOIA request was sent to the Air Force but they would not provide radar data from the military radar station that is located at the west end of the runway.

2. The FAA replied negative to a FOIA request for the airport control tower logs because they had turned over maintenance to a private company, Robinson Aviation. The private company, exempt from FOIA regulations, would not respond to requests for information.

3. Although a basic overview of the Wescam MX-15D video system is available, a detailed manual that describes specifics of the system was not available to the public.

4. The readout of the Wescam system's latitude and longitude coordinates is rounded to the nearest second. This rounding can produce a maximum potential error of 60 feet in the location of the aircraft or its sited ground coordinates. This potential error was taken into consideration in all calculations.

5. There is a consistent one second delay between latitude/longitude values displayed on the Wescam video and the latitude/longitude values as reflected by the true coordinates of the objects shown in the video. Due to its consistent variation, this shift is believed to be due to an inherent system delay that does not affect the system's operational capabilities and was taken into account in all calculations.

III. ANALYSIS AND CHARACTERIZATION

Witness Testimony The witness testimony was from a secondary witness whose direct testimony cannot be discussed in this report due to a request of anonymity. Additionally, it was the secondary witness who contacted this team's investigator labeled as special investigator and provided the original video. The primary witness is referred to in the remainder of the report as *Witness A*. Similarly, the secondary witness is *Witness B*.

Witnesses A is an officer and pilot employed by the CBP division of Homeland Security. *Witness A* was the pilot of the aircraft and one of four crew members that witnessed the event from the aircraft. *Witness B*, who asked not to be identified, was the only means of contact with *Witness A* who was not willing to talk to us at the time of the initial investigation of this report. Questionnaires were given to both *Witnesses A* and *B*. *Witness B*, in turn, provided one

[8] http://earthquake.usgs.gov/hazards/products/prvi/2003/documentation/

of the questionnaires to *Witness A*. The completed questionnaires were then returned to this investigative team by *Witness B*.

Multiple phone calls were made with *Witness B* as well as a personal meeting with two of this team's investigators on February 15, 2014, at an undisclosed location. The following testimony is from *Witness B* and it describes what was seen prior to the thermal video.

Witness A and his crew took off on a routine aircraft patrol of the Puerto Rican coast on the night of April 25, 2013. The DHC-8 Turboprop aircraft took off from the runway heading east at 9:16 pm. The aircraft contained four crewmen including the primary witness, a copilot, and two instrument operators (one manning the on-board radar system and the other manning the thermal image mounted camera system). *Witness A* looked out his left window and saw a pinkish to reddish light over the ocean northwest of the airport. The light was moving towards the airport. He believed the light to be at a higher elevation than his aircraft, which was at 1600 to 2100 feet, based on the radar data and the thermal video system engaged a moment before. The pilot confirmed visual contact with the tower personnel. The tower personnel also confirmed visual contact. As the target approached shore, its light went out. The pilot then requested monitoring of the craft with the on-board surveillance equipment. According to the reporting witness the on-board radar did not pick the object up, but the thermal imaging camera did detect the object. (The CBP's DHC-8 aircraft are equipped with SeaVue Marine search radar primarily for detecting seacraft.[9,10])At this time, *Witness A* no longer had visual contact with the object but did see the object in his thermal imaging display in the cockpit along with the thermal imaging display in the rear of the aircraft under control of the instrument operator. He continued tracking the object while on routine patrol in the aircraft. The pilot made no attempt to intercept the unknown target nor did the target seem to react in any way to the tracking aircraft.

Witness B stated the close presence of this unknown object caused the delay of a commercial aircraft's departure from the airport. This statement from the witness could not be verified since the authors of this report were denied access to the airport tower logs. However, the statement's claim was supported when it was found that Fed Ex flight 58 was scheduled to depart the airport at 9:10 pm but did not actually depart until 9:26 pm. It would also be logical to believe the tower would delay departures if there was an unknown aircraft in the airport's immediate airspace. Nonetheless, it cannot be known for certain that this departure delay was due to the unknown object. There was only one arriving flight during this time period. It was MartinAir flight 5713 that landed at 9:00 pm prior to the onset of this event. No arriving flights were affected. This information was obtained from the FlightStats, Inc database and is available in Appendix D.

Witness B indicated the video provided in this report was the entire unedited video and that knowledge of this video was widespread within the CBP office located at an undisclosed location. According to *Witness* B, Air Force Intelligence was contacted and subsequently was provided a copy of the video. Air Force Intelligence offered no explanation to CBP and recommended other agencies to contact. The identity of those agencies is not known. It is not

[9]http://www.cbp.gov/sites/default/files/documents/FS_2014_DHC-8%20Bombardier.pdf
[10]http://www.raytheon.com/capabilities/products/seavue/

clear, based on discussions with *Witness B*, whether the evidence for this event had an official security level. Since the event, *Witness A* indicated there have been no follow up investigations by any other government agencies nor has any debriefing ensued with any of the CBP officers.

Auxiliary Witness Testimony During research and field investigations pertaining to the subject video evidence, additional indirect witness testimony was obtained regarding the event and other similar events near and above Rafael Hernandez airport in Aguadilla, Puerto Rico. *Witness A* indicated another independent fellow CBP pilot was east of the base and on his way back to the airport about 15 to 30 minutes before the primary witness's sighting. This officer witnessed a formation of pinkish/red lights flying extremely low over the airfield in an unusual flight pattern. According to *Witness A*, the fellow pilot made a call to the base to notify personnel of his observations. Additionally, according to *Witness A,* the primary witness's son witnessed a light similar to the observed unknown object exit and enter the ocean just off the coast north of the airport one to two evenings after the main event of April 25, 2013.

An anonymous email was sent to investigator and researcher Morgan Beall from an individual with the alias "John" and from a secure email address[11]. The IP address within the email sent to the email server was received showing only the service provider server locations. The writer stated he or she had worked for the CBP and could vouch that the video was real. The writer's subsequent statements supported their claims. The writer mentioned the specific model of the thermal imaging IR system used, an L-3 MX 15D and the writer named the CBP DCH-8 maritime patrol aircraft specifically, which the research for this report had already confirmed through *Witness A.* The writer goes on to describe the events of April 25, 2013 with information we have only been able to glean directly from cooperative witnesses to this event. The information provided by this anonymous writer is considered credible and corroborates information from *Witness A* and *B*'s testimonies. Uniquely, the writer mentions the unknown object first appeared as a "forward flying horseshoe" shaped craft and gradually changed its configuration to a spherical shape before entering the water. It is not known if this is his or her interpretation of the video or if it is information witnessed by airport personnel or other privy information to which the witness had access. Conversely to this report's observations and conclusions, the writer makes a statement that the object did not split into two parts but rather the original object was met by a second craft and both proceeded to enter the water together. It is suspected this witness is either an active duty CBP person on site or is acquainted with personnel actively serving on the base.

Another anonymous communication was posted under a YouTube commentary section next to a lesser quality copy of this video at https://www.youtube.com/watch?v=Hee70AwwUJ8. This statement was posted in Spanish in June of 2014 by an individual with the alias "Red Bill". This individual is suspected to have some inside knowledge of the event because contrary to the original user's post of the video, "Red Bill" correctly states the source of the video as the U.S. Customs and Border Protection and correctly states that the video was taken from an airplane and not a helicopter. He also indicates (unverified by the authors of

[11] john@truth.com is a fake email used under a secure or untraceable email address.

this report) that the video was analyzed in Quantico, Virginia and claims that two other videos were made in the same area on different dates. All attempts to initiate communication with "Red Bill" were unsuccessful.

A third anonymous communication was sent to John Greenewald Jr., creator of the web site Black Vault (http://theblackvault.com/), in October 2014. The statements made in that communication were nearly identical to that of the anonymous email sent to investigator Morgan Beall. It is suspected that all three of these anonymous communications may be from the same person. It was confirmed these communications were not made by *Witness B* when questioned directly about the content and the source. The factual information concerning the agency involved, the aircraft used by CPB and the object described is considered credible.

It should be noted that all primary research and witness interviews by the authors of this report were completed prior to any of the afore mentioned leaks of a video and commentary on YouTube and Facebook.

Radar Analysis—Verification of Thermal Imaging Video Information As noted earlier in this report, data used in this analysis was from the primary radar site known as QJQ and is a long range radar located 90 miles ESE of the area of interest and is at 3,417 feet elevation. The radar is a FPS-20E and has a range of 200 nautical miles.[12] The radar was manufactured by Bendix and is an L-Band radar that operates at 1280-1350 MHz and has a transmission power of 2.0-2.5 megawatts.[13] Based on the lowest altitudes detected of identified aircraft in the area of interest, this radar is capable of detecting objects, if near the airport, at 400 feet altitude. A graph and discussion of how this information was derived is in Appendix F.

The radar data was used to verify that there was a government aircraft on the day, time and location as noted in the thermal imaging video. Hoaxes were eliminated once the aircraft that took the video had been verified on radar from QJQ site.

It is a straightforward exercise to determine whether the aircraft on radar is an exact match to the aircraft that filmed the thermal video. The video provides the exact time and location of the aircraft as it was taking video of the unknown object. The radar data can verify if an aircraft was present at the same time and location.

The CBP aircraft's location at specific times using the thermal video's time and latitude/longitude stamps of the CBP aircraft was compared against radar data to verify the existence and location of the aircraft. Radar data confirmed an aircraft tracking the same path and time as shown on the thermal video. Figure 1 shows the path taken by the CBP aircraft. The aircraft traveled north over the ocean once it departed the airport (north is at the top of the map), then gradually to the southwest before traveling back over land and to the south. Radar data indicated the transponder number of this aircraft as 4406. This transponder number itself indicates that the aircraft is a military or law enforcement aircraft. FAA Order

[12] Lincoln Laboratory, MIT, *Correlated Encounter Model for Cooperative Aircraft in the National Airspace*. October 24, 2008.
[13] OCEANA NAS, Harvey Clute, Jr., Bendix Engineer.

7110.66 stipulates that all transponder codes between 4401 and 4433 are controlled by FAA Order 7110.67, which is named "Special Aircraft Operations by Federal, State Law Enforcement, Military Organizations and Special Activities."

Based on the radar data, there is no doubt that the thermal video is a real video taken by a law enforcement or military controlled aircraft. Because we have time and distance information, the speed of the aircraft can be calculated. The aircraft's speed always varied from 180 mph to 240 mph, which indicates it is not a helicopter but is a fixed wing aircraft. All of this information supports the information in the thermal video as well as the story told by the CBP witness. (A detailed analysis of this work and the aircraft's calculated speeds is included in the Appendix F.)

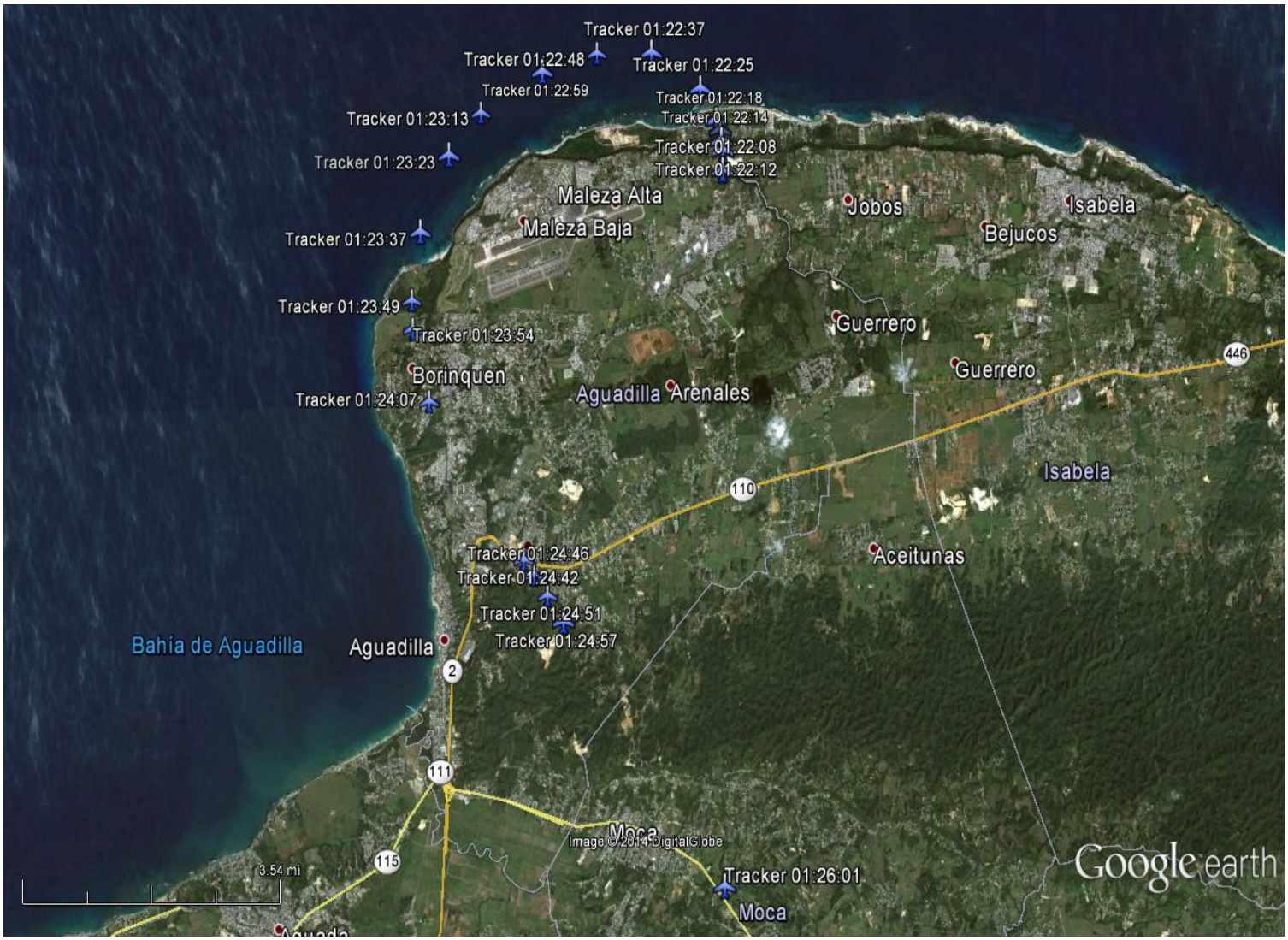

FIGURE 1: Tracking aircraft's location based on thermal and radar data. The name "Tracker" represents the CBP aircraft and the value to the right is Zulu time at that location. Radar data supports the time and location coordinates provided by the thermal imaging video.

Radar Analysis—Verification of Witness Testimony of Visual Sighting The witness indicated that the unknown aerial object was sighted just after takeoff and at the beginning of his standard nightly patrol. Visual confirmation of an approaching red light was made both by the pilot and the control tower.

Radar data shows that the aircraft made an extra search pattern around the airport before commencing what appeared to be its standard patrol and operational activities down the Puerto Rican coast. Although the thermal video shows the aircraft's path for only four minutes, the radar data shows the aircraft's path prior to and after the thermal video being engaged. In the Google Map in Figure 2 the aircraft images in blue represent both the matching thermal and radar data while the aircraft images in red are only radar data. It is clear that before the thermal imaging video was engaged (red colored plane), the aircraft circled the airport and then engaged the thermal video on its second pass (blue colored plane). This supports the witness testimony that the pilot was aware of an unknown target in the area, searched for the unknown target, and after finding it, engaged the thermal video tracking system prior to resuming the aircraft's normal course near the coast. Data that is discussed in the next section indicates that there is evidence to support the pilot's and control tower's claim of an unknown object in the area.

FIGURE 2: Radar only data of a law enforcement or military aircraft shown in red with Thermal Imaging & Radar data of the aircraft's location show in blue. The aircraft locations in red show the aircraft's flight pattern before engaging its thermal imaging video.

Radar Analysis—Verification of Unknown Targets

Radar data was reviewed for any primary data without a transponder code that would signify an unknown radar track in the area of interest. Primary radar tracks are those created by the actual reflection of the radar beam from a target. Known aircraft such as the law enforcement or military aircraft transmit a transponder code, which appears in the radar data, is also known as secondary radar. The radar picked up 50 primary radar strikes (no transponder) to the north and northwest of the airport of what appears to be a single object from Zulu time 00:58hrs to 01:14hrs, a 16 minute period of time. The CBP aircraft, which transmitted a transponder code, departed the airport runway at 01:16hrs. These 50 radar tracks (the radar sweeps every twelve seconds) of this unknown object are visually displayed in Figure 3. The amount of information in Figure 3 requires considerable commentary.

The first four radar strikes of the unknown target, seen at the far left area of Figure 3, occurred after each twelve second sweep of the radar and are designated as a, b, c, and d. The unknown target was not picked up for the next four sweeps, which equates to 48 seconds of no radar contact. The fifth radar strike designated as 1a++++[14] indicates the unknown was at the same location as it was one minute earlier. That does not necessarily mean that the object was stationary because the accuracy of the radar is only within 1/8 mile. If those first four target strikes are a single object then the movement indicates 7800 +/- 660 feet moved in 36 seconds or a speed of 135-160 mph. The altitude of the object is not known but based on the radar's minimum altitude detection limit at that distance, the object must have been about 800 feet altitude or higher. See Appendix F for detailed information.

The sixth radar strike occurs immediately after the fifth radar strike, i.e. the next twelve second sweep of the radar. Beginning with this sweep of the radar, the object shows up on almost every sweep of the radar for the next ten minutes. It could be that the first six radar strikes were not related to the next 42 radar strikes identified as 1b thru 1aq. Symbols 1b through 1aq are in consecutive order[15] and represent consecutive radar strikes 12 seconds apart. In total there were 42 radar strikes out of 50 possible in a ten minute period of time to the northwest of the airport. This level of activity would be sufficient to cause concern for anyone monitoring the radar system.

Within 18 minutes of this flurry of radar activity, the law enforcement aircraft with the thermal video imaging capability took off from the airport just before 01:16hrs, which is when the aircraft was first detected on radar at an altitude of 800 feet at the eastern end of the runway. Figure 3 reveals that the CBP aircraft made an extra sweep into the area where the unknowns were picked up on radar. Likely, the pinkish-reddish light seen to the northwest of the airport by the pilot was the unknown target seen on radar and the object later recorded by the CBP aircraft's thermal imaging video; it would be too coincidental to think otherwise.

The unknown target that appeared on radar for 16 minutes does not display characteristics expected of ordinary aircraft in flight. The speed variation and sudden changes in direction do not support mundane aircraft. Nonetheless, there are characteristics that can be attributed to the unknown target.

[14] The four plus signs indicate that four radar sweeps were missed.
[15] 1b 1c 1d … 1y 1z 1aa 1ab 1ac … 1ap 1aq.

First, this target's appearance on radar occurred at the right time and location to likely have been the object visually confirmed by the control tower and the CBP aircraft. Second, although the target jumped around, its overall directional movement was from the northeast to the southwest. Third, the target strength was strong as it was detected on almost every sweep of the radar for eight of the ten minutes it was on radar. Lastly, the target was no longer detected on radar during the time that the unknown was detected on the thermal imaging video. At that point in time the object was believed to be below the Pico Del Este radar's detectable altitude of 800 feet.

The authors of this report have looked for other explanations for the unknown radar strikes to the northwest of the airport. A temperature inversion is a possible cause of false radar returns. These occur when the upper air temperature is higher than lower air temperature. This possibility is discussed in Appendix F and discounted due to the lack of any temperature inversion layer in the area. One of the strongest arguments against some type of anomalous propagation is the consecutive radar returns every 12 second radar sweep within a small geographic area for a solid eight minutes coupled with the lack of these returns prior to this incident and the lack of these returns after the unknown is picked up on the thermal video at a lower altitude over land. It seems reasonable to consider the possibility that the visual confirmation of the object by the pilot and the control tower, the detection of these unknown radar returns on FAA radar data, and the detection of the unknown object on the thermal video are all related to the same event and the same object. No other reasonable explanation has yet been found.

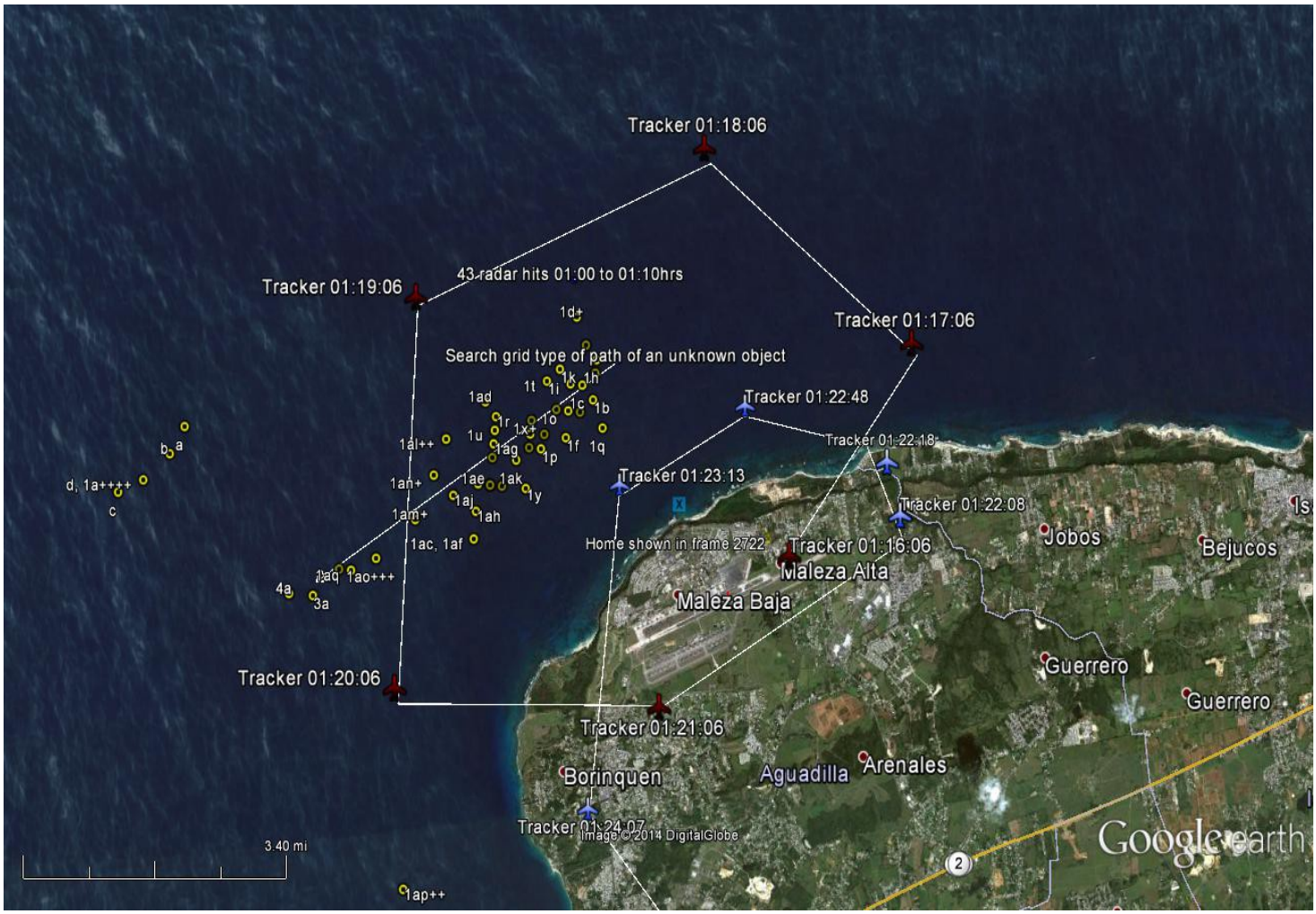

FIGURE 3: Radar plot of unknown that showed up off shore prior to the departure of the aircraft with thermal imaging capabilities. Tracks are designated in order of time beginning with a-d (segregated because of distance from the other radar tracks), followed by 1a-1aq, and followed by 2a, 3a, and 4a (segregated because of significant time delays of greater than one minute between radar tracks.

The radar sweeps every twelve seconds. Each "+" after a radar hit indicates that the target was not detected in the previous radar sweep. A designation such as "1ac,1af" indicates that two different radar sweeps occupied approximately the same physical location to within 1/8 of a mile of each other. (There is no difference between green & yellow circles and is due to a Google Earth issue.)

Object Size The object in this video was tracked using a state of the art Wescam MX-15D multi-sensor multi-spectral targeting system. The MX-15D was mounted on the underbelly of a DHC8 turbo prop aircraft operated by U.S. Customs and Border Protection. This system has high definition thermal imaging, short range IR for enhanced haze penetration, a laser rangefinder and illuminator, and stabilization features. The video lasted more than three minutes and due to familiar objects in the background, the approximate size, speed, and path of travel of the object were identified. The camera's video output included the latitude and longitude coordinates, azimuth heading, and the altitude above sea level of the tracking aircraft. It also provided a target latitude/longitude, an altitude above sea level, and the distance in nautical miles as well as meters. Due to the capabilities of this particular camera its sale outside of the United States requires approval from the U.S. Government.

The video consists of 3 minutes and 54 seconds of video imagery of which 2 minutes and 56 seconds displays an unknown object arriving from over the ocean, traversing land, and then disappearing back into the ocean. The entire video was broken into individual frames for analysis of the unknown object. There were a total of 7027 frames with each frame approximately 1/30 of a second exposure. Breaking the video into individual frames allowed for detailed evaluations of the object's characteristics.

Specific information is provided as to how the size, speed, and location of this object were determined. The basic determinations were based upon trigonometry related to the actual object size, angular size, and distance of the object. If two of those variables are known then the third variable can be calculated.

The angular size of the object was calculated from the angular size of each pixel in the video at a given magnification. The angular size of a pixel was determined from several different objects of known size, known distance, and the number of pixels that made up the object's length in a video frame. Using the known distance and size, the angular size of the known object was calculated in degrees. Dividing this by the object's length in pixels provided the angular size in pixels at that particular magnification. A value of .001483º +/- .000045º per pixel was obtained. An example of one of the known objects and distances used is shown in Figure 4. The angular size of a pixel is proportional to the magnification used in the video. A detailed discussion of the technique and calculations used is available in Appendix G.

The angular size of the object can be used to calculate the object's true size if we know the distance to the object. Although distance and altitude of the object is shown on the thermal video display, these values are actually the distance to the terrain behind the object. An example is shown in Figure 5 where the altitude of zero feet is clearly that of the ocean as is the distance of 3.5 nautical miles. The unknown object's true altitude in Figure 5 is some value greater than zero and its true distance is some value less than 3.5 nautical miles.

The distance can be accurately calculated whenever the object is at a known or a very low altitude. This occurs towards the end of the video when the object passes behind a telephone pole, behind trees, and then finally enters the water. During these periods of time there are means to measure the distance.

FIGURE 4: Frame 0892. Known tank size and distance along with unknown.

FIGURE 5: Frame 0141. Unknown object near center of cross-hairs.

For example, in the right triangle shown in Figure 6 the camera is at point 'C'. The cross-hairs of the camera are pointing towards 'A'. Any object in the cross-hairs (represented by point 'D') of the camera could be at any location along line 'AC'. However, when foreground objects such as trees or a telephone pole or the water surface itself interact with point 'D' then one knows that point 'D' is close enough to point 'A' (point 'A' is on the ground) to allow for a reasonably accurate determination of the distance from the object to the camera.

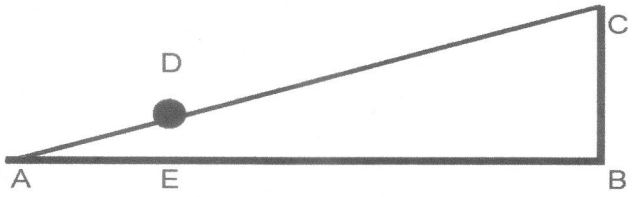

FIGURE 6: Right triangle

Calculations of the object's size were done on multiple frames whenever the object was a known distance from the ground which allowed accurate values of the object's distance and its size. Two examples are shown in Figure 7, where the object is seen four seconds after it had exited the water, and in Figures 8-10 that show the object moving behind a tree. In both examples the distance of the object is known because its approximate altitude is known; with a known distance then the object's size can be determined. The size values obtained for the object varied significantly from a minimum size of 3.0 feet to a maximum size of 5.2 feet. The variation in size could be due to either varied angular sides of the object as it is appears to be tumbling or temperature variations as seen by the IR camera that could distort the object's apparent shape. Regardless, the variations in apparent size seen by the IR camera are due to properties intrinsic to the object.

Object Path The path taken by this object during the video cannot be ascertained simply by plotting the latitude/longitude coordinates that are displayed by the thermal imaging system based on the cross-hairs. Those coordinates are driven by a laser range finder, which is not striking the object itself but the ground and other large objects in the background. This was done empirically using known objects in the background and verifying the longitude/latitude coordinates belonged to the background object. *Witness B* also supported this when he indicated to the authors that their laser range finder is used for ground targeting and only rarely has it been able to capture aerial targets. As a result, when the object is at altitudes above about 40 feet there can be significant differences in the actual distance between the object and the camera. This is the same issue discussed in the determination of the object's size. A powerful tool used in this analysis was “Image J” software that allows one to zoom in on groups of frames and run/reverse/stop the video at higher magnifications. This software was developed by the U.S. government.[16]

[16] ImageJ 1.47v. National Institute of Health, July 8, 2013. http://imagej.nih.gov/ij

FIGURE 7: Frame 5085. Unknown object in center of cross-hairs.

FIGURE 8: Frame 2697. Unknown object visible.

FIGURE 9: Frame 2705. Unknown object disappears behind trees.

FIGURE 10: Frame 2713. Unknown object reappears from behind trees.

The path was determined from various frames in the video where the approximate altitude of the object was known. This occurs during the last half of the video when the object's altitude was less than 40 feet and was descending into the ocean. Details of the calculations that identified the object's path are displayed in Appendix G.

The best determination of the object's possible paths is shown by the brightest of the three blue lines in Figure 11, a Google Earth image of the northwest coast of Puerto Rico. The airport that is seen in the image is the Raphael Hernandez Airport and is a joint civil-military airport located in Aguadilla, Puerto Rico. The top of the page faces west and the right hand side of the page faces north. The dark blue aircraft icons indicate the actual locations of the aircraft with the thermal camera. The locations were verified by both the thermal camera system's latitude/longitude values and by radar from the Pico Del Este radar site. In Figure 11, the numbers next to the aircraft represent the time in Zulu (aka Greenwich Mean Time) hours that the plane was at that specific location. A corresponding UAP (Unidentified Anomalous Phenomenon) location is on the map for the same time period. The UAP locations marked in red are exact locations of the object at those times due to accurate altitude values being available. The first exact location of the object is marked in red on the map at time 01:23:37 as the object passed behind a tree as shown in Figures 8-10. The UAP locations marked in orange represent approximate locations of the object within 500 feet. The UAP locations marked in yellow with a time value next to them and the darker blue line connecting them represent a “best guess” of the object's location based on the previous path of the object and its known direction from the aircraft. The brighter blue line begins at a question mark that represents the uncertainty of the object's location at the beginning of the video. The object's route does raise the possibility that its origin could have been its final destination or its origin could have been up to one mile farther to the west as shown by the other two light blue lines. The light blue lines connect possible routes taken by the unknown object that are farther to the west. The yellow colored UAP locations represent a higher level uncertainty of the object's position than those colored in red.

The object approached the island of Puerto Rico out of the north from the ocean. Its exact origin is unknown. Heading south it crossed the airport runway, turned east, then north again to recross the airport runway on its way back out to sea. The object's path reflects a complete 180 degree change in direction over land and a continual drop in altitude during the last half of the video. The object left land at 01:24:04 and changed direction again heading northwest. At 01:24:13 the object impacts the water and travels just below the surface. The object's movement through the water can be seen if you look carefully at the video. It exited momentarily at 01:24:18 before moving just below the surface again. Once more, the object can be followed until it exited the water at 01:24:31. The object changed its direction while underwater from northwest to west. (It is believed the reason the camera is able to follow the object while underwater is due to the Bernoulli[17] hump created by any object moving underwater. This is discussed further in Appendix H.) Eleven seconds after exiting the water at 01:24:42 the object split into two equal parts, both the same size as the original, as it continued to the west. One of the two parts entered the water at 01:24:52 while the other part

[17] Stefanick, T.; "Strategic Antisubmarine Warfare and Naval Strategy"; Institute for Defense and Disarmament Studies; (1987): Appendix 3

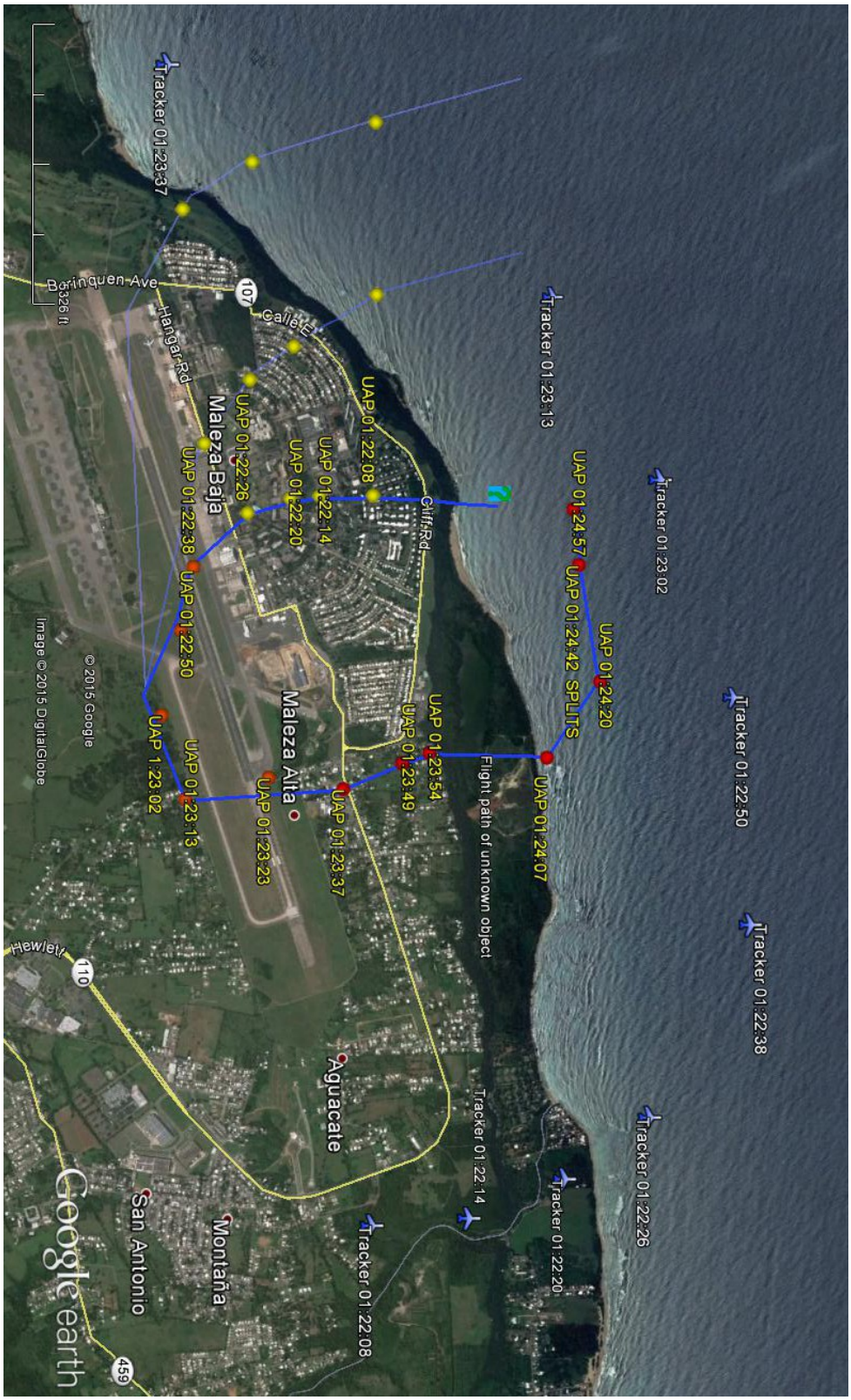

FIGURE 11: Google Map of three possible paths of the unknown object.

changed direction to the southwest before also disappearing into the water at 01:25:04.

Object Speed What is the energy source that propels the object in this video? The movements made by this object require some type of power source. The object traversed over four miles during the video and during that process changed direction; south to north to west then finally towards the southwest. No type of propulsion is evident from the thermal imaging video yet some form of propulsion is required for the object to maintain and vary its speed, change directions multiple times, and move in and out of the water. Again, the source that propels this object is not evident.

The speed of the object is most accurately calculated during the latter half of the video when the object's location can be more accurately determined. The calculation of the object's speed is straightforward and established from given distances and times. The thermal video system's clock and latitude/longitude locations allowed for the calculation of time and distance values. The clock accuracy is to the nearest 1/30 second due to the frame rate of the video. The main error is that the latitude/longitude values are in degrees, minutes, and seconds so that the location is a digitally displayed to the nearest second. The accuracy is within 0.5 seconds of a degree, which is roughly 51 ft. The rounding error is taken into consideration for the speed and distance calculations.

Table 1 shows the time of the latitude/longitude measurement, the distance traveled since the last measurement, and the calculated speed of the object. Although the speed of the object is fairly constant and normally varies from 70 mph to 110 mph, it is clear that the object accelerates and decelerates during this portion of the video, which again indicates some type of power source must be present. Some of the speeds shown in the table are noted as being through water. These speeds are average speeds and do not examine the possibility of higher speeds within short time bursts, which sometimes appear during the video.

ZULU TIME	ALT.	LAT./LONG.	DISTANCE TRAVELED	TIME	DIRECTION OF TRAVEL	SPEED
01:23:37	25 ft	18:30:08N 67:07:13W	------	------	------	------
01:23:49	16 ft	18:30:19N 67:07:18W	1213 ft	12.0”	north northwest	69 +/- 3 mph
01:23:54	16 ft	18:30:24N 67:07:20W	542 ft	5.0”	north northwest	74 +/- 7 mph
01:24:07	< 1 ft	18:30:46N 67:07:19W	2230 ft	13.0”	north	117 +/- 3 mph
01:24:20	**	18:30:56N 67:07:34W	1761 ft	13.0”	west northwest	92 +/- 3 mph
01:24:42	**	18:30:52N 67:07:57W	2246 ft	21.7”	west	70 +/- 2 mph
01:24:46	*	18:30:52N 67:08:01W	384 ft	3.95”	west	66 +/- 9 mph
01:24:51	*	18:30:53N 67:08:04W	305 ft	5.28”	west	39 +/- 7 mph
01:24:57	**	18:30:51N 67:08:08W	434 ft	6.03”	west southwest	49 +/- 6 mph

TABLE 1: Speed of object at known positions.

* Speed underwater. **Speed through water and air.

Table 1 uses 4 to 13 seconds in each calculation of the object's speed based on the latitude and longitude coordinates provided by the thermal imaging video.

Graph 1 shows speed averages over a total of about 800 frames. Average speeds were calculated for collections of about 50 frames each (covering approximately 1.5 seconds) from the 800 frames. Then, from all of the average speeds calculated, 15 sets of three each were used to generate a moving average. The purpose of the moving average was to emphasize longer term trends which may be seen in the curve of Graph 1. Even given the longer term speed trends of Graph 1, the object's speed is still seen to vary within a short period of time.

The speed of the object was also measured using a completely different method based on the object's ground speed by comparing its relative movement against background ocean waves whose speed was negligible. This method showed speed variations between frames 3769 to 3843 of 70 mph to 130 mph, which is comparable to the speeds found using latitude and longitude coordinates. Details on this second method are available in Appendix I. These two different methods clearly establish that this object moved at speeds above, through, and under the water that cannot be explained by simple conjectures such as a balloon, bird, or wind-blown object.

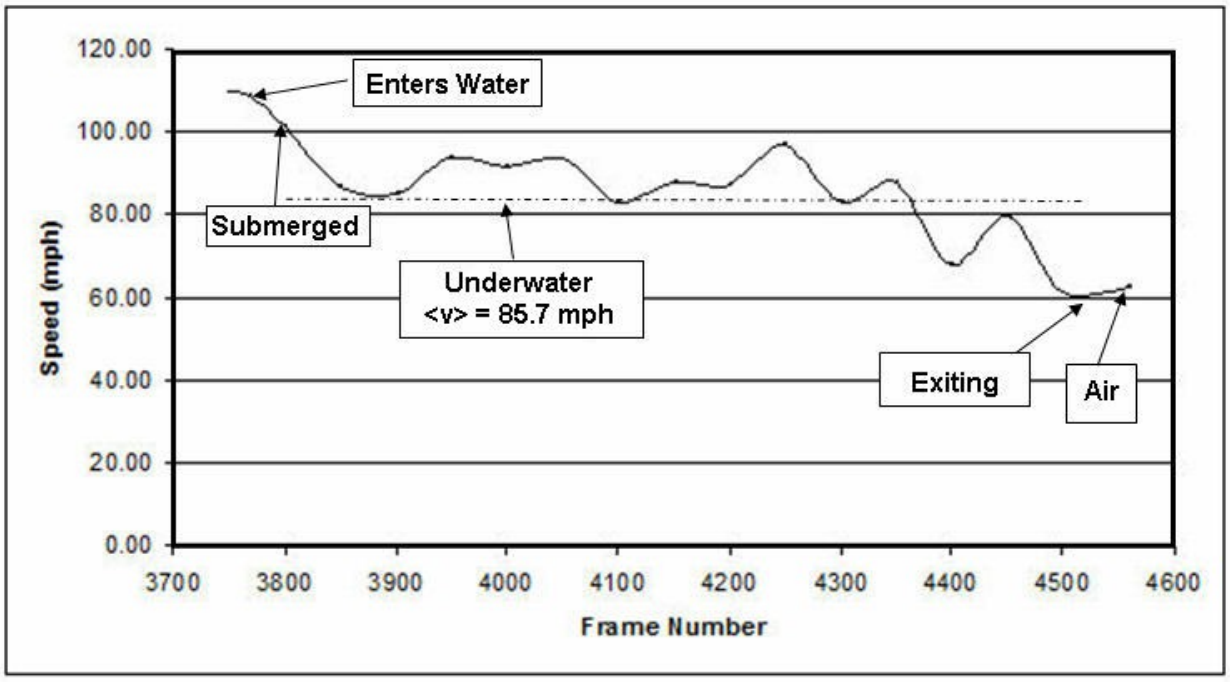

Graph 1: Speed measured every 50 frames

Object's Interaction with Water Although most of the video concerns the object moving through the air, there are portions in the latter part of the video when the object interacts with

the ocean. These include the object's actions immediately prior to impact in the ocean; entering the water; motion underwater; exiting the water; and object division.

Object's Interaction with Water: two seconds prior In the two seconds prior to ocean impact, there is no indication of the object slowing down. The object's speed prior to impact is near the highest speed measured during the latter part of the video. Frames 3700 through 3750 were used as the points of reference for measuring the object's speed prior to frame 3769 when the object began to impact the water. In order to minimize errors due to rounding, time to the nearest second and latitude/longitude to the nearest degree second, extrapolations were made using individual frames to provide higher accuracy. The speed calculated during the two seconds prior to impact was 109.7 mph with an error of +/- 11 mph. The details behind this calculation are shown in Appendix J.

Object's Interaction with Water: moment of impact In today's understanding of science, it is impossible to enter, leave and move through a fluid and not affect it. There is no visual indication within the video that the object immediately slows down on impact, (Graph 1 shows this minimal impact as the object slows by only 10% as it first impacts the water until total submersion.), creates an expected significant splash, or reacts with the water in any obvious fashion. The mystery around this lack of a splash is further compounded since the object doesn't appear streamlined but is more of an oval shape. The lack of a visual effect could be due to our difficulty in translating a heat signature into the more normal visual picture. A very detailed discussion of the object's shape is covered in Appendix H, “Modeling of the Object”.

At 01:24:13 Zulu hours, as shown in Frame 3769 and those following (see Figures 12 and 13) an object larger than three feet, traveling over 100 miles per hour, hit and entered the ocean seemingly with little or no splash. Although present science knows ways to minimize the splash, eliminating it is not possible. Effectively a splash is taking a volume of water and drastically increasing its surface area. Since both evaporative and radiative heat transfer are proportional to surface area, a splash enables that volume of water to become cooler. The change in temperature discussed here is very small and is nearly invisible in infrared as can be seen in Figure 14. In this figure, the red circle outlines the unknown object that has just hit the surface of the ocean. The red arrow indicates the object's direction of travel. As was stated above, even with a 300X zoom, no significant cooling (lighter shades) of the water can be seen.

A three-dimensional view of pixel intensities is helpful in looking for a splash. An “Image J” tool[18], "Surface Plot", was used to create a 3-D view. The software converts the pixel intensities (heat variations) in the IR frame to height variations with the lighter (cooler) pixels being represented as hills and the darker (hotter) pixels as valleys. The red outline in Figure 14 was provided to allow a direct comparison of that picture with the surface plot shown in Figure 15.

[18] ImageJ 1.47v. National Institute of Health, July 8, 2013. http://imagej.nih.gov/ij

FIGURE 12: Object's initial impact with water shown in Frame 3769

FIGURE 13: Object's < 1/6 of a second later in Frame 3773

Although still small, the cooler areas representing the splash are seen as raised areas around the upper-right corner of Figure 15. It is believed these represent a splash rather than simply cooler areas of the UAP since they only show up in these plots where the UAP is entering the water. The object in Figure 14 is moving to the left and slightly down. This raises an interesting observation. Rather than the splash being in front of the UAP, it is trailing. Since a frontal splash could not be found in this or any later frames, it is believed the splash was caused by the lower middle or back lower portion of the UAP. The UAP was angled such that it sliced into the water with little or no splash at a speed close to 109 mph. This feat requires a technology that would be at the forefront of the U.S. Navy's current capabilities. If it has been developed then it would most assuredly be highly classified.

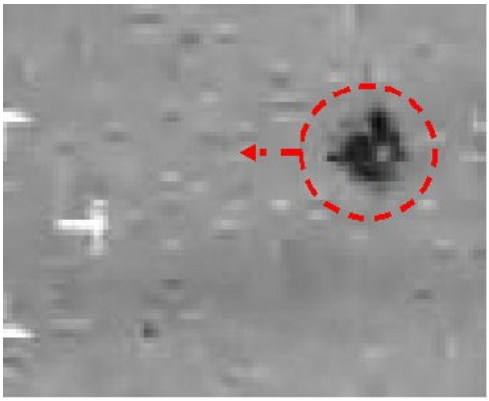

FIGURE 14: Frame 3769 - 300X zoom

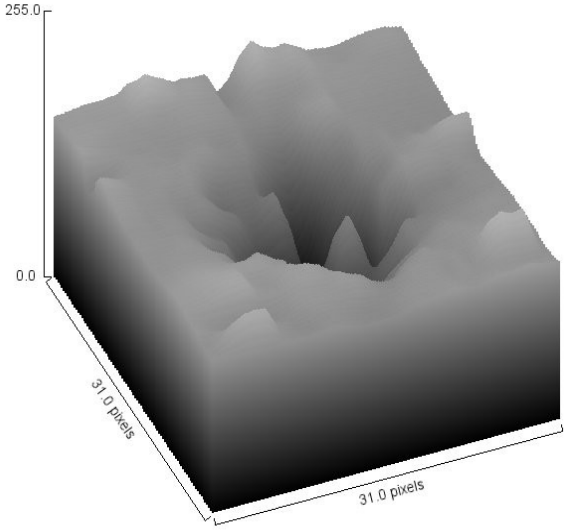

FIGURE 15: Frame 3769 – Surface Plot

Object's Interaction with Water: movement through water Although the video does not show the object for most of its underwater period, each time the object appears, the camera is found to be pointed almost directly at the unknown. Since one of the witnesses specifically rejected the idea that the camera was locked onto the object, this implies that the object has remained visible to either the camera operator or the pilot or both. It further implies that while traveling underwater the unknown object has remained relatively close to the surface throughout. Since these assumptions essentially mean the unknown is at an altitude of sea level and is placed at the target location printed on each frame, we can utilize the target location as the unknown's location throughout this period to calculate its speed.

During the first 26.7 seconds that the object is traveling underwater, it covers a distance of 3241.7 feet equating to an average speed of 82.8 mph. This is a slight drop from the object's aerial speed at impact. Whether that speed drop is due to the resistance in the water or is just coincidental is not known. The speed calculations made of the object's movement through the water is detailed in Appendix J. The speed of the object underwater is not beyond our current technological capabilities. These high speeds are easily exceeded by underwater torpedoes that reduce water resistance via a process known as super-cavitation.

At this point, it is worth discussing how the thermal imaging video is capable of seeing an object underwater. Infrared radiation is easily blocked by water and about one millimeter of water absorbs virtually all of the IR generated by the object; however, that does not necessarily eliminate detection of underwater objects using infrared.

When a solid object moves underwater, the water must be displaced and some of that water is displaced toward the surface which then manifests as a moving hump along the surface. Northrop Grumman is aware of this phenomenon, known as a Bernoulli Hump, and has mentioned this as one possible method to detect submarines.[19] Like the splash discussed earlier, that surface hump would increase the exposed surface area of the water and therefore decrease the temperature compared to the surrounding surface water. This thermal effect can be easily seen in the movie as a moving cool region and is easier to view than in individual frames. It is caused by the slight bulge in the surface due to water displaced by the motion of the unknown object. The infrared camera displays a lightly cooler (whitish) area associated with the object and can be seen in Figure 16. This whitish area, the Bernoulli Hump, increases with speed and cross sectional size of the object and decreases with depth. Using this information, the depth of the unknown object can be estimated. The average wave height off the coast of northern Puerto Rico is one to three feet on a typical day. The height of the waves seen in the video are then likely to be this height therefore the Bernoulli Hump seen in the video is also in this range. Consequently, from Graph 2, the maximum depth of the unknown object is in a range from 9 to 16 feet. See Appendix H for additional information.

[19] Haffa and Patton, "Analogs of Stealth," Northrup Grumman Analysis Center Papers, June 2002, p.14

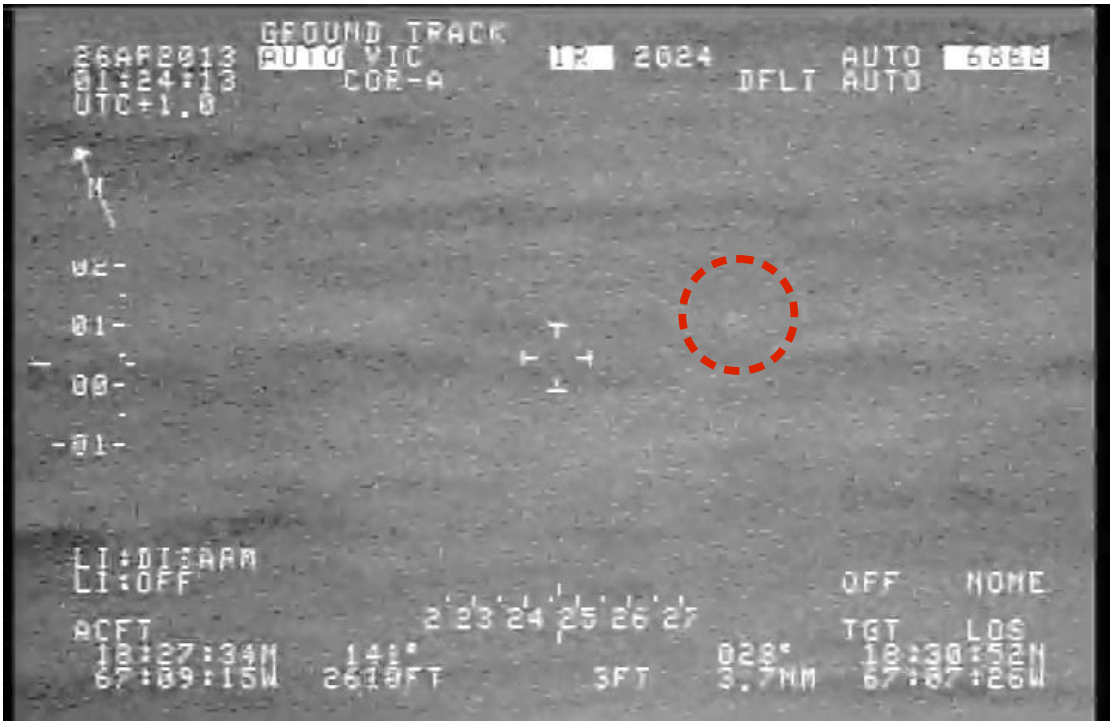

FIGURE 16: Cooler signature of object in frame 3781

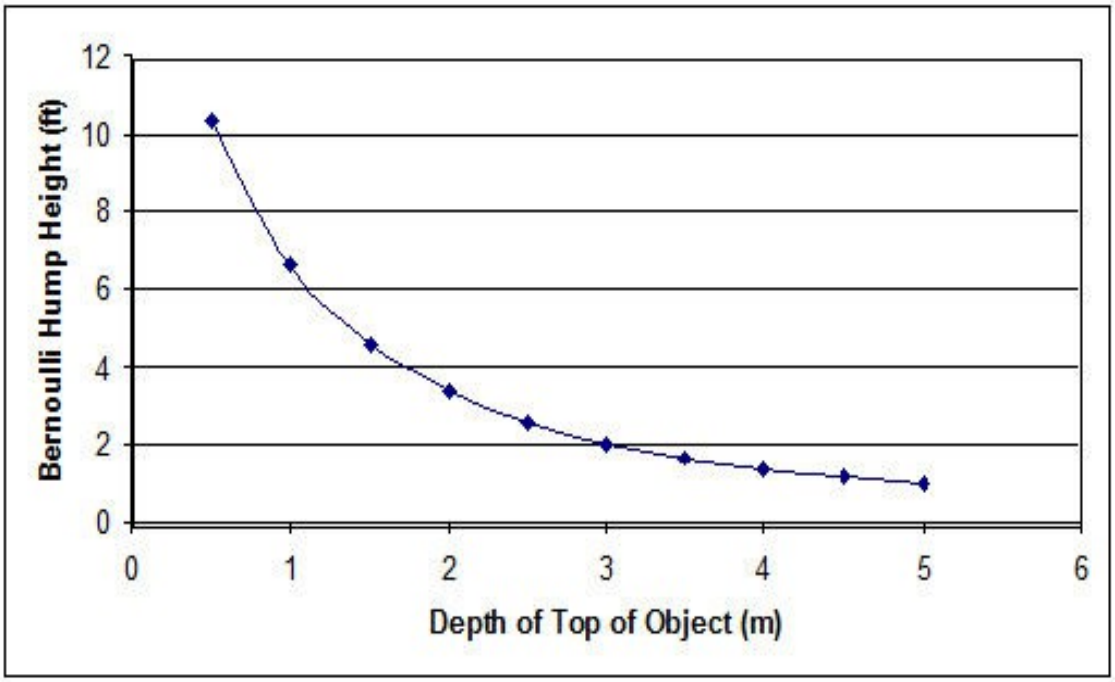

Graph 2: Bernoulli hump; height vs depth based on a 3 ft object moving at 83 mph

Object's Interaction with Water: exiting the water Five seconds after the object enters the water at 01:24:18, it re-emerges for about two seconds and either skims along the surface or is only partially submerged. During those two seconds, it is clear that the object's temperature is still hotter than the water around it because it is still a distinct black. It is also clear that there has been no slowing of the object through the water. The object must have some type of power source that maintains its movement through the water as well as maintain its temperature. Figure 17 demonstrates the heat of the object is still present and, as shown in Table 1, the object maintained a significant underwater speed for a lengthy period of time; almost a minute. When the object made its next exit at 01:24:31 hours, it continued to maintain a heat signature on the video.

FIGURE 17: Heat of object indicated by dark color in frame 3937

Object Divides into Two A significant and unusual characteristic exhibited by this object is the moment when the object splits in half. No indication could be found of a second object that joins the first does the video evidence suggest the second object is due to reflection. A careful frame by frame analysis indicates that the object split in half. In less than one second, the object's thermal image doubled in size; its center of heat then became bimodal; the object then split into two halves. The process appeared similar to mitosis observed during cell division with the splitting of the nucleus, the expansion of the cell, and the final separation into two cells. Due to the significance of this event, a considerable amount of time was spent illustrating this segment of the video evidence.

The initiation and completion of the splitting process occurs largely within one second. This second of time was separated into 32 frames (frame numbers 4602 through 4633) allowing the events to be examined every 1/32 of a second. In order to display the object's appearance before and after the split, some of the frames displayed are within the immediate one to two seconds before and after Zulu time 01:24:41 hours.

The object's appearance is illustrated using four approaches. One uses full frame of the video, the second uses frame magnification that enable individual pixels to be seen, the third displays pixel values (0-255) with 0 representing the hottest IR signature and 255 the coldest IR signature, and the last uses a two dimensional contoured surface plot. The frames selected are representative of the ongoing change in the object and are represented as figures ##A through ##H. A few frames were not usable because the system's white screen overlay interfered with the object image.

Table 2 displays the important parameters for each selected frame. The comment section primarily describes the object's pixel distribution.

Frame #	Time	Comments
4563(A)	01:24:39	Typical display. Hotter in center.
4590(B)	01:24:40	Typical display. Hotter in center.
4611(C)	01:24:41	Size of object begins to increase.
4623(D)	01:24:41	Object's internal heat distribution increases uniformity. Center area enlarges.
4631(E)	01:24:41	Object's size continues to increase.
4634(F)	01:24:42	Still one object but interior is exhibiting bimodal heat zones.
4640(G)	01:24:42	Bi-modality of center heat zone is now clear.
4652(H)	01:24:42	There are now two separate objects.

TABLE 2: Frames used in evaluation of object splitting in two.

Figures 18A through 18H are the video frames analyzed. The laser range finder reticle, in white and shaped like four “Ts”, can be seen at the screen center with the object nearby in all eight frames. Figures 19A through 19H are enlargements of the previous frames. These enlargements display the individual pixels making up the object. The object has the darker (hotter) pixels than its surroundings. Figures 20A through 20H are the pixel values positioned in their relative screen centered around the unknown object. The pixel values represent the level of infrared intensity relative to other pixels. The pixel values in the 110-140 range are from the ocean. Those are much cooler values than the object, which are in the lower and hotter range from 10-105. Values >160 that occasionally show up are from the laser range finder reticle, which are the bright white pixels.

Figure 18A: Frame 4563

Figure 18B: Frame 4590

Figure 18C: Frame 4611

Figure 18D: Frame 4623

Figure 18E: Frame 4631

Figure 18F: Frame 4634

Figure 18G: Frame 4640

Figure 18H: Frame 4652

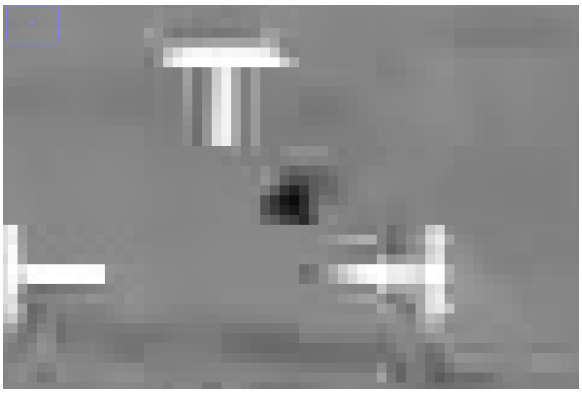

Figure 19A: Frame 4563

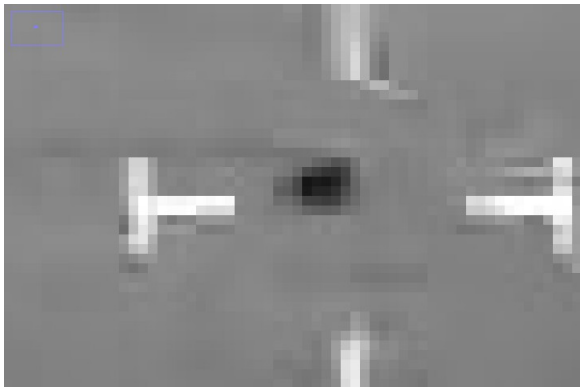

Figure 19B: Frame 4590

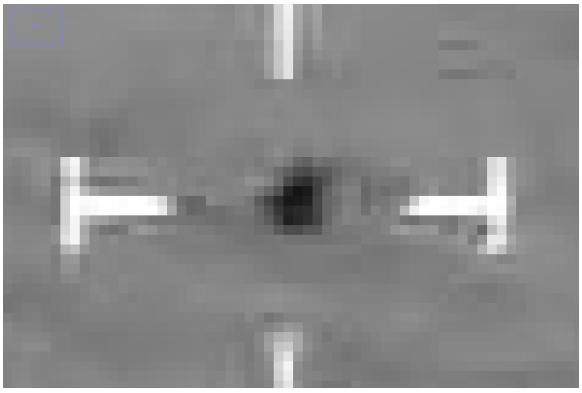

Figure 19C: Frame 4611

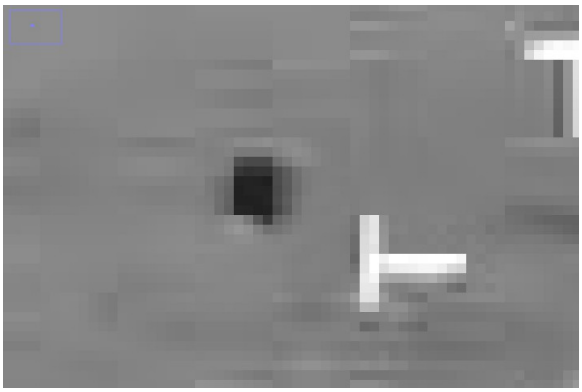

Figure 19D: Frame 4623

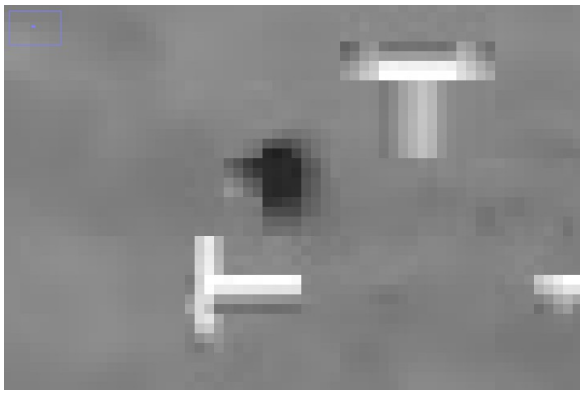

Figure 19E: Frame 4631

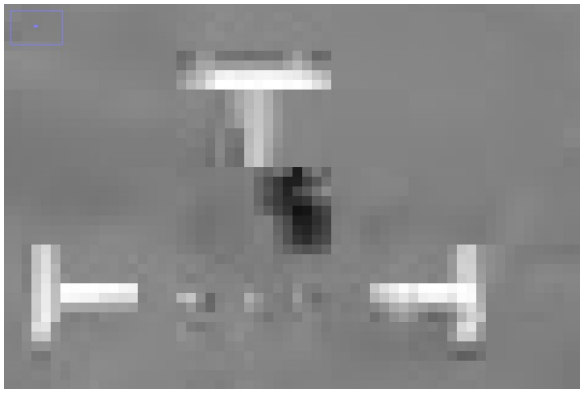

Figure 19F: Frame 4634

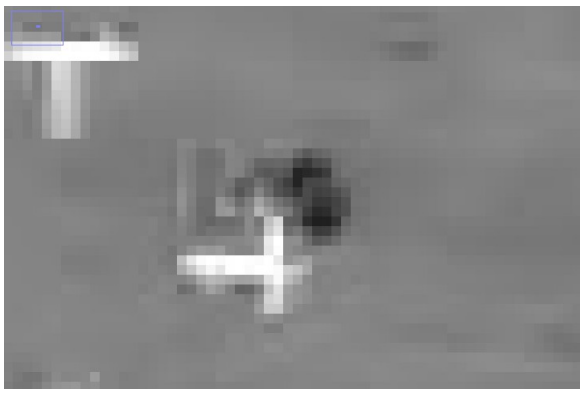

Figure 19G: Frame 4640

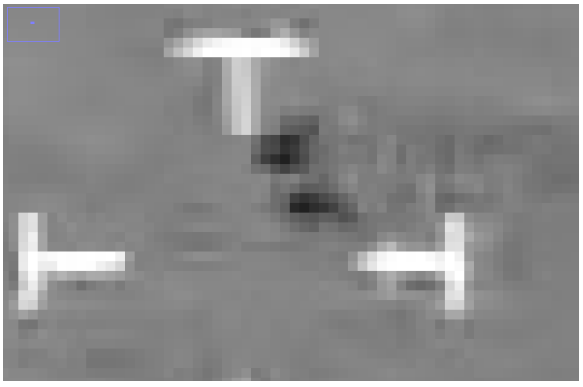

Figure 19H: Frame 4652

To make the object easier to visualize, the pixel values were color coded from the hottest (red = values <31) to the next hottest (orange = values 31-60) to the cooler parts of the object (yellow = values 61-105) all of which are distinct from the cooler areas of the ocean (no color). When white pixels belonging to the reticle were near the object, they were color coded as green. The ranges chosen for each color help visualize the changes in the IR emissions of the object as it split into two halves. The actual edge of the object cannot be discerned in any absolute way. The coloring of the pixels ends at the edge of the number that is closest to the arbitrary value ranges of <31, 31-60, etc. The infrared outline of the object can be seen when there is a significant change in the IR values of the object's periphery compared to the surrounding ocean.

138	129	124	135	143	141	142	141	129
128	128	124	128	130	133	130	130	128
129	142	128	108	97	103	104	107	117
130	147	129	92	76	76	92	98	108
137	124	94	52	33	54	91	102	105
132	82	52	24	11	43	93	115	112
133	82	58	35	23	46	95	130	130
133	104	93	69	60	42	85	131	139
136	136	136	136	136	136	134	134	129

Figure 20A: Frame 4563; normal image about two seconds prior to any change in the pixel.

133	133	134	135	136	140	144	147	142
116	116	116	117	119	123	129	132	136
126	121	114	114	101	95	83	90	115
124	120	104	74	63	53	50	67	109
106	99	73	21	27	24	35	63	102
96	93	72	25	37	37	48	77	101
109	110	97	65	64	60	65	91	108
123	122	114	102	97	95	98	113	118
129	130	127	130	134	132	134	135	128

Figure 20B: Frame 4590; normal image about 2/3 of a second prior to any changes.

129	127	128	134	141	133	126	126	133	134	129
126	128	121	128	132	122	103	97	115	110	113
126	132	128	123	109	95	79	75	89	90	103
133	144	143	132	109	74	52	47	67	85	107
132	134	120	104	82	34	20	25	65	98	115
127	118	92	69	45	24	25	32	71	102	109
120	119	102	82	54	36	42	45	71	102	114
115	114	104	92	66	32	39	48	67	103	121
117	115	110	108	91	77	76	86	89	112	121
117	116	116	117	119	114	114	114	114	115	117
121	120	119	119	119	123	123	124	124	125	125

Figure 20C: Frame 4611; size begins to increase.

129	131	133	139	138	140	143	137	139	138	133
127	128	131	122	122	122	122	131	138	142	139
128	128	123	80	73	73	73	110	122	134	137
130	127	120	55	49	51	51	77	93	112	123
122	113	105	34	35	34	31	76	91	110	122
122	110	101	32	35	36	36	74	90	109	122
124	111	99	32	32	33	37	76	94	114	126
127	110	97	37	36	32	34	71	91	115	126
130	131	137	138	120	86	58	101	112	122	127
134	137	145	151	145	128	113	116	122	128	129
134	135	138	141	141	136	132	129	131	131	129

Figure 20D: Frame 4623; center zone of object expands and the internal heat distribution increases in uniformity.

132	132	132	132	131	123	116	116	120	125	130
131	130	124	119	89	80	78	90	106	117	125
132	128	117	107	38	32	40	68	97	115	126
100	84	61	44	41	39	43	41	85	97	119
114	98	73	58	42	41	43	38	78	90	115
136	122	98	86	42	39	42	42	83	95	114
150	139	114	97	43	39	41	43	83	96	113
130	125	125	125	50	52	59	63	93	101	114
127	125	123	118	77	75	75	74	96	103	114
127	129	126	125	101	98	98	97	113	115	118
128	131	125	125	111	112	114	111	119	116	120

Figure 20E: Frame 4631; object's size continues to increase.

(green pixels due to white reticule)

186	202	165	136	131	133	133	132	129	131	131
129	114	101	114	90	28	95	123	101	129	129
128	102	79	56	30	31	65	87	114	130	129
126	103	85	60	36	69	89	115	140	127	128
125	102	76	59	42	43	53	88	99	123	126
124	111	93	67	50	18	22	53	71	121	125
124	127	129	95	73	29	30	47	65	124	127
123	130	128	102	80	42	36	53	69	126	129
123	131	127	108	81	53	44	65	75	125	130
127	126	127	113	101	89	82	87	101	133	130
126	125	128	120	121	123	128	124	126	129	132

Figure 20F: Frame 4634 at 1/10 of a second after Figure 20E; the center warmer area has become bimodal.

127	123	125	105	91	101	107	116	119	121	123
102	104	100	71	58	75	83	109	116	120	122
88	92	84	36	41	48	61	105	118	116	115
100	79	63	35	70	71	76	98	105	112	118
109	83	73	53	76	64	68	78	92	113	114
138	115	102	81	74	55	57	67	82	115	117
159	132	123	93	62	42	46	69	80	113	115
191	217	94	90	44	31	32	51	100	115	119
203	228	110	119	89	59	62	83	112	121	118
235	255	141	142	110	88	94	108	125	125	122
232	253	141	133	125	126	133	131	135	131	131

(green pixels due to white reticule)

Figure 20G: Frame 4640 at 1/5 of a second after Figure 20F; interior warm zones are now clearly bimodal and separate.

169	134	130	107	106	101	97	120	124	137	142	131	123
167	132	126	96	92	88	83	122	120	128	133	126	123
113	77	69	44	52	77	99	116	118	121	114	116	118
107	78	72	49	59	81	103	108	117	127	123	123	116
94	63	46	32	55	77	101	111	117	122	121	122	116
114	107	83	67	80	89	111	112	119	127	133	127	125
134	137	119	125	129	112	112	102	116	132	141	125	125
136	133	111	118	108	91	93	97	108	124	133	125	128
136	130	110	103	63	50	58	74	84	101	115	128	127
127	120	110	96	40	32	45	52	66	88	102	131	123
134	131	122	109	96	88	85	95	93	81	88	110	118
136	137	133	123	111	102	97	116	113	104	106	113	118
135	137	135	130	125	122	121	123	123	120	118	114	118

Figure 20H: Frame 4652 is 1/3 of a second after Figure 20G with two objects that are now separated.

The changes seen in these eight frames are representative of all the frames during that same time period. A ten-frame moving average was used to minimize any intrinsic pixel variation and/or subjective judgements as to whether a pixel was or was not part of the object. This change in pixel size is shown in Graph 3. Whenever the reticle cross obscured a significant part of the object then a note to that effect is shown on the graph. Those frames were not used in the calculation of the moving average.

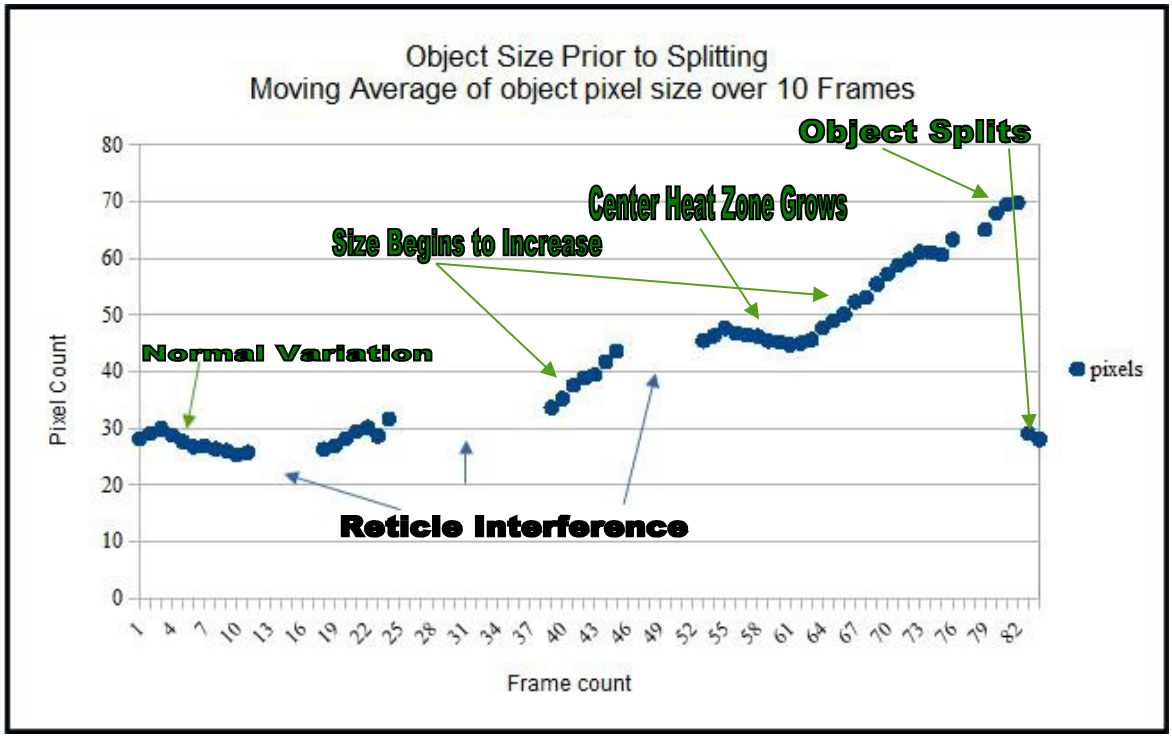

Graph 3: Frame by frame moving average of object's change in size

The last of the four approaches used surface plots from ImageJ software to create a 3-D view. These are displayed in Figures 21A through 21H. Highlighting was done with the LUT feature that provided six shades used to note the IR heat with the bluer (cooler) pixels being represented as hills and the redder (hotter) pixels as valleys. The blue area is the water and the red-orange area is the object with the yellowish-greenish color being a debatable zone of either the object itself or heated areas around the object. The tall pinkish capped peaks seen in Figures 21E through 21H are the effect of the laser range finder reticle image. The size of the area chosen for each frame was kept constant at 13 x 13 pixels so that the change in size, the bimodal heat zone, and the final splitting of the object would be easier to compare across the eight surface plots.

Figures 21A through 21E depict the heat signature consistently seen through the unknown's complete transit. In Figures 21F through 21H a clear representation of the heat signatures can be seen splitting in to two similar parts as depicted in Figures 20 A through 20H.

Frame by frame analysis provides no evidence any pre-existing and independent second object arose out of the water; nor is there any indication that the second object is some type of infrared reflection of the first object. Frame by frame analysis, which was every 1/30 of a second, did not support either possibility.

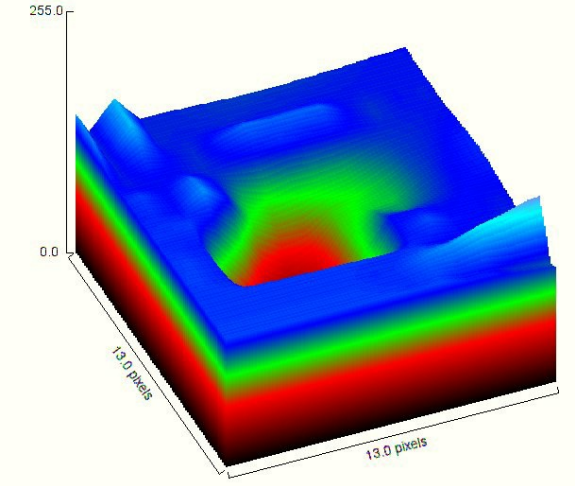

Figure 21A: Frame 4563

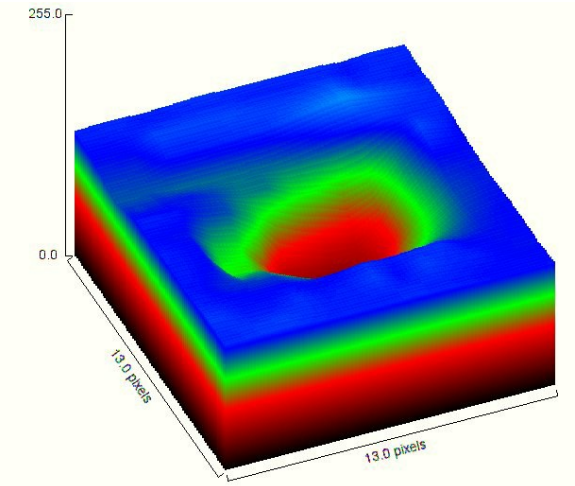

Figure 21B: Frame 4590

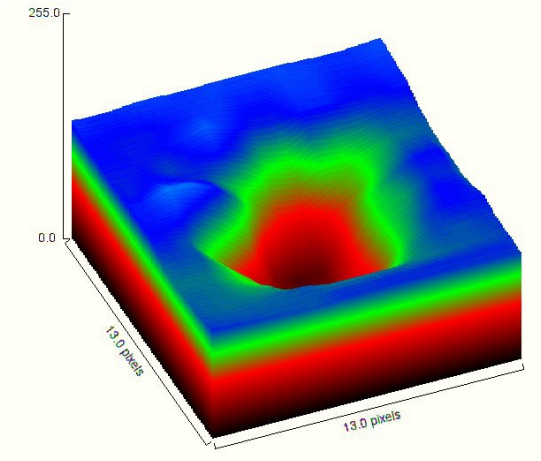

Figure 21C: Frame 4611

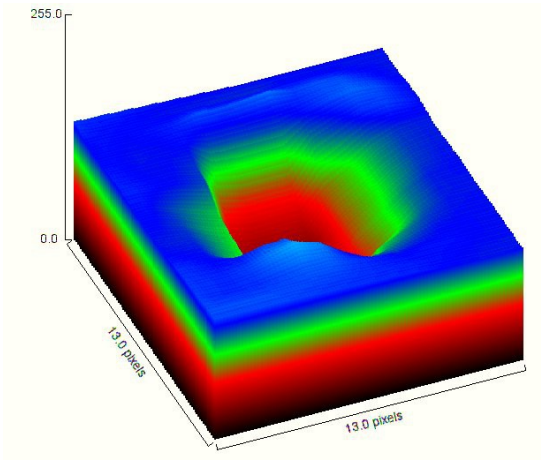

Figure 21D: Frame 4623

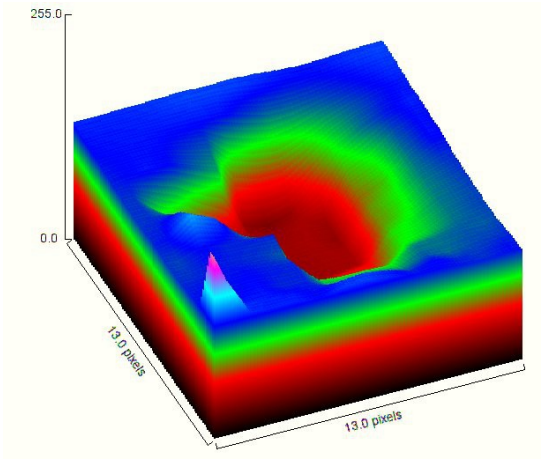

Figure 21E: Frame 4631

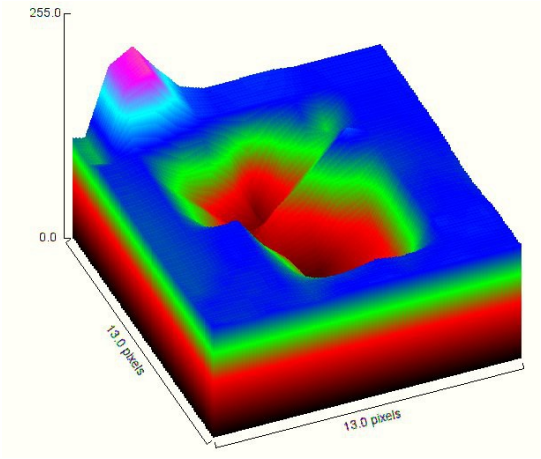

Figure 21F: Frame 4634

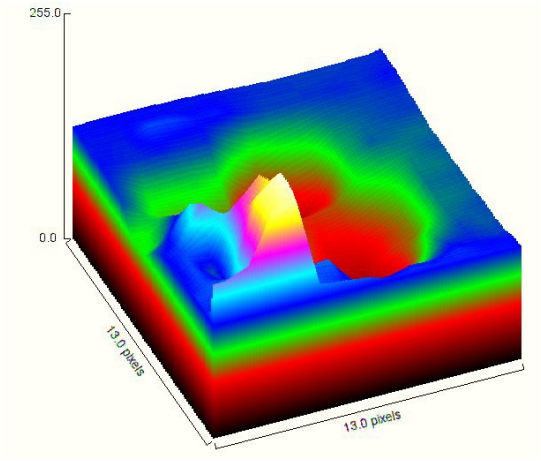

Figure 21G: Frame 4640

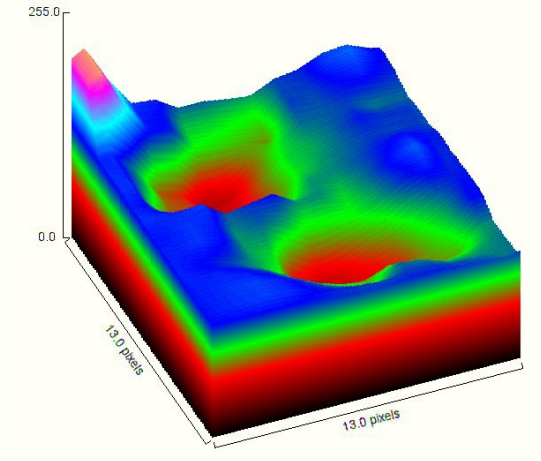

Figure 21H: Frame 4652

Power Source The unknown in the video displayed qualities and behaviors that require some type of power source. Over the course of more than four miles the object reached speeds of greater than 110 mph, made multiple changes in direction, accelerated and decelerated, maintained a temperature significantly greater than the ambient air temperature, entered and exited the ocean at speeds of over 100 mph, and finally split into two parts. The unknown object in the video clearly generated heat which statistically remained near its center with its outer areas at a lower temperature. The heat generated is usually much less than what is seen in the video from jet engines and automobiles. There is no exhaust plume or any other indication of an ordinary aircraft power source. It is also evident the unknown object generates more heat than the ambient air and continues to maintain its heat signature after submersing in the ocean and re-entering the air. These actions and characteristics cannot be achieved without some power source.

It was possible to determine approximate temperatures of the object. The thermal video contains gray scale pixel values between 0 to 255 where 0 is the hottest and is represented by 'black' while 255 is the coldest and is represented by 'white.' Using ImageJ software, the heat signature of the individual pixels comprising the object could be compared. This type of display has already been shown in Figures 20A through 20H where the object's lower IR pixel values of 10-60 in the object's center represent a hotter temperature than the ocean water's pixel values of 115-140, which represent an ocean temperature of about 79 to 83 degrees during April off the Puerto Rican coast. While we have the temperature of the ocean and its corresponding pixel values, for these particular frames with a single known temperature, we can only state that the object's pixel values of 10-60 is warmer than 79 to 83 degrees. Other portions of the video have been analyzed where objects such as cattle, roads and pastureland are in the same frame and enable the establishment of temperature reference points that permitted the temperatures of the object to be estimated. In Frame 1251, time stamped 01:22:49 hours in the video, the unknown object can be seen as well as cattle, an asphalt road, and a pasture. The temperatures of the latter two could be determined based on their natural characteristics and known cooling rates while the skin temperature of cattle is a known value. The details of this analysis are discussed in Appendix K. Graph 4 displays the temperature values vs. the pixel values using the three known temperatures in Frame 1251. The eight center pixel values of the object vary from 0 to 8, which on this graph equates to a temperature of 105 degree Fahrenheit assuming that the thermal video distributes the 255 pixel values linearly. If not then the temperature would be greater than 105 degrees. The sixteen pixel values surrounding those are slightly cooler with pixel values ranging from 16 to 96. Those temperatures range from 103 degrees to 87 degrees.

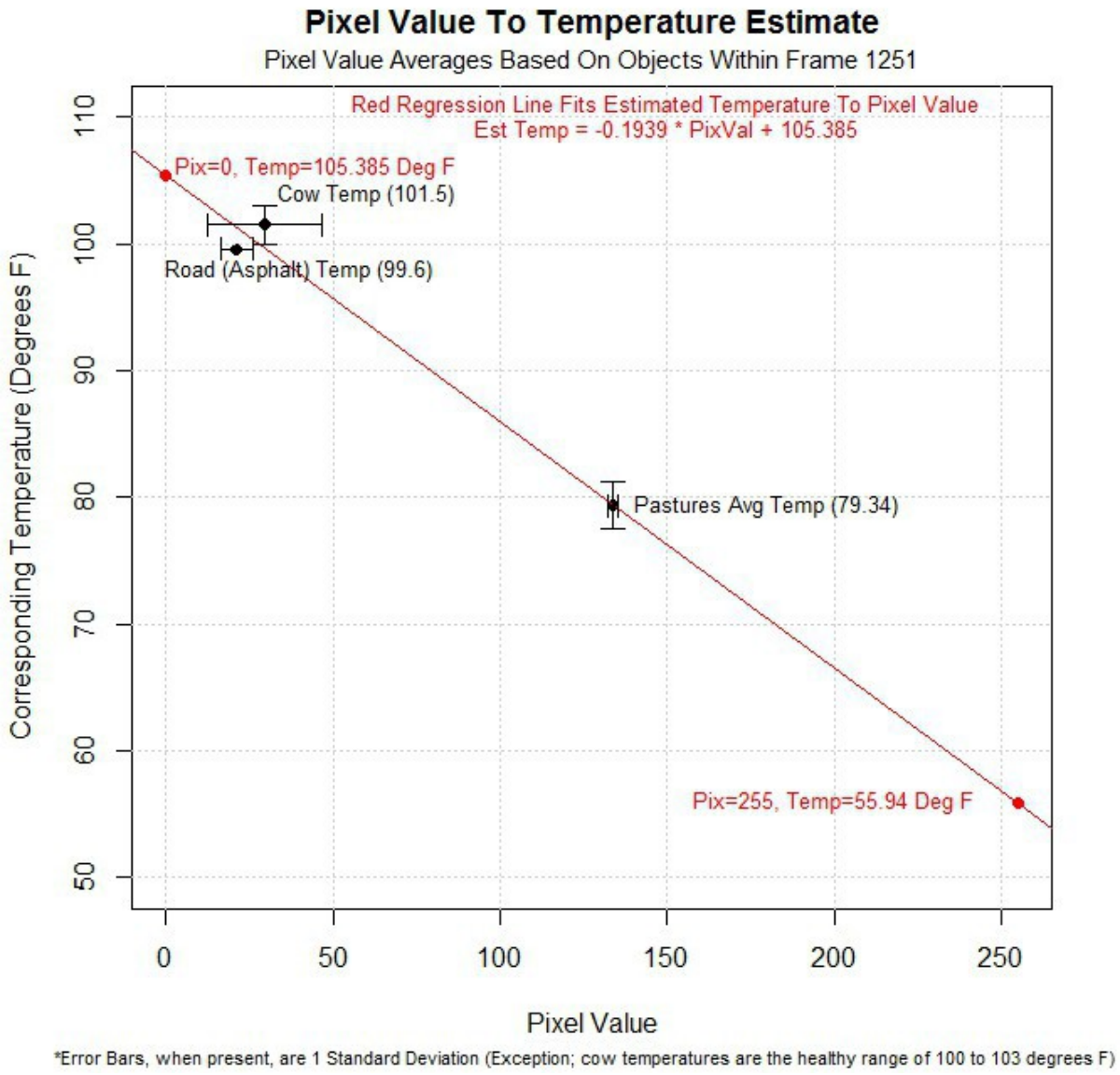

Graph 4: Temperature distributions in Frame 1251 at 01:22:49 hours.

A similar but less exact observation can be made by viewing the video from 01:22:33 to 01:22:36 during the time that the object is crossing in front of the airport's tarmac. In those frames the object's inner temperature is represented by pixel values from 1 to 23 and its outer temperature pixel values from 6 to 79. The tarmac registers a cooler temperature with pixel values of 100-115. There is no question that the object's temperature is significantly above the ambient and its center zone is usually hotter than its outer areas. Whether the object's warmest temperature is only 105 degrees Fahrenheit or hotter cannot be determined without knowing the specific algorithm used by the manufacturer of the thermal video which controls the video's pixel values.

Maneuverability The object's ability to maneuver at speeds of 80-100 miles per hour at low altitude is of interest. A notable characteristic of the object is its apparent tumbling as it moves through the air. This tumbling appearance ends prior to the object's entry into the water and as it moves through the water. At 01:23:37 hours in the video the object can be seen to disappear behind a tree momentarily, placing its altitude at below 40 feet. The ability to fly at that altitude at night and between trees requires precise control and a highly responsive propulsion system particularly given the apparent lack of control by aerodynamic devices (like wings). In terms of current technology, advanced GPS satellites and sophisticated vision pattern recognition in communications with an on board microprocessor might partially explain such maneuvers. More difficult to explain would be the willingness of any government or organization to expose this capability by traversing a residential area where malfunctions during flight could result in harm to the civilian population as well as compromise an advanced military technology.

IV. DISCUSSION AND CONCLUSIONS

Summary The authors of this paper received this video in October of 2013 and have spent more than a year and a half composing this report. Hundreds of hours of work has been spent in gathering information and analyzing the video, radar data, witness claims, and other information related to this event that took place in northwestern Puerto Rico on April 25, 2013. Additionally, our efforts took into consideration protection of the witnesses' identity; it is unfortunate that stigma often accompanies the reporting of what is commonly termed a UFO/USO, but what we have referred to as an UAP. It is hoped that the work that went into this report will inspire future work in the identification of any phenomenon that displays unusual technological capabilities.

We believe that there is sufficient information in the video to characterize this object as: three to five feet in size; the shape is circular to oval but changes; air speed varies from 70 to 120 mph; capable of changing direction; internal temperature of about 105 degrees Fahrenheit usually in the center of the object and exterior temperatures above the ambient air temperature; capable of traveling at low altitude through a residential area; able to enter the water with no obvious splash or impact; underwater speed varies from 39 to 95 mph; ability to exit and re-enter water; and the capability of splitting into two independent parts that appear to be the same size as the original object based on its infrared signature.

Examination of Possible Explanations Entire classes of animals and man-made objects may be eliminated by comparison of properties attributed to the unknown object. The most likely explanations of the unknown object are discussed here.

Examination of Possible Explanations: Hoax One of the first possibilities examined was that of a hoax. The authors of this report spent hundreds of hours in review of the video, detailed review of over 5,000 individual frames and that included pixel level enlargements. During all of this analysis there was never any indication of pixel manipulation. The background in the video corresponds, in extreme structural and geographic detail, to

hundreds of square miles of the actual location. Every on-screen GPS position corresponded to real locations verified by satellite images. Additionally, the location, date and time stamps of independent radar data verified the locations, dates and times of the aircraft taking the video. As noted earlier in this report in the section labeled “Radar Analysis---Verification of Thermal Imaging Video Information,” the radar data supports that there was an aircraft at the exact time and location indicated on the full three minutes of the video and the radar data verifies the pilot's claim that he flew a circle around the base before continuing on his standard surveillance mission along the Puerto Rican coast. The possibility of a hoax is therefore considered extremely unlikely.

Examination of Possible Explanations: Any Lighter Than Air Devices (Not Powered)

The possibility that the object in the video was a balloon or any other windblown object is discussed next. The appearance that the object is tumbling is a main attraction of the balloon theory. Although it is difficult to give this serious consideration, as mentioned previously there was a poor quality copy of this video released on the internet that caused a lot of speculation with the leading explanation being a balloon carried by the wind. The balloon theory posits that a balloon was basically stationary and the movement seen in the video was actually that of the aircraft as it moved in a semi-circle around the balloon. There are multiple reasons why the object in the video cannot be explained as a balloon and they are listed as follows:

1. The object's speed was too great. The actual path of the object was derived in the section of this report labeled “Object Path.” Based on portions of the video where the approximate altitude of the object is known, it was straight forward to calculate the speed of the object which approached 120 mph at times. The wind speeds were 8-13 mph out of the east at ground level and 12-18 mph out of the northeast at elevations of 400 to 3200 feet---much too slow to support a balloon explanation.

2. The object changed directions multiple times, which cannot be explained by a balloon with winds out of the east or northeast. The pilot saw the object traveling from north to south and the video also confirmed that. The object then turned east into the wind then headed back north towards the ocean. Multiple directional changes cannot be explained by a balloon.

3. Temperature information from the thermal video indicates that the object was hotter than the ambient and the center of it was near 105 degrees Fahrenheit with a cooler exterior. A balloon would be near ambient temperatures and there would not be the large temperature gradient as seen in the unknown object. Chinese lanterns would not display the area of heat seen in the video nor could they continue to burn underwater nor could they split into two parts while maintaining the same speed well in excess of the wind.

4. The object impacts the water, and this is clearly seen when analyzing the video frame by frame. The object disappears into the water, travels underwater at an average speed of 82.8 mph then exits back into the air. Prior to impacting the water and after departing the water, the object's heat signature was still present. A balloon or Chinese lantern cannot enter water and stay underwater due to its buoyancy, and it certainly cannot maintain a temperature hotter than the ambient during the process.

5. The splitting of the object into two parts also eliminates a balloon as a possibility.

6. Line of sight movement seen during the video based on the latitude/longitude of the CBP aircraft eliminates any possibility of the object being a balloon. Some arguments have been advanced that the motion of the balloon relative to the background is an illusion created by the motion of the plane circling the balloon. This argument is not valid since the object can be seen moving past background objects even while the background was stationary in certain frames. Further, angular analysis reveals that a balloon, traveling at 15 mph, could be no farther away than 1520 feet from the plane. Using the on-screen GPS data across frames, this relatively short distance creates major line of sight inconsistencies. The details of this analysis are found in Appendix L.

The authors of this report do not consider a wind-blown object as a reasonable explanation for the object in the video due to speed characteristics, directional changes, temperature, buoyancy issues in water, splitting into two parts, and line of sight issues related the movement of a windblown object.

Flying Animals One possibility that is supported by the object's temperature is the possibility of some species of large fast flying bird. This could explain the ability to maintain a temperature above the ambient, the capability to dive into water, and the ability to change directions. The key to a "bird explanation" is the ability of a bird to fly continuously, without diving, at an average speed of about 80 mph, maximum speeds of up to 120 mph, and the ability to dive into water at high speed. There are three large birds capable of sustained horizontal speeds of 80 mph: the golden eagle, the grey-headed albatross, and the peregrine falcon. The golden eagle is about three feet tall with a wingspan of 6-8 feet and its average horizontal speed is 28 to 35 mph with a maximum horizontal speed of 80 mph. It does not live near dense populations of humans and is not native to Puerto Rico. The grey-headed albatross is almost three feet in size with a 7 foot wingspan and has been recorded flying horizontally for eight hours at 79 mph with a South Atlantic tail wind. This albatross is native to the colder areas of the South Atlantic and South Pacific near Antarctica. Lastly, the peregrine falcon does visit Puerto Rico during the winter. Its body is one to two feet in size and it has a three foot wingspan. Although it can dive at extreme speeds, its average horizontal speed is 40-56 mph with a maximum horizontal speed of 65-68 mph. None of these birds, along with being native to the area, fits all the characteristics of speed and size of the unknown object. Nor is there ever any indication of flapping wings during this three minute video, which would be expected over that period of time especially when making directional changes. Additionally, none of these birds are capable of moving underwater at a speed of 95 mph. The fastest swimming bird is the Gentoo penguin at a paltry 22 mph. There is no type of flying animal that can mimic the object seen in the video.

Aircraft Including Drones An explanation worthy of consideration would be some new type of military drone that is perhaps launched from an ocean platform such as a ship or submarine. The size of the object at three to five feet fits into the drone category as does its speed through the air. Currently the Navy is working on a drone capable of traveling in water and air. "The goal is to basically fly as an airplane, splash down and become a submarine,"

according to an aerospace engineer at the Naval Research Laboratory.[20] With both flying and swimming characteristics, it is referred to as a Flimmer. The current model can fly at 68 mph and a swimming speed that has not yet been tested. It is reasonable to suspect that the Navy's current capabilities exceed what is released to the public. It may be within our current technological capability to build a drone that can match the air and water speeds of the object in the video. Although the splash seen in the photo is quite large, there are torpedoes capable of minimizing their interaction with water and it would not be unreasonable to suspect that the same capability might be possible with an advanced drone. This could potentially explain the speed, movement capabilities over land, underwater movement, and the seeming lack of interaction with the water on impact.

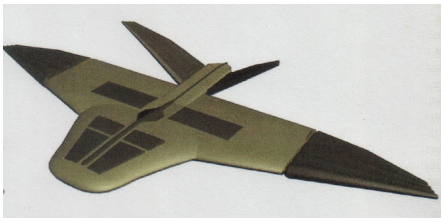

Rendition of the Navy's new Flimmer (fly and swim)

Early Flimmer model splashing into the Potomac

Still to be explained is the thermal heat signature of the object and its ability to split in half. There is no indication of the power sources that would be expected with the familiar types of drones or an air/water drone such as the Flimmer. Any type of internal combustion engine, jet engine or rocket would have been consistently detectable by the thermal imaging system as seen with the automobiles and jets on the tarmac. This characteristic eliminates a drone such as the Flimmer. However, the absence of any comparable heat signature could be addressed by some type of drone more similar to an artillery shell than an aircraft. It is conceivable such a projectile could change direction multiple times after launch and perhaps that is related to the apparent tumbling action. It might even be possible for such a projectile to enter the water with very little impact. As mentioned before, there are missiles and torpedoes designed with that capability. An advanced drone without a power source and that is launched could explain the changes in direction, low altitude maneuverability among trees if equipped with advanced vision/GPS/navigational technology and the ability to impact water with very little disturbance. But a non-powered drone cannot explain the increases and decreases in speed that occur multiple times during the object's flight, the ability to enter and leave water, nor can it explain the ability to split into two parts. Lastly, a drone powered by a lithium battery or low temperature fuel cell might be able to fly with a minimal heat signature. A lithium powered torpedo has traveled at over 50 mph underwater.[21] The military has published aerial drones such as the Wasp III with speeds of 40 mph so it would expected that classified battery powered military drones might reach speeds in the air of 100 mph. It might be possible that a new drone has been developed that can travel in water and air at the speeds of the object in the video. Still, this leaves two capabilities that such a drone would need to match the characteristics of the unknown object: the ability to move in and out of water at high speed; and the ability to split into two parts with both sections capable of independently

[20]Signal Magazine, "Fast-Flying Flimmer No Underwater Fluke". December 1, 2014.

[21]DCNS Jan. 23, 2013. http://en.dcnsgroup.com/news/a-torpedo-powered-by-a-lithium-ion-battery-breaks-speed-records-in-complete-safety/

traversing through air and water.

Careful consideration has been given to the “drone theory” but the authors do not believe that it is a sufficient explanation of what was seen in the video. There are four arguments against a drone as a possible explanation. The first; the authors' question that an advanced drone would be tested at night over civilian areas where there is possible exposure of advanced technology and the risk of loss of the drone when the same testing could be safely achieved over a military operating area. It is also difficult to believe that our military would accept the inherent safety risks of flying a drone across airport runways at low altitude with commercial jets active on the tarmac. Second is the ability of the object to maintain a high speed, even accelerate, underwater, along with the ability to move back and forth between air and water. Third is the appearance of the object in the video; there is nothing in the video to indicate the presence of any type of wings. Lastly, which begs explanation, how one drone splits into two distinct drones of the same size as the initial drone.

Commercial or military aircraft larger than 8 feet are summarily dismissed as impossible given the maximum size of the unknown object as well as some of the same arguments listed in the previous paragraph.

Recommended Actions Further examination and study of this video is warranted as well as collection of additional information. There are remaining questions. Are there additional videos from the Puerto Rico area from other dates in the possession of the CBP as claimed by the anonymous source discussed earlier? Could the FAA provide copies of the Tower logs? Could the military provide radar from the radar facility located at the airport?

Efforts should continue to enlist professional and academic help for work already done as well as suggestions for further research into this video. There remains more follow up that can be done on the software algorithms used in the infrared video system. We should continue efforts to obtain technical manuals for this equipment. What cannot be gleaned from technical manuals that we may or may not obtain, we should attempt experimental projects to determine the visual and measurable limitations of this camera's infrared technology.

Methodologies need to be developed and refined to measure, within this video, object altitudes, angular and absolute velocities and acceleration both in the air and underwater. These accelerations need to be compared to the object temperature fluctuations to determine any correlations. This will help determine any possible relationship between the heat emitted by the object and its motions. Means of measuring the curvature (sharper turns) in the path of the object should be explored.

Conclusion The study of unknown anomalous phenomenon often referred to as UFOs usually carries with it many negative connotations. This negativity has often been brought about due to claims of aliens and little green or grey men in our midst. These types of claims are then further dramatized and stigmatized in the media. This stigma prevents the type of open minded evaluation of aerial phenomena that needs to be undertaken. It is this stigma along with the fact that this object could be labeled a UFO and a USO that we choose instead to refer to this as Unidentified Anomalous Phenomenon. This bypasses the arguments and instead focuses on the fact that it does not fit any logical classification commonly used.

Logically, there should be nothing negative associated with the study of a video that displays an object that appears to be capable of movements not readily explainable by current technology. If others can establish a plausible explanation that reasonably accounts for the characteristics of the object in this video, then so be it. But any explanation must be supported by a detailed report and not assertions or what-ifs. This video is the best documentation of an unknown aerial and submerged nautical object exhibiting advanced technology that the authors of this report have seen.

V. ACKNOWLEDGEMENTS

Robert Powell
B.S. Chemistry
Research Analyst

Morgan A. Beall
B.S. Earth Science
Coordinator

Daina Chaviano
Masters English Literature
Special Field Investigator

Larry Cates
B.S. Mathematics
Computer based analysis & statistics

Carl Paulson
B.S. Physics
Nuclear Physicist – Grumman/Lockheed

Richard Hoffman
B.A. Communications
I.T. Strategic Planner – Defense Dept

Refer to Appendix A for author biographical information.

APPENDIX

APPENDIX A

Author Acknowledgements

Robert Powell has a B.S. in Chemistry from Southeastern Oklahoma State University. He has 28 years experience in engineering management in the semiconductor industry. While working at Advanced Micro Devices he took numerous internal courses related to device physics, design of experiments, and statistical analysis. He helped the company develop its first flash memory technology used in today's flash cards. His experience includes managing a state-of-the-art chemistry laboratory and managing a Research and Development group that worked on nanotechnology using atomic force microscopes, near-field optical microscopy, and other techniques. Mr. Powell is also a co-holder of four patents related to nanotechnology. He has held the position of Director of Research at MUFON (Mutual UFO Network) since 2007 and is also the head of MUFON's Science Review Board. He is a member of the National Space Society and the Society for Scientific Exploration.

Morgan Beall has a B.S. in Earth Science from Frostburg State University. He has worked in the field of environmental consulting and OSHA/EPA regulations for the last 12 years. He has learned and developed team building skills and discipline both in the classroom and in the university athletic program. Mr. Beall has been a MUFON field investigator since 2009 and has had vested interest for many years in the investigative field of the UFO phenomenon. He has conducted many investigations throughout Florida both privately and publicly through MUFON. He is currently the MUFON State Director for Florida, a MUFON STAR Team investigator, and has held held many project management positions within the MUFON organization.

Larry Cates has a B.S. in Mathematics from Jacksonville University. He has 40+ years of programming experience; systems analysis, application and hardware development. He did statistical work for Florida Health and Rehabilitative Services which included design of statistical methods and setting up data analysis queries. Mr. Cates has investigated and researched the UFO phenomenon for over eight years including fielding investigations and analysis of radar data.

Carl Paulson has a B.S. *magna cum laude* in Physics and spent four years working on a PhD in Physics at New York University's Dept of Physics Graduate program. He previously served four years in the United States Air Force. During his career he designed power systems for the Tokamak fusion reactor at the Princeton Plasma Physics Laboratory and then worked for Grumman Aerospace in their Advanced Energy department located at Princeton. This work led to similar positions at Northrop-Grumman and Lockheed Martin. Simultaneously, Mr. Paulson provided the physics designs for multiple linear accelerators. Those designs included the entire CWDD linear accelerator at Argonne National Laboratory and portions of the BEAR accelerator which was placed and operated in space. He is a MUFON STAR Team investigator and is a member of the MUFON Science Review Board.

Richard Hoffman has a B.A. in Organizational Communications from Wright State University. He is an Information Technology consultant and strategist. He has been a defense contractor for over 20 years working primarily for the Army Materiel Command HQ with a variety of companies. Currently, Mr. Hoffman is a Senior Engineer supporting the U.S. Army Network Enterprise Technology Command (NETCOM) at Redstone Arsenal in Huntsville. He has 51 years of experience as an investigator, researcher, writer, and presenter on the

subject of the UFO phenomenon. He was one of the first to join MUFON in 1969 and is currently the MUFON STAR Team Manager as well as the State Director for Alabama.

Daina Chaviano has a B.A. in English Language Translation from the University of Havana in Cuba. She began her career as a literary and cultural consultant. While in Cuba she published several fantasy and science fiction books and became the best-selling author in both genres in the island's history. She has lived in Miami, Florida, for the last 23 years and has won several international literary awards. Her works have been translated into 30 languages.

APPENDIX B

WESCAM Model MX-15D

MX™ SERIES ROCK SOLID FLIGHT PROVEN

MX™-15D

L3 WESCAM

WESCAM's MX-15D. Fully Digital. High Definition.

An Extreme Multi-Sensor, Multi-Spectral Targeting System in a single LRU configuration.

Ideal for: Medium-Altitude; Covert Intelligence, Surveillance & Reconnaissance, Armed Reconnaissance, CSAR, Target Designation

Airborne Installations: Fixed-Wing, Rotary-Wing, UAV

FEATURES & BENEFITS: MX-15D

Weight-Optimized System
- 113 lb turret
- Electronics unit inside the turret
- Built-in GPS receiver

Interface Flexibility
- Simultaneous SMPTE HD digital & analog (NTSC or PAL) video outputs
- 720p or 1080p HD video
- Supports all standard MX-Series command & control, moving map, radar & searchlight interfaces
- Wide range of electrical interfaces: ARINC 429, Ethernet, MIL-STD-1553B, RS-422/232

High Resolution Imaging
- <5 microradian stabilization minimizes platform-induced image degradation
- Individually optimized optics to maximize performance in each sensor
- MX-Series steering eases workload & ensures steady high magnification video

Sensor Flexibility
- 10 sensor payload
- Delivers 6 separate digital imaging modes & 4 discrete laser capabilities
- Precision zoom low light & HD color optics for situational awareness
- Long range low light, HD color & short wave IR (SWIR) spotter optics for day and night positive target ID
- Laser illuminator, dual mode rangefinder/ designator & spot tracker
- Multi-FOV 640x512 mid-wave IR with option for 1280x1024 High Definition mid-wave IR

Short Wave IR Imaging
- Enhanced haze penetration & target contrast
- Laser spot imaging

Advanced Image Processing
- 14-bit IR and 12-bit EO digital cameras
- Advanced image processing on all sensors improve haze penetration, feature recognition & identification
- Image blending

Consistent Targeting Accuracy
- Simple integration
  - Built-in IMU, GPS & MX-GEO software
  - Connect to GPS antenna
  - Automatic alignment to aircraft
- High target location accuracy
- Automatic video & GEO tracking
- Full laser stabilization minimizes spot jitter
- Internal isolator minimizes vibration-induced boresight shifts
- Operationally proven precision target designation

Ruggedness and Reliability
- MIL spec environmental & EMC
- Sealed heat exchanger does not degrad stabilization
- Built-in vibration isolation protects internal payload components
- High fielded reliability for intense op tempo ISRT applications

See our products in action on YouTube Search:
- MX-15D Product Video
- MX-Series Product Video

Product Enhancements:
- **10 Sensor Payload Capability**

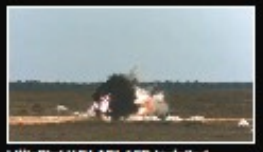

LittleBird UAV: MX-15D Installed

WESCAM's EO/IR/Laser Systems

wescam.com

Previous Description, MX-15Di

MX-15D

PAYLOAD SPECIFICATIONS - SELECT UP TO 10 IMAGING & LASER SENSORS

Sensor Options for Thermal Imager

Sensor #1a - **Thermal Imager:**
Type: 3-5µm staring array
Fields of View: 26.7°, 5.4°, 1.1°, 0.36°

or

Sensor #1b - **HD IR:**
Type: 3-5µm staring array
Fields of View: 35.5°, 9.4°, 1.9°, 1.3° 720p & 1080p
Resolution: 1280 x 1024

Sensor #2 - **Daylight Continuous Zoom TV:**
Type: 5 Megapixel Color HD
Fields of View: 36.3° to 1.1° - 720p
27.6° to 1.6° - 1080p

Sensor #3 - **Lowlight Continuous Zoom TV:**
Type: Electron Multiplied CCD (Mono)
Fields of View: 40.8° to 2.38°

Sensors #4 & #5 - **Laser Designator/Rangefinder:**
Laser Type: Diode Pumped - Nd:YAG/OPO (Class 4)
Wavelenght: 1064nm/1570nm Selectable
Code Compatibility: US & NATO Laser Guided Munitions
Range: Up to 20km
Range Resolution: ±2m

Sensor #6 - **Laser Illuminator (LI)[1]:**
(Used in conjunction with Sensor 3)
Laser Type: Diode - (Class 4)
Wavelength: 860nm
Modes: Continuous, Pulsed
Beam Divergence: Narrow or Ultra Narrow

Sensor #7 - **Daylight Spotter TV with Triple Channel Spotter Lens:**
Type: 2 Megapixel Color HD
Fields of View: 0.37° 720p
0.55° 1080p

Sensor #8 - **Lowlight Spotter TV:**
(Requires Sensor #7)
Type: Electron Multiplied CCD (Mono) 640 x 480
Fields of View: 0.37°

Sensor #9 - **SWIR Spotter TV:**
(Requires Sensor #7)

Sensor #10 - **Laser Spot Tracker**
Type: Quadrant Detector
Wavelength: 1064nm
Code Compatibility: US & NATO Laser Guided Munitions

Note:
• Consult factory for Analog Video specifications.

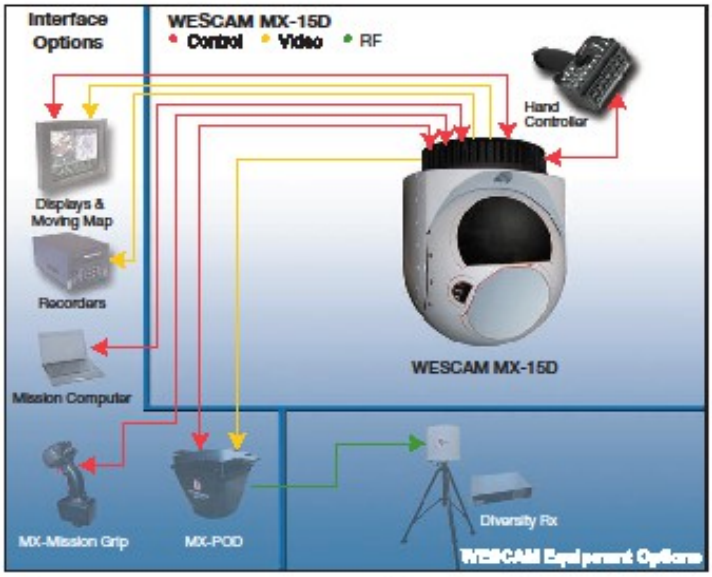

Equipment described herein may require Canadian and/or U.S. Government authorization for export purposes. Diversion contrary to Canadian and/or U.S. law is prohibited.

SYSTEM SPECIFICATIONS

MX-15D Turret
<113 lbs / 51.4 Kg (all sensors)
16.5"(D) x 19.75"(H)
419mm (D) x 495mm (H))

Power
MIL-STD-704E, 280W - 430W (Avg.) 1000W (Max.)

Hand Controller Unit (HCU)
2.2 lbs / 1.0 Kg
4.25"(W) x 8.97"(L) x 3.00"(D)
108mm (W) x 228mm (L) x 76mm (D)
Powered by turret; 5W (Max.)

Cables
Consult factory for available variants

Environmental
MIL-STD-461, MIL-STD-810

TURRET SPECIFICATIONS

Line-of-sight Stabilization
Typically <5 µradians
Consult factory for performance under specific vibration conditions.

Stabilization and Steering
(2) Axis Inner (pitch/yaw)
(2) Axis Outer (azimuth/elevation)

Vibration Isolation
(6) Axis Passive (x/y/z/pitch/roll/yaw)
AZ/EL Slew Rate: 0-60°/sec
Azimuth Field of Range: Continuous 360°
Elevation Field of Range: +90° to -120°

MCU STANDARD INTERFACES
6 Simultaneous EO/IR Digital and Analog Video channels; 1080p configurable for 720p,1080I, 525I & 625I digital options
MX-Hand Controller

OPTIONS AVAILABLE

Interfaces Types:
RS-232
RS-422
MIL-STD-1553B
ARINC 429
Ethernet

Functional Interfaces:
Moving Map
Remote Control
Searchlight
Radar
Microwave/Data Linkz
Aircraft INS/GPS
Metadata

Controller:
MX Mission Grip

Microwave Equipment:
MX-POD, Digital Transmitter
Diversity Rx

WESCAM has a policy of continuous product improvement. Specifications are therefore subject to change without notice.

642996 / July 2012

Inquiries: 1 800 668 4355
sales.wescam@l-3com.com

APPENDIX C

FOIA Requests and Replies

1.0 Initial Letter - Investigator Larry Cates Letter to USAF Regarding 84 RADES

Email to: acc.foia@langley.af.mil
11/04/2013

Dear Sir or Madam:

This is a request under the Freedom of Information Act. I am willing to =
pay up to $50 for this request for the cost of
duplication. If fees will exceed this amount, please contact me first.

This request is to the 84 Radar Evaluation Squadron (84 RADES) for all =
primary and secondary(transponder) surveillance
radar information related to the continuous time period of 23:00hrs Zulu =
Time on April 25, 2013 through 02:00hrs Zulu
Time on April 26, 2013. I request that a radar data extraction be =
produced using the following latitude and longitude
coordinates: a boundary box of upper left N19=BA 00=92 00=94, W68=BA =
00=92 00=94 to lower right N18=BA 00=92 00=94, W066=BA 00=92 00=94. If
possible, please send radar data on a CD in a text or excel format with =
data such as date, time, transponder code or
lack of, range, azimuth, altitude, longitude, and latitude. If you need =
any additional information regarding this
request, please feel free to contact me via email or telephone.

In order to determine my status to assess fees, you should know that my =
fee category is: an individual seeking records
for personal use and not for profit. Thank you for your consideration of =
this request.

Regards,

Larry Cates

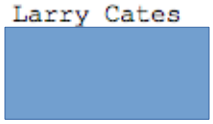

2.0 Response E-mail - Acknowledgment Letter - FOIA Case # 2014-0638

Bautista, Jesica <jesica.bautista@langley.af.mil>
11/5/13
Dear Mr. Cates

This is an acknowledgement for receipt of your 4 November 2013 Freedom =
of Information Act request for a copy of all 84
Radar Evaluation Squadron (84 RADES) primary and secondary transponder =
surveillance radar information related to the
continuous time period of 23:00hrs Zulu Time on April 25, 2013 through =
02:00hrs Zulu Time on April 26, 2013.

We received your request on 5 November 2013. Your case has been =
assigned case number 2014-0638. For all future FOIA
request please submit through the PAL for immediate processing: =
https://www.efoia.af.mil/palMain.aspx
In addition before we can process your request, FOIA Case 2014-0638, we =
require your mailing address.

If you have any questions concerning your request, you may contact us =
at 757-764-7633 or email us at
acc.foia@langley.af.mil. Please reference your assigned case number =
when making inquiries.

Sincerely

JESICA L. BAUTISTA, SrA, USAF
Assistant Freedom of Information Act Manager
FOIA Case 2014-0638

In addition before we can process your request, FOIA Case 2014-0638, we =
require your mailing address. If you have any
questions concerning your request, you may contact us at 757-764-7633 =
or email us at . Please reference your
assigned case number when making inquiries. Sincerely JESICA L. =
BAUTISTA, SrA, USAFAssistant Freedom of Information
Act Manager FOIA Case 2014-0638

3.0 Phone Call Reference Response - FOIA Case# 2014-4053

Bautista, Jesica <jesica.bautista@langley.af.mil>
11/7/13

Mr. Cates,

This is response to your recent telephone call on 7 November 2013. We =
have received your address and updated your
information in our system. Your request FOIA Case 2014-0638 is =
currently being processed. Our target completion date
is 5 December 2013. If you have any questions concerning your request =
please call me at 757-764-7633 or email us at
acc.foia@us.af.mil.

V/r

JESICA L. BAUTISTA, SrA, USAF
Assistant Freedom of Information Act Manager
Air Combat Command

FOIA Case 2014-0638

4.0 FOIA Case# 2014-0638-F Official Response

DEPARTMENT OF THE AIR FORCE
HEADQUARTERS AIR COMBAT COMMAND
JOINT BASE LANGLEY-EUSTIS VA

20 November 2013

HQ ACC/A6XP (FOIA)
180 Benedict Avenue, Suite 210
Joint Base Langley-Eustis VA 23665-1993

Mr. Larry Cates
[redacted]

Dear Mr. Cates

This is in response to your 4 November2013 Freedom of Information Act request for a copy of radar information from the 84th Radar Evaluation Squadron at Hill AFB Utah.

The subject records requested are fully releasable and attached. Department of Defense Regulation 5400.7 indicates fees be assessed for processing this request; however, there were no chargeable fees.

Sincerely

JESICA L. Bautista, SrA, USAF
Assistant FOIA Manager
Air Combat Command

Attachment:
Releasable Records

FOIA Case 2014-0638-F

Agile Combat Power

4.1 FOIA Case# 2014-0638-F Example of data provided

Id	Time	MsgType	Rng(nmi)	Az(deg)	Hgt(ft)	MC(ft)	MCV	M3	M3V	M2	M2V	Lat	Lon	Date
QJQ	23:00:00.040	Sch	86.625	270.615								18.16.41.614 N	067.16.26.937 W	25 Apr 2013
QJQ	23:00:00.055	Bcn	62.125	274.482		3600	1	4743	1	0	0	18.20.48.585 N	066.50.37.558 W	25 Apr 2013
QJQ	23:00:00.118	Reinf	78.375	272.549		16200	1	4046	1	0	0	18.19.19.333 N	067.07.45.226 W	25 Apr 2013
QJQ	23:00:00.149	Bcn	76.75	278.262		1100	1	401	1	0	0	18.26.54.783 N	067.05.24.771 W	25 Apr 2013
QJQ	23:00:00.211	Sch	70.75	276.592								18.24.01.878 N	066.59.23.247 W	25 Apr 2013
QJQ	23:00:00.227	Sch	71.125	275.449								18.22.39.358 N	066.59.55.539 W	25 Apr 2013
QJQ	23:00:00.352	Sch	29.125	279.756								18.21.01.975 N	066.15.40.948 W	25 Apr 2013
QJQ	23:00:00.414	Sch	67.125	283.359								18.31.28.497 N	066.54.12.468 W	25 Apr 2013
QJQ	23:00:00.414	Sch	98.5	283.271								18.38.21.181 N	067.26.22.744 W	25 Apr 2013
QJQ	23:00:00.695	Bcn	26.375	293.906		1100	1	1200	1	0	0	18.26.49.258 N	066.10.52.968 W	25 Apr 2013
QJQ	23:00:00.789	Sch	58.875	293.555								18.39.35.138 N	066.42.19.891 W	25 Apr 2013
QJQ	23:00:00.898	Bcn	16.5	297.686		900	1	4515	1	0	0	18.23.48.229 N	066.00.52.945 W	25 Apr 2013
QJQ	23:00:00.913	Bcn	23.25	298.74		200	1	1200	1	0	0	18.27.19.235 N	066.06.57.709 W	25 Apr 2013
QJQ	23:00:00.929	Bcn	40.75	299.795		4700	1	3272	1	0	0	18.36.23.041 N	066.22.44.974 W	25 Apr 2013
QJQ	23:00:00.945	Bcn	24.875	299.971		1100	1	1200	1	0	0	18.28.34.268 N	066.08.11.413 W	25 Apr 2013
QJQ	23:00:01.038	Bcn	18.75	301.729		400	1	4746	1	0	0	18.26.00.219 N	066.02.17.454 W	25 Apr 2013
QJQ	23:00:01.054	Sch	22.625	300.059								18.27.28.235 N	066.06.06.470 W	25 Apr 2013
QJQ	23:00:01.116	Bcn	17.375	305.244		-100	1	23	1	0	0	18.26.10.244 N	066.00.26.418 W	25 Apr 2013
QJQ	23:00:01.116	Bcn	49.25	306.123		80000	1	1274	1	0	0	18.44.09.608 N	066.25.57.072 W	25 Apr 2013
QJQ	23:00:01.147	Bcn	17.25	305.508		-100	1	1200	1	0	0	18.26.09.805 N	066.00.17.072 W	25 Apr 2013
QJQ	23:00:01.147	Bcn	17.25	305.332		-100	1	2000	1	0	0	18.26.07.207 N	066.00.19.003 W	25 Apr 2013
QJQ	23:00:01.584	Bcn	30	321.24		90000	1	1275	1	0	0	18.36.43.428 N	066.02.53.044 W	25 Apr 2013
QJQ	23:00:11.413	Sch	27.5	250.752								18.06.59.602 N	066.12.45.896 W	25 Apr 2013
QJQ	23:00:11.459	Sch	29	252.949								18.07.33.157 N	066.14.37.012 W	25 Apr 2013
QJQ	23:00:11.522	Sch	40	255.674								18.06.07.022 N	066.26.11.556 W	25 Apr 2013
QJQ	23:00:11.522	Sch	27.75	253.125								18.08.00.320 N	066.13.23.357 W	25 Apr 2013
QJQ	23:00:11.647	Reinf	48	255.674		4700	1	4423	1	0	0	18.04.05.754 N	066.34.19.781 W	25 Apr 2013
QJQ	23:00:11.849	Sch	82.5	265.078								18.08.42.005 N	067.11.44.091 W	25 Apr 2013
QJQ	23:00:11.912	Sch	63.5	267.188								18.12.48.127 N	066.52.06.304 W	25 Apr 2013
QJQ	23:00:12.052	Reinf	77.25	272.637		15900	1	4046	1	0	0	18.19.23.956 N	067.06.34.179 W	25 Apr 2013

5.0 Initial Request Letter - Investigator Daina Chaviano

Daina Chaviano
[redacted]

March 26, 2014
Federal Aviation Administration
Eastern Service Center Air Traffic Organization FOIA Coordinator, AJO-2E5
P.O. Box 20636
Atlanta, GA 30320

FOIA Coordinator:

This is a request under the Freedom of Information Act. I request that a copy of the following documents (or documents containing the following information) be provided to me:

Dear Sir or Madam, this request is for a copy of the Daily Record of Facility Operation (FAA Form 7230-4) from the Rafael Hernandez Airport located in Aguadilla, Puerto Rico. The Daily Record of Facility Operation being requested are those for the time period of April 23 through April 27 of 2013.

In order to determine my status to assess fees, you should know that my fee category is: an individual seeking records for personal use and not for profit.

The maximum dollar amount I am willing to pay for this request is $25. Please notify me if the fees will exceed $25.00 or the maximum dollar amount I entered.

Thank you for your consideration of this request.

Sincerely,

Daina Chaviano

[redacted]
dch_000@yahoo.com

6.0 FAA Certified Mail - Return Receipt - FOIA Case# 2014-008277(ES)

U.S. Department
of Transportation
**Federal Aviation
Administration**

1701 Columbia Avenue
College Park, GA 30337

APR 10 2014

Certified Mail – Return Receipt

Mr. Daina Chaviano
[redacted]

RE: Freedom of Information Act (FOIA) Control No. 2014-008277(ES)

Dear Mr. Chaviano:

This is an Air Traffic Organization, Eastern Service Center no records response to your FOIA request received in this office on April 4, 2014 made under the provisions of Title 5 United States Code, Section 552. You requested a copy of the Daily Record of Facility Operation from the Rafael Hernandez Airport (BQN), in Aguadilla, Puerto Rico from April 23 through April 27, 2013.

Unfortunately, we were not able to conduct a search because BQN is a Federal Contract Tower. These facilities are non-government entities operated by Robinson Aviation, Inc., under contract to the FAA. They are not obligated to provide records pursuant to the FOIA program. You may contact them at:

Robinson Aviation, Inc.
9063 Farmoor Road
Germantown, TN 38139

There were no fees incurred in processing your request.

Your request has also been assigned for action to other FAA offices for any other responsive records. They will be responding directly to you.

There were no fees associated with your request.

The undersigned and Mr. Mark D. Ward, Director, Air Traffic Organization, Eastern Service Center, are responsible for this no records determination. You may request reconsideration of this determination by writing to:

Assistant Administrator for Finance and Management, AFN-1
Federal Aviation Administration
800 Independence Avenue, S.W.
Washington, DC 20591

7.0 April 2014 Request - Regarding 84 RADES

Dear Sir or Madam:

This is a request under the Freedom of Information Act. I am willing to pay up to $50 for this request for the cost of duplication. If fees will exceed this amount, please contact me first.

This request is to the 84 Radar Evaluation Squadron (84 RADES) for all primary and secondary(transponder) surveillance radar information related to the continuous time period of 23:00hrs Zulu Time on April 25, 2013 through 02:00hrs Zulu Time on April 26, 2013. I request that a radar data extraction be produced using the following latitude and longitude coordinates: a boundary box of upper left N19° 00’ 00”, W68° 00’ 00” to lower right N18° 00’ 00”, W066° 00’ 00”. If possible, please send radar data on a CD in a text or excel format with data such as date, time, transponder code or lack of, range, azimuth, altitude, longitude, and latitude.

If you need any additional information regarding this request, please feel free to contact me via email or telephone.

In order to determine my status to assess fees, you should know that my fee category is: an individual seeking records for personal use and not for profit. Thank you for your consideration of this request.

Regards,

Larry Cates
[redacted]

8.0 FOIA Case# 2014-0638-F Official Response - 84th Radar Evaluation Squadron

DEPARTMENT OF THE AIR FORCE
HEADQUARTERS AIR COMBAT COMMAND
JOINT BASE LANGLEY-EUSTIS VA

16 May 2014

HQ ACC/A6XP (FOIA)
180 Benedict Avenue, Suite 217
Joint Base Langley-Eustis VA 23665-1993

Mr. Larry Cates
[redacted]

Dear Mr. Cates

This is in response to your Freedom of Information Act requests for radar data from the 84th Radar Evaluation Squadron at Hill AFB Utah.

Your requests have been reviewed by the Air Combat Command, Department of Defense/Department of Homeland Security Long Range Radar Joint Program Office and they have determined that the 84 RADES will no longer process FOIA requests to create a federal record for release to the public.

The radar data is jointly owned by the Department of Defense, Department of Homeland Security and the Federal Aviation Administration. Even though the 84 RADES has been processing previous requests and providing records, they have never received or requested approval to release this information to the public. Also, in accordance with DoDr 5400.7 the 84 RADES is not obligated to create a record to satisfy a FOIA request. Creating these records are not considered minor operations for day-to-day operations because a trained radar technican must perform the radar data extraction and parsing of the radar data to create a usable product.

If you are dissatisfied with this response, you may contact the Air Force Public liaison officer to address your concerns to the Air Force FOIA Public Liaison Office, Ms. Anh Trinh at usaf.pentagon.saf-cio-a6.mbx.af-foia@mail.mil or 703-614-8500.

Department of Defense Regulation 5400.7 indicates fees be assessed for processing this request; however, there were no fees assessed in this instance.

Sincerely

JESICA L. Bautista, SrA, USAF
Assistant FOIA Manager
Air Combat Command

FOIA Case 2014-4053-F

Agile Combat Power

APPENDIX D

Delay of Fed Ex Flight 58

information provided by Flight Stats

BQN Departures: Thu Apr-25-2013 from All day

Choose Destination
— All Airports —
Show Codeshares
Hide Codeshares
What is a Codeshare?
Choose Airline
— All Airlines —
Update

LEGEND
^ CODESHARE FLIGHT
~ ESTIMATED TIME
SET FLIGHT ALERT
FLIGHT TRACKER
FLIGHT NOTES (DRILLDOWN)
ON-TIME
DELAYS 15-29 MIN.
DELAYS 30-44 MIN.
DELAYS 45+ MIN.
CANCELLED

For details, click on Airport Code, Flight Number or On-time Rating

Destination	Flight	On-time Rating	Airline	Departure Sched	Departure Actual	Term Gate	Status	Equip	Track
EWR Newark	UA 1162	★★★★☆	United Airlines	1:50 AM	2:05 AM		Landed On-time	738	
EWR Newark	AC 2211^	★★★★☆	Air Canada	1:50 AM	2:05 AM		Landed On-time	738	
MCO Orlando	B6 730	★★★★☆	JetBlue Airways	3:19 AM	3:04 AM		Landed On-time	320	
JFK New York	B6 728		JetBlue Airways	5:01 AM	4:57 AM		Landed On-time	320	
CUR Curacao	AMF 8118		Ameriflight	9:35 AM	9:46 AM		Unknown		
PLS Providenciales	MTN 8115		Mountain Air Cargo	9:40 AM	9:40 AM ~		Unknown		
SLU Saint Lucia	AMF 8110		Ameriflight	9:55 AM	9:57 AM		Unknown		
BGI Bridgetown	AMF 8106		Ameriflight	9:55 AM	9:49 AM		Unknown		
POS Port Of Spain	MTN 8129		Mountain Air Cargo	10:05 AM	10:52 AM		Unknown		
AUA Aruba	AMF 8120		Ameriflight	10:10 AM	10:05 AM		Unknown		
SJU San Juan	AMF 6911		Ameriflight	7:20 PM	7:29 PM		Landed On-time		
FRA Frankfurt	LH 8263		Lufthansa	7:45 PM	7:55 PM ~		Unknown	M1F	
FRA Frankfurt	GEC 8263		Lufthansa Cargo	7:55 PM	7:35 PM		Unknown		
MEM Memphis	FX 58		FedEx	9:10 PM	9:26 PM		Landed On-time		
AMS Amsterdam	MP 1158		Martinair	10:20 PM	12:26 AM		Unknown	M1F	
IND Indianapolis	FX 9302		FedEx	11:10 PM	10:56 PM		Landed On-time		
GSO Greensboro/High Point	FX 9306		FedEx	11:44 PM	11:33 PM		Landed On-time		

[1]

[1]The "Landed On-Time" statement refers to FedEx flight 58's arrival at its destination on time. The delay in departure is shown by the scheduled time of 9:10pm vs the actual time of 9:26pm.

BQN Arrivals: Thu Apr-25-2013 from All day

Choose Origin
— All Airports —

Choose Airline
— All Airlines —

Show Codeshares
Hide Codeshares
What is a Codeshare?

Update

LEGEND
^ CODESHARE FLIGHT
~ ESTIMATED TIME
SET FLIGHT ALERT
FLIGHT TRACKER
FLIGHT NOTES (DRILLDOWN)
ON-TIME
DELAYS 15-29 MIN.
DELAYS 30-44 MIN.
DELAYS 45+ MIN.
CANCELLED

For details, click on Airport Code, Flight Number or On-time Rating

Origin	Flight	On-time Rating	Airline	Arrival Sched	Arrival Actual	Term Gate	Status	Equip	Track
EWR Newark	UA 1071	★★☆☆☆	United Airlines	12:36 AM	1:02 AM		Landed △ 26 min	738	
EWR Newark	AC 2210^	★★☆☆☆	Air Canada	12:36 AM	1:02 AM		Landed △ 26 min	738	
MCO Orlando	B6 729	★★★★☆	JetBlue Airways	2:04 AM	1:43 AM		Landed ● On-time	320	
JFK New York	B6 727		JetBlue Airways	3:39 AM	3:24 AM		Landed ● On-time	320	
MEM Memphis	FX 57		FedEx	7:45 AM	8:03 AM		Landed △ 18 min		
GSO Greensboro/High Point	FX 9305		FedEx	7:46 AM	7:33 AM		Landed ● On-time		
IND Indianapolis	FX 9301		FedEx	8:54 AM	8:33 AM		Landed ● On-time		
STT Saint Thomas	AMF 6910		Ameriflight	12:31 PM	1:29 PM		Diverted		
SJU San Juan	AMF 6910		Ameriflight	5:43 PM	5:45 PM		Landed ● On-time		
UIO Quito	LH 8262		Lufthansa	6:45 PM			Unknown	M1F	
BGI Bridgetown	AMF 7106		Ameriflight	7:31 PM	8:00 PM		Landed △ 29 min		
CUR Curacao	AMF 7120		Ameriflight	7:56 PM	7:37 PM		Landed ● On-time		
SLU Saint Lucia	AMF 7110		Ameriflight	8:02 PM	7:50 PM		Landed ● On-time		
BOG Bogota	MP 5713		Martinair	9:00 PM	9:00 PM ~		Unknown		
BOG Bogota	MP 1158		Martinair	9:20 PM	10:59 PM		Landed ■ 99 min	M1F	
POS Port Of Spain	MTN 7129		Mountain Air Cargo		8:19 PM		Landed		

APPENDIX E

Auxiliary Witness Communications

1.0: Anonymous Email to John Greenewald and the Back Vault

This information is location on BlackVault site
(http://www.theblackvault.com/m/events/view/

Anonymous-Letter-Authenticates-Puerto-Rico-UFO-Video-And-Sets-Record-Straight) and sent sometime in October 2014. Items of interest are highlighted in yellow.

Recently, I received a letter from an anonymous source, authenticating a UFO video that has circulated for a couple months. Although he claims that the video is authentic, he does mention the information circulating about the video's origins are false, and seems to have quite a bit of knowledge about the videos origin, the technology used, and how the information about the video that is circulating (like it was shot from a Black Hawk helicopter) is actually not true. This letter is in regards to a UFO video, shot by an infrared camera, in Puerto Rico. Special thanks to Jorge Martín, Journalist and UFO researcher in Puerto Rico, for this higher resolution, and clearer, version of the UFO video: The anonymous letter is also below:

The anonymous letter, is as follows:

Hello John,

I was reading about your involvement in getting documents from the NSA concerning UFO's. Sir, if you want undeiable proof of UFO's on earth from a government source it is in the video below. Try a FOIA request for this video that was leaked onto youtube.

I can vouch that the following video is 100% real. I am remaining anonymous to avoid government reprisals. https://www.youtube.com/watch?v=Hee70AwwUJ8

If you ever wanted to truly see how aliens are monitoring or studying us, and witness their technology, this is it. The video is a black and white infrared recording using a L3 MX15 EOIR camera. The IR video uses back hot, meaning the blacker something is the hotter, or fuller of energy it is. The video was leaked onto youtube because the Federal Agents who recorded it realized the Federal Government was not interested in disclosing it. The video was recorded from the screen of a laptop using a iPhone type device. Spanish is heard as background noise to distort the leaker's voices so they are not discovered, so disregard all audio. Lastly, the poster of the video speculates it was recorded from a CBP Blackhawk. In reality it was recorded by a CBP DHC8 turboprop maritime patrol aircraft. This is not a maybe, this is 100% alien technology on earth, in our skies, and under our oceans. The video was taken in Aguadilla Puerto Rico, and can be verified by calling CBP Caribbean Air and Marine Branch, and Aguadilla airport control tower (the UFO was over the airport without permission and tower controllers saw it and tracked it on radar.

On April 25, 2013 at 2122 Local/April 26, 2013 0122Z a Customs and Border Protection Caribbean Air and Marine Branch DHC8 maritime patrol aircraft was on a routine patrol when it encountered a UFO immediately after takeoff. The object was spotted visually by the Captain of the aircraft, and the Aguadilla control tower operator. It appeared to have a strange red light. The Customs and Border Protection crew thought the aircraft might be a smuggler so they began to follow the UFO, and record a IR video. The UFO circled the Aguadilla airport and made its way to the ocean. Initially the UFO appears as a forward flying horseshoe, then as it makes its way to the ocean, it changes its configuration to a more spherical shape. The UFO skims on top of the ocean, and submerges, unaffected by the hydrodynamic forces. Watch the video carefully at 01:24:39 (time in upper left corner) when the object gets really dark (hot) another UFO actually pops out of the ocean and joins the original UFO in formation. Then both UFO's make controlled entries into the ocean. Alien technology is no doubt under the ocean near Puerto Rico!

Final note from The Black Vault: *Unfortunately, I can not verify the above letter. There was no contact information whatsoever, and it was sent via my online contact center. Although a false email address was given, I was able to verify the IP address (unique number given to every computer on the internet) was from the Miami area - but I will not list the IP address for obvious privacy reasons. I feel by disclosing in the Miami area - is not a breach of anything.*

2.0 Anonymous Email to Florida MUFON State Director from Alias John Truth

to:Xxxxxxxxxxxxxxxx (Morgan Beall personal email)
date:Sun, Aug 17, 2014 at 3:43 PM
subject:MUFON Florida: UFO recorded by Customs and Border Protection Aircraft

Having worked for CBP I can vouch that the following video is 100% real. I am remaining anonymous to avoid government reprisals. https://www.youtube.com/watch?v=Hee70AwwUJ8

If you ever wanted to truly see how aliens are monitoring or studying us, and witness their technology, this is it.

The video is a black and white infrared recording using a L3 MX15 EOIR camera. The IR video uses back hot, meaning the blacker something is the hotter, or fuller of energy it is. The video was leaked onto youtube because the Federal Agents who recorded it realized the Federal Government was not interested in disclosing it. The video was recorded from the screen of a laptop using a iPhone type device. Spanish is heard as background noise to distort the leaker's voices so they are not discovered, so disregard all audio. Lastly, the poster of the video speculates it was recorded from a CBP Blackhawk. In reality it was recorded by a CBP DHC8 turboprop maritime patrol aircraft. This is not a maybe, this is 100% alien technology on earth, in our skies, and under our oceans. The video was taken in Aguadilla Puerto Rico, and can be verified by calling CBP Caribbean Air and Marine Branch, and Aguadilla airport control tower (the UFO was over the airport without permission and tower controllers saw it and tracked it on radar.

On April 25, 2013 at 2122 Local/April 26, 2013 0122Z a Customs and Border Protection Caribbean Air and Marine Branch DHC8 maritime patrol aircraft was on a routine patrol when it encountered a UFO immediately after takeoff. The object was spotted visually by the Captain of the aircraft, and the Aguadilla control tower operator. It appeared to have a strange red light. The Customs and Border Protection crew thought the aircraft might be a smuggler so they began to follow the UFO, and record a IR video. The UFO circled the Aguadilla airport and made its way to the ocean. Initially the UFO appears as a forward flying horseshoe, then as it makes its way to the ocean, it changes its configuration to a more spherical shape. The UFO skims on top of the ocean, and submerges, unaffected by the hydrodynamic forces. Watch the video carefully at 01:24:39 (time in upper left corner) when the object gets really dark (hot) another UFO actually pops out of the ocean and joins the original UFO in formation. Then both UFO's make controlled entries into the ocean. Alien technology is no doubt under the ocean near Puerto Rico!

3.0 Youtube Account Anonymous Informant

The statement below was placed in the YouTube commentary on roughly June of 2014 by an individual who has some inside knowledge of the event because he indicates that the video was taken by the U.S. Customs and Border Patrol. The location of the YouTube site at the time of the postings is https://www.youtube.com/watch?v=Hee70AwwUJ8

Interestingly, this individual claims that there are two other videos made in the same area. He/she also claims the video was analyzed in Quantico, Virginia.

Two emails were sent to Red Bill through his YouTube homepage. The emails asked if he could communicate with the researcher of the current investigation. No reply has been received to the date of this report.

The YouTube page has no information in it and it appears that Red Bill created this name for the express purpose of making his YouTube comment.

Red Bill

2 months ago

No se cómo tiene ese video, no fue en un helicóptero. Fue en un avión de Us Customs and border protection. El video original es en blanco y negro, tiene audio, fue examinado en Quantico, Virginia. Hay 2 video más y son de la misma área, de diferente fecha y como punto de referencia es la playa surfers beach.

TRANSLATION:

No way in that video, it was not a helicopter. It was an airplane of the US Customs and Border protection. The original video is in black and white, has audio, was examined in Quantico, Virginia. There are 2 more videos and are of the same area, different date and point of reference is the beach surfers beach.

Below is a second comment made by Red Bill on a different YouTube site that has posted the same video. This comment was made in July of 2014. The site of that YouTube video was the following at the time of this report:
https://www.youtube.com/watch?v=Pm-Sg_J_hB8

In this comment, Red Bill claims that he/she was there. It is difficult to tell if he/she means that he was on the airplane or at the airport when this occurred.

Saludos, fue un avión. Lo que gira es la cámara. El avión de color gris de Aduana. Para las dudas yo estaba ahí, cuando paso. Desde el año pasado esta y hay dos videos de diferentes fechas. Si quiere preguntar dos semanas antes los vecinos de la Base Ramey llamaron a la policía en relación a unas luces que salían del mar. Varios policías llegaron a ver esas luces. Todo se quedo en secreto. Hay una playa que tiene un portón, hay noches que lo cierran. En ese lugar puedes ver esferas de luces, no todo el tiempo, pero pasa a menudo.

TRANSLATION:

Cheers, it was a plane. It is the camera that rotates. The plane is a gray colored Customs. For the doubters, I was there when it happened. From this last year, there are two videos of different dates. If you want to ask two weeks before residents of the Ramey Base called police regarding some lights coming out of the sea. Several policemen came to see those lights. All remained in secret. There is a beach that has a gate, there are nights that close. In this place you can see fields of lights, not all the time, but it happens often.

APPENDIX F

Analysis of Radar Information

Radar Information on the Puerto Rico Thermal Video

Introduction

The purpose of this radar analysis is to verify the legitimacy of the video by identifying the aircraft that took the video through correlation of exact times and radar locations of the aircraft taking the video. A search will also be made to identify any unknown aerial objects that were detected on radar.

1.0 Acquisition of Radar Information

The thermal system's latitude/longitude coordinates indicated that the video of this unknown object occurred over Puerto Rico and the time stamp indicated that the video was taken between 01:22:07 UTC+1 and 01:26:01 UTC+1 on April 26, 2013. Based on this, a request was made for all primary and secondary radar data related to the continuous time period of 23:00hrs Zulu Time on April 25, 2013 through 02:00hrs Zulu Time on April 26, 2013, from FAA radar sites in the vicinity of Puerto Rico. The request included information such as date, time, transponder code or lack of, range, azimuth, altitude, longitude, and latitude.

Radar data was received for that time period from the following radar sites:

QJQ located 92 miles to the east southeast at Pico Del Este, Puerto Rico, at an elevation of 3417 feet and 18º16'07”N 65º45'31”W.

SJU located 75 miles to the east in San Juan, Puerto Rico, at an elevation of 20 feet and 18º27'06”N 65º59'29”W.

STT located 144 miles to the east in St Thomas, Virgin Islands.

The data included a time stamp for each radar contact, type of radar beacon, azimuth/range bearings, latitude, longitude, transponder identification, and altitude. This information is sufficient to verify if the thermal information matches with an aircraft at the exact time and location as shown on radar, thus verifying the validity of the thermal video.

2.0 Radar Analysis of Aircraft Matching Time/Location of Thermal Video

It is a straightforward exercise to determine if there is an aircraft on radar that is an exact match for the aircraft that filmed the thermal video. The thermal video provides the exact time and location of the aircraft as it was taking video of the unknown object. The radar data can verify if an aircraft was present at the same time and location. If there was an aircraft present, then there is no doubt that the video in question was taken by an actual aircraft in maneuvers over Puerto Rico.

The aircraft's location at specific times was obtained from the thermal video and is represented on the Google Map in Figure 1. The initial thermal video shown in Figure 2 indicates that the aircraft was ½ mile east of the Rafael Hernandez airport at 01:22:07 hours at an altitude of 1875 feet. The aircraft departed in an easterly direction, turned towards the north, passed over the coastline in a westerly direction, and finally headed to the south along the coastline. The last frame of the thermal video shows the aircraft located one mile to the southeast of the village of Moca at 01:26:01 hours and at an altitude of 4523 feet.

The radar data was examined and an aircraft was detected that matched the signature of the aircraft that created the thermal video. The transponder number on this aircraft was 4406. This aircraft showed up on the radar data from all three radar sites. Data from the QJQ radar site at Pico Del Este was used to correlate against the thermal video. The following table displays latitude and longitude coordinates from a portion of both the thermal and the radar data. All of these coordinates are at the same time and are within ¼ mile of each other. No other aircraft was in this area with a similar flight pattern at the time. The date based on Zulu time is 04/26/2013 for this table.

Time (Zulu)		thermal Lat/Long	Radar Lat/Long	thermal Alt	Radar Alt	Speed
01:22:08		18º30'11”N 67º05'48”W	18º29'52”N 67º05'51”W	1875'	1600'	
01:22:25		18º31'00”N 67º06'05”W	18º30'44”N 67º06'01”W	1912'	1700'	209 mph
01:22:59		18º31'09”N 67º08'04”W	18º31'09”N 67º07'55”W	1784'	1500'	230 mph
01:23:23		18º30'19”N 67º09'14”W	18º30'30”N 67º09'05”W	2075'	1700'	239 mph
01:23:49		18º28'53”N 67º09'41”W	18º29'06”N 67º0'39”W	2491'	2300'	238 mph
01:24:07		18º27'53”N 67º09'27”W	18º28'05”N 67º09'37”W	2561'	2300'	236 mph
01:24:42		18º26'20”N 67º08'15”W	18º26'27”N 67º08'25”W	3222'	2900'	228 mph
01:26:01		18º23'06”N 67º05'43”W	18º23'16”N 67º05'53”W	4523'	4200'	211 mph

TABLE 1: Correlation of thermal data to radar data

The transponder code on this aircraft is 4406. This indicates that it is a military or law enforcement aircraft. FAA Order 7110.66 stipulates that all transponder codes between 4401 and 4433 will be controlled by FAA Order 7110.67, which is named “Special Aircraft Operations by Federal, State Law Enforcement, Military Organizations and Special Activities.”

Based on the radar data, there is no doubt that the thermal video is a real video taken by a law enforcement or military controlled aircraft. Because we have time and distance information in Table 1, the speed of the aircraft can be calculated. The aircraft's speed varied from 209 mph to 239 mph, which indicates it is not a helicopter but is a plane.

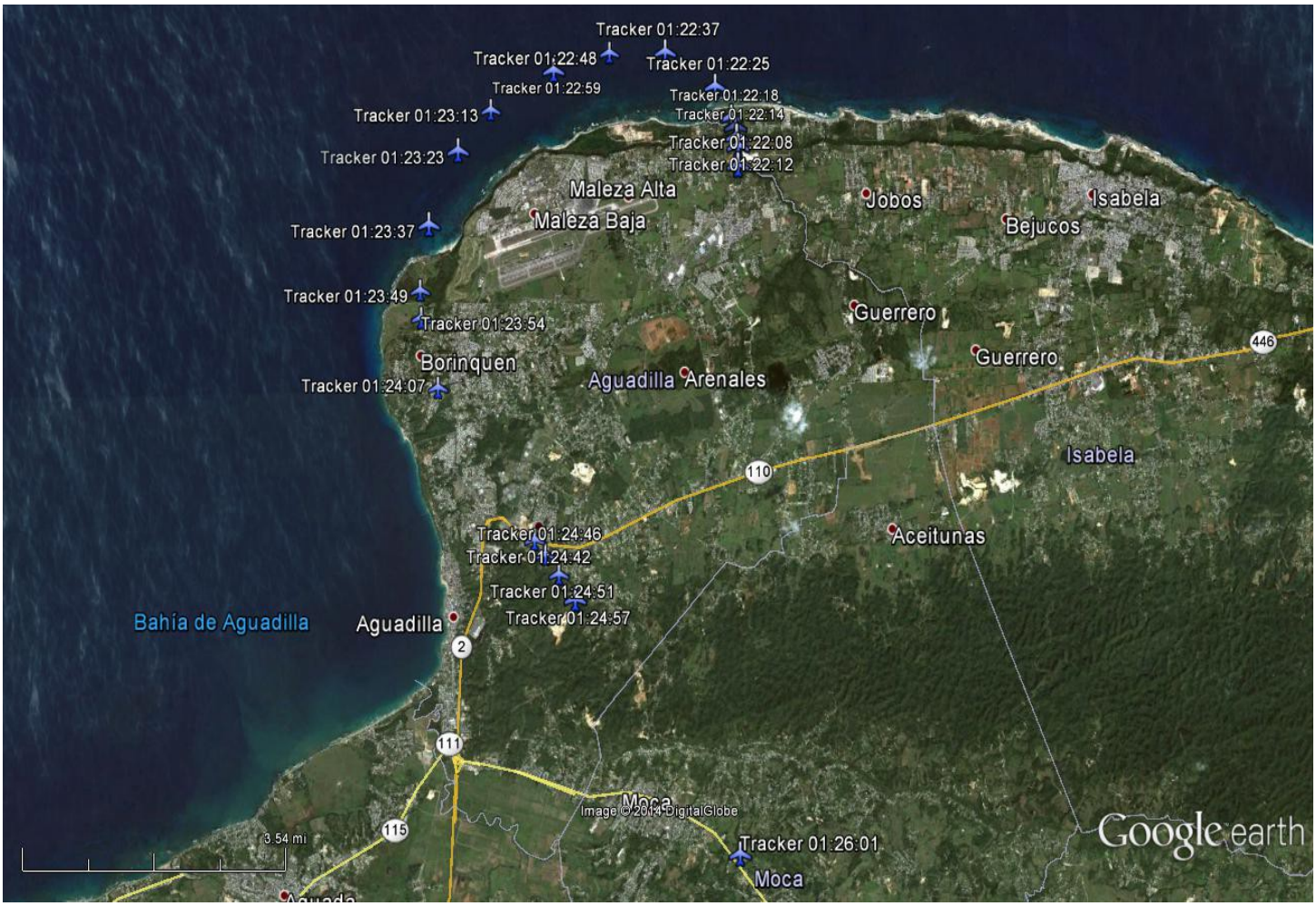

FIGURE 1: Tracking aircraft's location based on video and radar data. The name "Tracker" represents the aircraft and the value to the right is Zulu time at that location.

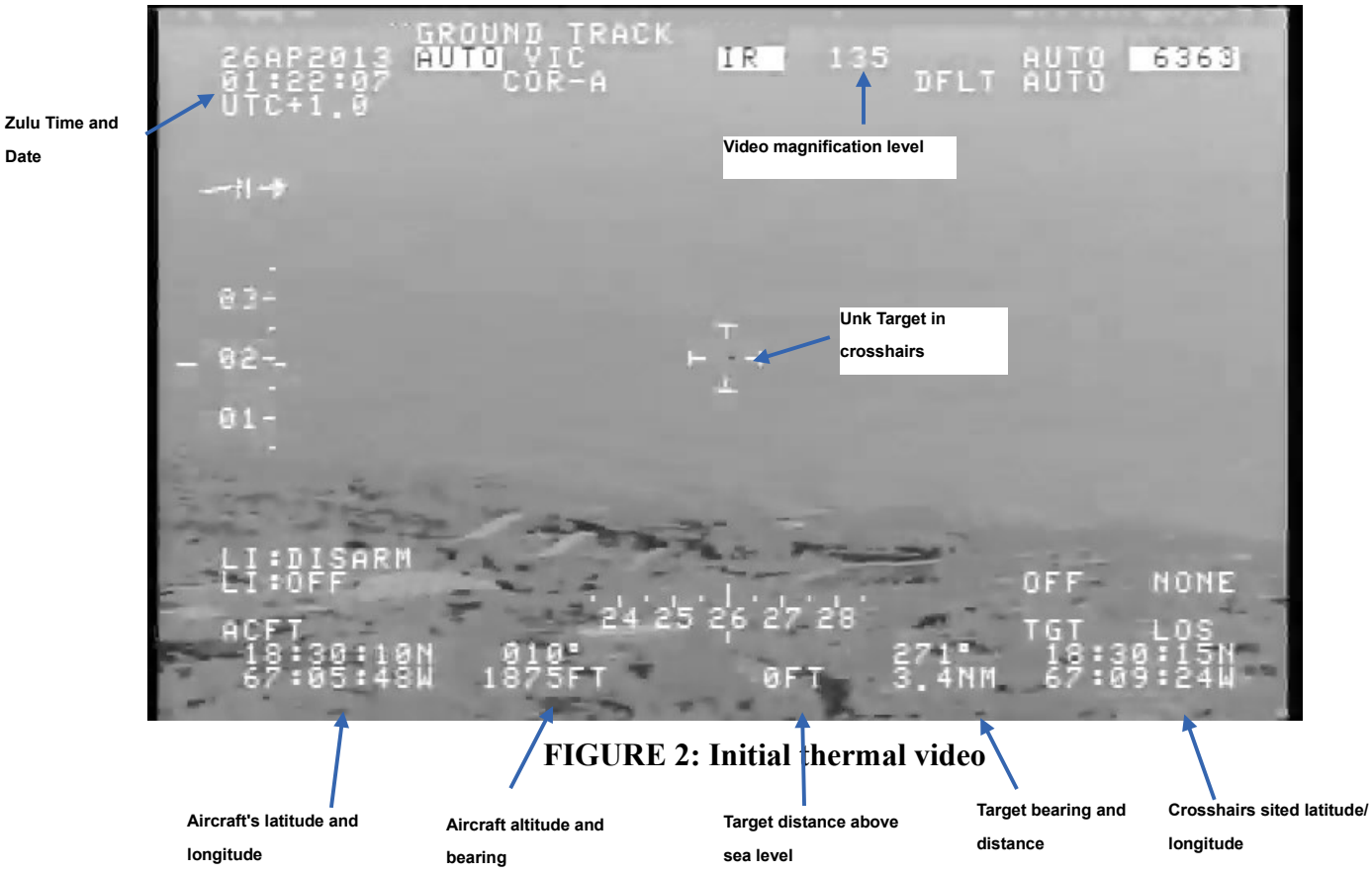

FIGURE 2: Initial thermal video

It is also worth noting that the aircraft made what appears to be an extra search pattern over the ocean to the north and northwest of the airport before commencing what is probably its standard patrol and operational activities down the Puerto Rican coast. Although the thermal video shows the aircraft's path for only four minutes, the radar data shows the aircraft's path prior to and after the thermal video was engaged. In the Google Map in Figure 3 the aircraft images in blue represent both the matching thermal and radar data while the aircraft images in red are only radar data. It is clear that before the thermal video was engaged (red colored planes), the aircraft circled to the north and northwest of the airport and then engaged the thermal video on its second pass of the airport (blue colored planes). This may indicate that the pilot was aware that an unknown target was in the area, searched for the unknown target, and upon finding it, engaged the thermal video system prior to resuming the aircraft's normal course down the coast. Data that will be discussed in the next section indicates that there was a potential reason for the pilot to suspect there was an unknown object in the area.

FIGURE 3: Radar only data of a law enforcement or military aircraft shown in red with Thermal Imaging & Radar data of the aircraft's location show in blue

3.0 Radar's Minimal Detection Elevation near Airport

It has been determined in conversations with the witnesses that the initial indication of an unknown object came from the Raphael Hernandez Control Tower. That means that at least at some point, the object had to be high enough such that the radar system used could resolve it as a target. Since not all agencies are required to answer FOIA (Freedom of Information Act) requests, this investigation could not determine which radar system made this determination. The only radar system in the area, other than a military radar system, that could have detected the target is Pico Del Este located at 3417 feet altitude and approximately 91.5 miles from the middle of the Raphael Hernandez airport and on the opposite (eastern) end of Puerto Rico. It is therefore important that the minimum detection height of the radar system be determined.

It is known that in standard conditions the vertical gradient of the index of refraction decreases with height. This tends to bend the beam down toward the Earth's surface. It is also

known that being a oblate spheroid, the Earth's surface tends to fall away from a horizontal line. Therefore a radar beam will tend to travel farther than normally thought; however, since the second effect is normally larger than the first, the beam will still slowly move away from the Earth's surface.

Further complicating this effect is beam divergence. This means the beam spreads as it moves away from its antenna and widens the envelope in which the beam is able to resolve targets. Since this spreading is a function of the design of the beam's antenna, this effect cannot be calculated without knowledge of the complete design plans of the system.

Although the exact beam envelope cannot be determined, given data of targets seen by the radar system, it is possible to make an approximation of the envelope. Figure 4 is a 2 hour plot of height verses range of all transponders up to 10,000 feet regardless of azimuth and time. The maximum height of 10,000 feet was chosen since it highlights the sloped area under review. This plot will help determine the minimum resolving height of the radar at the target's location. The red dashed line to the right in Figure 4 is the height based on distance from the radar. It was found to have a slope of ~114.34 ft/mile and an intercept of ~88.3 miles. The distance of the unknown targets to the northwest of the airport in Figure 4 vary from 94 to 104 miles from the radar at Pico Del Este. At those distances the radar's minimum detection altitude would vary from 652 feet to 1795 feet. A target directly over the airport (91.5 miles from the radar) would need a minimum altitude of 366 feet to be detected.

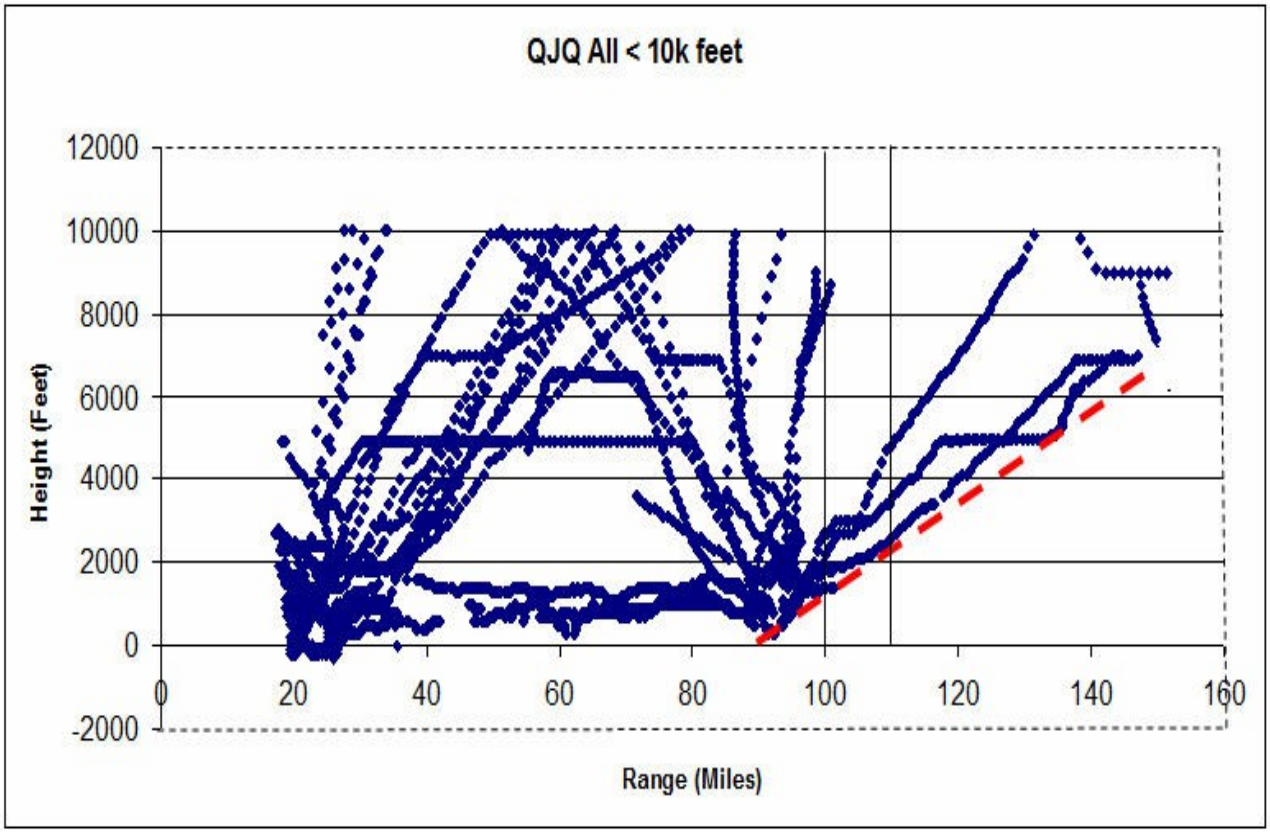

Figure 4: Minimal altitude detection level of the Pico Del Este radar system QJQ

4.0 Radar Analysis of Unknown Target in Area Prior to Aircraft Launch

The data from radar site QJQ was reviewed for any primary data without a transponder code that identified an unknown radar track in the area of interest. Primary radar tracks are those created by the actual reflection of the radar beam from a target. Known aircraft such as the law enforcement or military aircraft that took the thermal video will transmit a transponder code, also known as secondary radar. Primary radar tracks are identified with the designation "Sch" as shown in column 2 (Msg Type) of Table 2. As can be seen in that table, the radar picked up 50 primary radar tracks of what appears to be a single object from Zulu time 00:58hrs to 01:14hrs, a 16 minute period of time. The CBP aircraft departed the runway with instructions to look for an unknown to the northwest of the airport at 01:16hrs. These 50 radar tracks (the radar sweeps every twelve seconds) of this unknown object are visually displayed in Figure 5. The amount of information requires considerable commentary.

The first four radar strikes occurred after each twelve second sweep of the radar and can be seen at the far left area of Figure 5 and are designated as a, b, c, and d. The object is not picked up in the next four sweeps, which equates to 48 seconds. The fifth radar strike designated as 1a++++ (the four plus signs indicate that four previous radar sweeps were missed) indicates the unknown is at the same location as it was one minute earlier. That doesn't necessarily mean that the object is stationary because the accuracy of the radar is only to within 1/8 mile. A list of the radar target's longitude/latitude locations, speed and its direction of movement is shown in Table 3. Due to the potential 1/8 mile (660 feet) possible error in the primary radar, the speeds when the object is traveling less than 1200 feet could vary by almost 100% therefore the speeds shown in Table are not meant to be accurate. A statistical analysis of those speed numbers gives a mean of 168 mph with a standard deviation of 97 mph. The altitude of the object is not known but based on the minimum altitude in which the radar picked up the tracking aircraft, the object must be at 652 feet altitude or higher.

The sixth radar strike occurs immediately after the fifth radar strike, i.e. the next twelve second sweep of the radar. Beginning with this sweep of the radar, the object shows up on almost every sweep of the radar for the next ten minutes; however, if the sixth radar strike was created by the same object that created the first five then its speed is a minimum of 1700 mph. This calculation is not significantly affected by the radar error due to the large distance of 30,000 feet that was traveled. This perceived speed is unlikely so it is possible that the first six radar strikes are not related to the next large set of radar strikes identified as 1b thru 1aq. Symbols 1b through 1aq are in chronological order and represent the results of each subsequent 12 second radar sweep. Each plus sign following a symbol indicates that there was no strike on the previous radar sweep.

The group of radar strikes from 1b through 1aq cover 42 radar hits during 10 minutes. These radar hits occur with almost every sweep of the radar and they are all in the same general area.

Radar Site: QJQ 26 Apr 2013

Time	MsgType	Rng(nmi)	Az(deg)	Lat	Lon
00:58:16.909	Sch	85.25	280.811	18.31.48.965 N	067.13.32.938 W
00:58:28.874	Sch	85.375	280.635	18.31.34.812 N	067.13.43.643 W
00:58:40.902	Sch	85.875	280.371	18.31.16.718 N	067.14.19.057 W
00:58:52.899	Sch	85.625	280.459	18.31.21.911 N	067.14.02.078 W
00:59:52.882	Sch	85.625	280.459	18.31.21.911 N	067.14.02.078 W
01:00:04.941	Sch	81	281.25	18.31.39.674 N	067.09.01.791 W
01:00:16.922	Sch	81.125	281.338	18.31.48.439 N	067.09.08.066 W
01:00:40.900	Sch	81.25	281.777	18.32.26.646 N	067.09.08.238 W
01:00:52.866	Sch	81	281.426	18.31.54.354 N	067.08.58.828 W
01:01:04.909	Sch	81.25	280.986	18.31.20.395 N	067.09.21.664 W
01:01:16.875	Sch	81.125	281.602	18.32.10.482 N	067.09.03.561 W
01:01:28.871	Sch	81	281.514	18.32.01.690 N	067.08.57.329 W
01:01:40.837	Sch	81.25	281.338	18.31.49.862 N	067.09.15.816 W
01:01:52.880	Sch	81.375	281.162	18.31.36.533 N	067.09.26.518 W
01:02:04.970	Sch	81.375	281.426	18.31.58.658 N	067.09.22.072 W
01:02:16.842	Sch	81.5	281.074	18.31.30.543 N	067.09.35.733 W
01:02:28.855	Sch	81.125	281.162	18.31.33.732 N	067.09.11.009 W
01:02:40.883	Sch	81.125	281.162	18.31.33.732 N	067.09.11.009 W
01:02:52.910	Sch	81.25	281.162	18.31.35.133 N	067.09.18.764 W
01:03:04.954	Sch	81.5	280.898	18.31.15.756 N	067.09.38.618 W
01:03:16.997	Sch	80.875	281.074	18.31.23.597 N	067.08.56.951 W
01:03:29.103	Sch	82	281.074	18.31.36.098 N	067.10.06.759 W
01:03:41.178	Sch	81.625	280.898	18.31.17.122 N	067.09.46.379 W
01:03:53.159	Sch	81.5	281.338	18.31.52.708 N	067.09.31.316 W
01:04:05.203	Sch	82	280.986	18.31.28.660 N	067.10.08.216 W
01:04:17.231	Sch	81.625	281.074	18.31.31.932 N	067.09.43.489 W
01:04:29.243	Sch	81.375	281.162	18.31.36.533 N	067.09.26.518 W
01:04:53.361	Sch	81.625	280.986	18.31.24.528 N	067.09.44.940 W
01:05:05.405	Sch	81.625	280.635	18.30.54.891 N	067.09.50.624 W
01:05:29.507	Sch	82	280.811	18.31.13.778 N	067.10.11.095 W
01:05:41.504	Sch	82	280.635	18.30.58.887 N	067.10.13.925 W
01:05:53.485	Sch	81.875	280.635	18.30.57.555 N	067.10.06.158 W
01:06:05.529	Sch	82.125	280.283	18.30.30.367 N	067.10.27.217 W
01:06:17.541	Sch	82.125	281.162	18.31.44.934 N	067.10.13.044 W
01:06:29.678	Sch	82.125	280.635	18.31.00.219 N	067.10.21.692 W
01:06:41.737	Sch	82.125	280.283	18.30.30.367 N	067.10.27.217 W
01:06:53.656	Sch	82	280.898	18.31.21.220 N	067.10.09.661 W
01:07:05.668	Sch	82.125	280.459	18.30.45.297 N	067.10.24.478 W
01:07:17.696	Sch	82	280.635	18.30.58.887 N	067.10.13.925 W
01:07:29.708	Sch	82.375	280.547	18.30.55.399 N	067.10.38.629 W
01:07:41.705	Sch	81.75	280.811	18.31.11.069 N	067.09.55.569 W
01:08:17.835	Sch	82.5	280.898	18.31.26.683 N	067.10.40.705 W
01:08:41.766	Sch	82.75	280.371	18.30.44.320 N	067.11.04.719 W
01:09:05.838	Sch	82.5	280.283	18.30.34.225 N	067.10.50.542 W
01:09:53.762	Sch	83.125	280.107	18.30.25.533 N	067.11.32.140 W
01:10:29.643	Sch	82.625	278.086	18.27.27.119 N	067.11.28.651 W
01:10:41.780	Sch	83.375	280.02	18.30.20.472 N	067.11.49.044 W
01:12:53.743	Sch	83.5	280.02	18.30.21.723 N	067.11.56.826 W
01:13:53.836	Sch	83.75	279.844	18.30.08.979 N	067.12.15.055 W
01:14:17.923	Sch	84	279.844	18.30.11.435 N	067.12.30.625 W

TABLE 2: Raw radar data that shows targets northwest of the airport

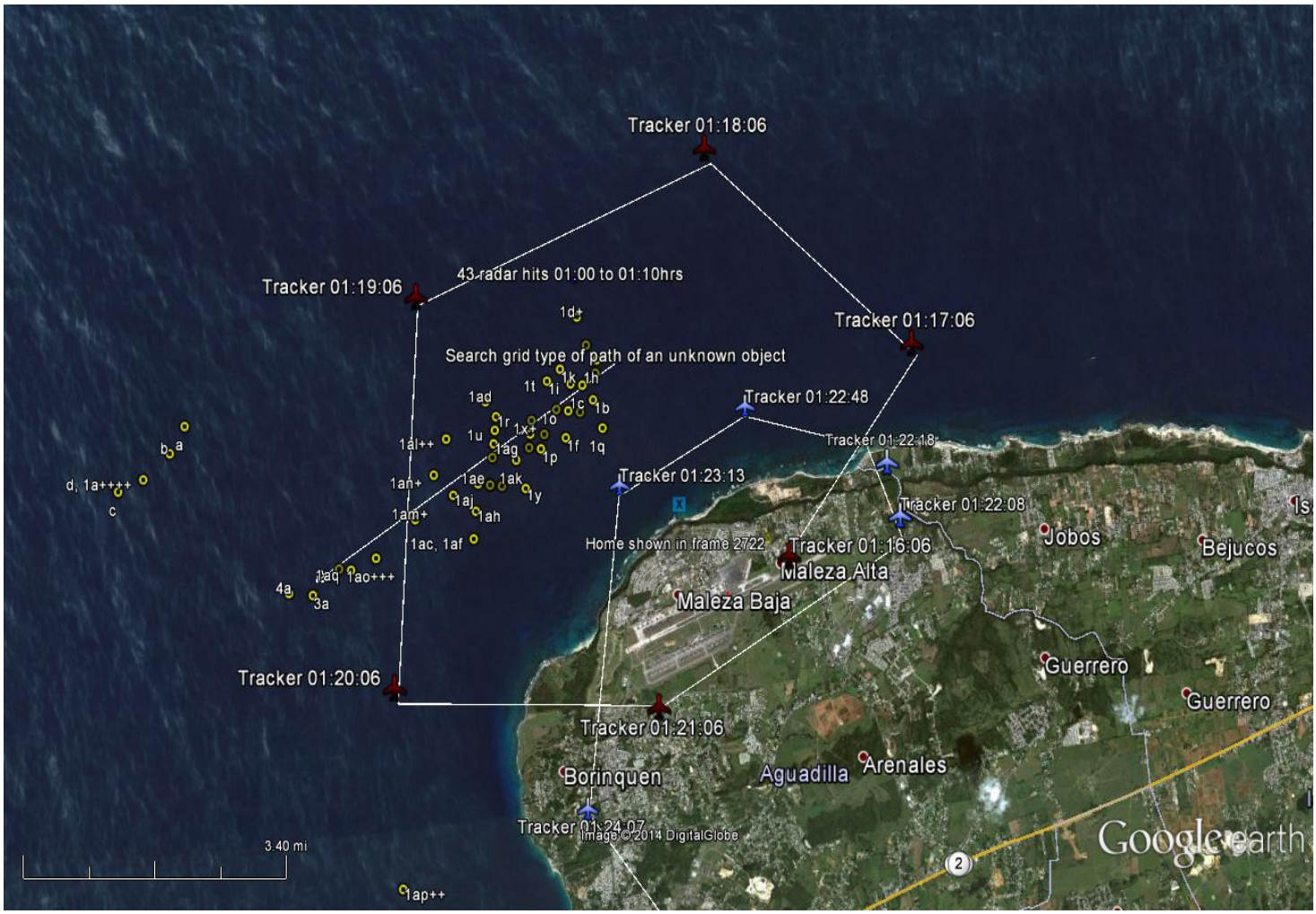

FIGURE 5: Radar plot of unknown that showed up off shore prior to the departure of the aircraft with thermal imaging capabilities. Tracks are designated in order of time beginning with a-d (segregated because of distance from the other radar tracks), followed by 1a-1aq, and followed by 2a, 3a, and 4a (segregated because of significant time delays of greater than one minute between radar tracks.

The radar sweeps every twelve seconds. Each "+" after a radar hit indicates that the target was not detected in the previous radar sweep. A designation such as "1ac,1af" indicates that two different radar sweeps occupied approximately the same physical location to within 1/8 of a mile of each other.

	Elapsed Time	GPS Points: Start Point		GPS Points: End Point		Points: Distance (ft)	Heading (Degrees)	Speed	Radar Skips
1	11.965 sec	From 18.530268	-67.225816	To 18.526337	-67.228790	1798.27	215.6	102.47	
2	12.028 sec	From 18.526337	-67.228790	To 18.521311	-67.238627	4029.98	241.7	228.44	
3	11.997 sec	From 18.521311	-67.238627	To 18.522753	-67.233911	1799.25	72.1	102.26	
4	59.983 sec	From 18.522753	-67.233911	To 18.522753	-67.233911	0.00	---	0.00	+++++
5	12.059 sec	From 18.522753	-67.233911	To 18.527687	-67.150498	30482.85	86.4	1723.51	
6	11.981 sec	From 18.527687	-67.150498	To 18.530122	-67.152241	1092.37	325.8	62.16	
7	23.978 sec	From 18.530122	-67.152241	To 18.540735	-67.152288	3871.82	359.8	110.10	++
8	11.966 sec	From 18.540735	-67.152288	To 18.531765	-67.149674	3408.47	164.6	194.21	
9	12.043 sec	From 18.531765	-67.149674	To 18.522332	-67.156018	4146.99	212.5	234.78	
10	11.966 sec	From 18.522332	-67.156018	To 18.536245	-67.150989	5397.00	18.9	307.52	
11	11.996 sec	From 18.536245	-67.150989	To 18.533803	-67.149258	1092.07	146.1	62.07	
12	11.966 sec	From 18.533803	-67.149258	To 18.530517	-67.154393	2224.02	236.0	126.72	
13	12.043 sec	From 18.530517	-67.154393	To 18.526815	-67.157366	1732.21	217.3	98.07	
14	12.090 sec	From 18.526815	-67.157366	To 18.532961	-67.156131	2286.90	10.8	128.97	
15	11.872 sec	From 18.532961	-67.156131	To 18.525151	-67.159926	3167.60	204.7	181.92	
16	12.013 sec	From 18.525151	-67.159926	To 18.526037	-67.153058	2526.17	82.3	143.38	
17	12.028 sec	From 18.526037	-67.153058	To 18.526037	-67.153058	0.00	---	0.00	
18	12.027 sec	From 18.526037	-67.153058	To 18.526426	-67.155212	798.58	280.8	45.27	
19	12.044 sec	From 18.526426	-67.155212	To 18.521043	-67.160727	2811.32	224.2	159.15	
20	12.043 sec	From 18.521043	-67.160727	To 18.523221	-67.149153	4296.45	78.8	243.24	
21	12.106 sec	From 18.523221	-67.149153	To 18.526694	-67.168544	7186.55	280.7	404.75	
22	12.075 sec	From 18.526694	-67.168544	To 18.521423	-67.162883	2821.86	134.5	159.34	
23	11.981 sec	From 18.521423	-67.162883	To 18.531308	-67.158699	3915.92	21.9	222.85	
24	12.044 sec	From 18.531308	-67.158699	To 18.524628	-67.168949	4463.28	235.5	252.67	
25	12.028 sec	From 18.524628	-67.168949	To 18.525537	-67.162080	2527.56	82.1	143.28	
26	12.012 sec	From 18.525537	-67.162080	To 18.526815	-67.157366	1781.84	74.0	101.14	
27	24.118 sec	From 18.526815	-67.157366	To 18.523480	-67.162483	2228.21	235.5	62.99	++
28	12.044 sec	From 18.523480	-67.162483	To 18.515248	-67.164062	3058.05	190.3	173.12	
29	24.102 sec	From 18.515248	-67.164062	To 18.520494	-67.169749	2822.50	314.2	79.85	++
30	11.997 sec	From 18.520494	-67.169749	To 18.516358	-67.170535	1536.02	190.2	87.30	
31	11.981 sec	From 18.516358	-67.170535	To 18.515988	-67.168377	798.56	100.3	45.44	
32	12.044 sec	From 18.515988	-67.168377	To 18.508435	-67.174227	3484.95	216.3	197.29	
33	12.012 sec	From 18.508435	-67.174227	To 18.529148	-67.170290	7691.67	10.2	436.59	
34	12.137 sec	From 18.529148	-67.170290	To 18.516728	-67.172692	4615.24	190.4	259.27	
35	12.059 sec	From 18.516728	-67.172692	To 18.508435	-67.174227	3076.48	190.0	173.94	
36	11.919 sec	From 18.508435	-67.174227	To 18.522561	-67.169350	5451.73	18.1	311.86	
37	12.012 sec	From 18.522561	-67.169350	To 18.512583	-67.173466	3937.82	201.4	223.52	
38	12.028 sec	From 18.512583	-67.173466	To 18.516358	-67.170535	1743.61	36.4	98.84	
39	12.012 sec	From 18.516358	-67.170535	To 18.515389	-67.177397	2528.22	261.5	143.51	
40	11.997 sec	From 18.515389	-67.177397	To 18.519741	-67.165436	4643.46	69.0	263.90	
41	36.130 sec	From 18.519741	-67.165436	To 18.524079	-67.177974	4839.82	290.0	91.33	+++
42	23.931 sec	From 18.524079	-67.177974	To 18.512311	-67.184644	4934.68	208.3	140.59	++
43	24.072 sec	From 18.512311	-67.184644	To 18.509507	-67.180706	1763.64	126.9	49.95	
44	47.924 sec	From 18.509507	-67.180706	To 18.507092	-67.192261	4306.39	257.6	61.27	++++
45	35.881 sec	From 18.507092	-67.192261	To 18.457533	-67.191292	18083.37	178.9	343.62	+++
46	12.137 sec	From 18.457533	-67.191292	To 18.505687	-67.196957	17688.18	353.6	993.67	

TABLE 3: Time, location, and direcitonal movement of targets northwest of the airport

The unknown target(s) seen on the QJQ radar were likely the same unknown target(s) that caused the control tower to request the CBP aircraft to look in the area to the northwest of the airport. Figure 5 shows that the CBP aircraft flew directly into the area where the unknowns were picked up on radar. It is reasonable to consider that the pinkish-reddish light seen to the northwest of the airport by the pilot may have been the cause of the unknown target seen on radar in the same area and that same object picked up by the CBP aircraft's thermal imaging video. If those objects were not related then it is a very unusual coincidence that an unknown object on video was in the same area as an unknown target on radar during a similar period of time.

The unknown target that was detected on radar for 16 minutes does not display characteristics that would be expected of an aircraft in flight. The speed variation and sudden changes in direction are nonsensical. Nonetheless, there are characteristics that can be attributed to the unknown target. First, this target's appearance on radar occurs at the right time and location to likely be the object detected by the control tower and the resulting subsequent alert to the CBP aircraft. Second, although the target jumps around, its overall directional movement is from the northeast to the southwest. Third, the target strength is strong as it is detected on almost every sweep of the radar for eight of the ten minutes it is on radar. Lastly, the target is no longer detected on radar during the time that the unknown is detected on the thermal imaging video. At that point in time the object is below the Pico Del Este radar's detectable altitude.

Conclusion

The authors of this report have examined other explanations for the unknown radar strikes to the northwest of the airport. A temperature inversion is a possible cause of false radar returns. These occur when the upper air temperature is higher than lower air temperature. This possibility was examined and discounted due to the lack of any temperature inversion layer in the area. A copy of the upper atmospheric conditions was obtained and is shown in Table 4. One of the strongest arguments against some type of anomalous propagation is the continuation of the radar returns within a small geographic area for ten minutes and with almost every 12 second sweep of the radar, the lack of these returns prior to this incident, and the lack of these returns after the incident of the unknown object recorded on thermal video at a lower altitude over land. It seems reasonable to consider the possibility that the control tower decision to vector an aircraft into the same area as this unknown radar return, the detection of these unknown radar returns on FAA radar data, the visual by the pilot of an unknown object with a red light, and the detection of the unknown object on the thermal video are all related to the same event and the same object. No other reasonable explanation has yet been found.

78526 TJSJ San Juan Observations at 00Z 26 Apr 2013

PRES hPa	HGHT m	TEMP C	DWPT C	RELH %	MIXR g/kg	DRCT deg	SKNT knot	THTA K	THTE K	THTV K
1015.0	3	25.8	20.8	74	15.49	55	4	297.7	342.8	300.4
1000.0	137	25.0	20.5	76	15.43	60	12	298.1	343.2	300.9
980.9	305	23.4	20.2	82	15.41	60	12	298.1	343.1	300.9
947.3	610	20.4	19.6	95	15.38	65	16	298.1	342.9	300.9
943.0	649	20.0	19.5	97	15.38	64	15	298.1	342.9	300.9
925.0	816	19.2	17.5	90	13.79	60	13	298.9	339.3	301.4
914.5	914	18.6	16.5	88	13.11	60	13	299.3	337.8	301.6
898.0	1071	17.6	15.0	85	12.08	60	11	299.8	335.4	302.0
882.6	1219	16.5	13.7	84	11.31	60	9	300.2	333.6	302.2
881.0	1234	16.4	13.6	84	11.23	59	9	300.2	333.4	302.2
876.0	1283	15.6	14.3	92	11.83	56	8	299.9	334.7	302.0
865.0	1390	15.8	9.8	68	8.86	49	7	301.2	327.6	302.8
858.0	1459	16.2	9.2	63	8.58	45	7	302.3	328.1	303.9
853.0	1509	15.8	11.4	75	10.02	42	6	302.4	332.3	304.2
850.0	1539	15.6	11.0	74	9.79	40	6	302.5	331.8	304.3
845.0	1589	15.2	11.5	79	10.18	38	6	302.6	333.0	304.4
832.0	1721	14.2	8.2	67	8.26	34	7	302.9	327.8	304.4
827.0	1772	13.6	11.2	85	10.20	32	7	302.7	333.3	304.6
823.0	1812	13.2	11.4	89	10.39	31	7	302.7	333.8	304.6
821.4	1829	13.2	10.8	85	10.02	30	7	302.9	332.9	304.8
809.0	1957	13.4	6.4	63	7.50	5	7	304.4	327.3	305.8
792.1	2134	12.1	6.8	70	7.91	330	7	304.9	329.0	306.4
783.0	2232	11.4	7.1	75	8.14	324	7	305.1	329.9	306.6
770.0	2372	11.4	3.4	58	6.38	314	7	306.6	326.4	307.8
763.9	2438	10.8	3.7	62	6.57	310	7	306.6	326.9	307.8
757.0	2514	10.0	4.0	66	6.78	316	8	306.6	327.5	307.9
752.0	2569	9.8	1.8	57	5.83	321	9	307.0	325.1	308.0
744.0	2658	9.2	3.2	66	6.52	328	10	307.2	327.4	308.4
740.0	2702	9.2	-0.8	50	4.90	332	10	307.7	323.1	308.6
736.4	2743	9.0	0.0	53	5.23	335	11	307.9	324.3	308.9
733.0	2781	8.8	0.8	57	5.56	334	11	308.1	325.5	309.1
721.0	2918	8.4	-7.6	31	3.01	331	10	309.1	318.9	309.7
700.0	3161	6.4	-8.6	33	2.87	325	9	309.5	318.9	310.1
696.0	3208	6.0	-10.0	31	2.58	327	9	309.6	318.1	310.1
683.0	3362	6.2	-16.8	17	1.51	333	10	311.5	316.6	311.8
674.0	3471	5.4	-11.6	28	2.35	337	11	311.8	319.6	312.2
670.0	3519	5.8	-20.2	13	1.15	339	11	312.8	316.8	313.0
658.7	3658	6.2	-30.4	5	0.47	345	12	314.7	316.5	314.8
653.0	3729	6.4	-35.6	3	0.28	344	13	315.8	316.8	315.8
641.0	3881	5.6	-37.4	3	0.24	343	14	316.5	317.4	316.6
610.8	4267	2.3	-37.9	3	0.24	340	18	317.1	318.0	317.1
566.0	4877	-2.9	-38.6	4	0.24	325	17	317.9	318.9	318.0
550.0	5106	-4.9	-38.9	5	0.24	310	16	318.2	319.1	318.3
544.7	5182	-5.1	-41.2	4	0.19	305	16	318.9	319.6	318.9
528.0	5426	-5.7	-48.7	2	0.09	321	22	321.0	321.4	321.0
523.9	5486	-6.1	-48.2	2	0.09	325	24	321.2	321.6	321.2
500.0	5850	-8.5	-45.5	3	0.13	315	28	322.6	323.1	322.6
484.3	6096	-10.5	-45.0	4	0.14	305	32	323.1	323.7	323.1
475.0	6245	-11.7	-44.7	5	0.15	303	35	323.4	324.0	323.4
465.4	6401	-12.3	-46.0	4	0.13	300	39	324.6	325.1	324.6
462.0	6458	-12.5	-46.5	4	0.13	300	39	325.0	325.5	325.0
435.0	6914	-16.7	-45.7	6	0.15	304	37	325.3	325.9	325.3
410.0	7357	-18.9	-54.9	3	0.05	308	35	328.0	328.2	328.0
400.0	7540	-20.3	-55.3	3	0.05	310	34	328.5	328.8	328.5
395.6	7620	-20.9	-55.0	3	0.06	310	34	328.8	329.0	328.8
363.9	8230	-25.4	-52.9	6	0.08	285	37	330.6	331.0	330.7
353.0	8453	-27.1	-52.1	7	0.09	289	36	331.3	331.7	331.3
320.0	9144	-33.2	-52.2	13	0.10	300	32	332.2	332.6	332.2
300.0	9600	-37.3	-52.3	19	0.10	285	34	332.7	333.1	332.7
284.0	9975	-40.7	-54.7	21	0.08	281	33	333.1	333.4	333.1
280.5	10058	-41.3	-55.0	21	0.08	280	33	333.3	333.6	333.3
256.1	10668	-46.1	-57.5	26	0.06	275	44	335.1	335.4	335.1
252.0	10777	-46.9	-57.9	27	0.06	278	48	335.4	335.7	335.4
250.0	10830	-47.1	-58.1	27	0.06	280	50	335.9	336.2	335.9

245.0	10964	-46.9	-65.9	10	0.02	281	53	338.1	338.3	338.2
239.0	11128	-47.3	-71.3	5	0.01	283	56	339.9	340.0	340.0
233.6	11278	-48.0	-71.6	5	0.01	285	59	341.1	341.1	341.1
200.0	12290	-52.9	-73.9	6	0.01	290	64	348.8	348.9	348.8
197.0	12388	-53.3	-74.3	6	0.01	291	65	349.7	349.8	349.7
187.0	12725	-52.7	-78.7	3	0.00	295	68	355.9	355.9	355.9
186.0	12759	-52.9	-78.9	3	0.00	295	68	356.2	356.2	356.2
184.8	12802	-53.0	-79.2	3	0.00	295	68	356.6	356.6	356.6
169.0	13376	-55.5	-82.5	2	0.00	297	59	361.7	361.7	361.7
157.0	13844	-58.3	-83.3	3	0.00	299	51	364.6	364.7	364.6
150.0	14130	-60.7	-84.7	3	0.00	300	46	365.3	365.3	365.3
124.8	15240	-69.2	-87.6	5	0.00	280	28	369.7	369.7	369.7
118.7	15545	-71.5	-88.4	7	0.00	255	35	370.8	370.8	370.8
115.0	15733	-72.9	-88.9	7	0.00	263	37	371.5	371.5	371.5
114.0	15785	-72.5	-88.5	7	0.00	265	38	373.2	373.2	373.2
107.0	16155	-74.1	-90.1	7	0.00	280	43	376.9	376.9	376.9
100.0	16550	-72.9	-88.9	7	0.00	300	30	386.6	386.6	386.6
86.8	17374	-75.7	-91.7	7	0.00	340	9	397.1	397.1	397.1
82.3	17678	-76.7	-92.7	6	0.00	335	14	401.0	401.0	401.0
80.6	17801	-77.1	-93.1	6	0.00	7	13	402.6	402.6	402.6
79.0	17916	-75.9	-91.9	7	0.00	37	12	407.4	407.4	407.4
75.0	18216	-76.5	-92.5	7	0.00	116	9	412.2	412.2	412.2
74.1	18288	-77.1	-92.9	7	0.00	135	8	412.4	412.4	412.4
71.5	18489	-78.9	-93.9	7	0.00	185	7	412.8	412.8	412.8
70.0	18610	-77.9	-92.9	8	0.00	245	6	417.4	417.4	417.4
65.4	19002	-73.9	-89.9	7	0.00	165	3	434.3	434.3	434.3
63.2	19202	-73.5	-90.1	6	0.00	125	2	439.6	439.6	439.6

TABLE 4: Upper Air Wind Conditions; San Juan, PR.

Univ of Wyoming, Dept of Atmospheric Sciences.

APPENDIX G

Object Location, Speed, Size

Introduction

The object in this video was tracked using a state of the art Wescam MX-15D multi-sensor multi-spectral targeting system. The MX-15D is mounted on the underbelly of a DHC8 turbo prop aircraft operated by U.S. Customs and Border Patrol. This system has high definition thermal imaging, short range IR for enhanced haze penetration, a laser rangefinder and illuminator, and stabilization features. The video lasted for about three minutes and due to familiar objects in the background, we were able to identify the approximate size, speed, and path of travel of the object. The camera's video output included the latitude/longitude coordinates, azimuth heading, and the altitude above sea level of the tracking aircraft. It also provided the latitude/longitude of any object within the crosshairs of the camera, the altitude above sea level, and the distance in nautical miles of any object in the crosshairs of the camera. Due to the capabilities of this particular camera its sale outside of the United States requires approval from the U.S. Government.

The video consists of 3 minutes and 54 seconds of video imagery of which 2 minutes and 56 seconds displays an unknown object arriving from over the ocean, transversing land, and then disappearing back into the ocean. The entire video was broken into individual frames for analysis of the unknown object. There were a total of 7027 frames with each frame equating to 1/30 of a second exposure. Breaking the video into individual frames allowed for detailed evaluations of the object's characteristics.

Specific information will be provided as to how the size, speed, and location of this object were determined. The basic determinations hinge on the trigonometry related to the actual object size, angular size, and distance of the object. If two of those variables are known then the third variable can be calculated using trigonometry.

1.0 Angular size of pixels in the video frame

The angular size of an object represents the angle subtended by an object in the sky. This is measured in degrees, arcminutes, and/or arcseconds. As an example, the angular size of the moon is approximately 0.5 degrees or 30 arcminutes or 1800 arcseconds.

The angular size of any object in the camera frame can be calculated using the number of pixels that comprise the object's apparent length. The pixel size is constant for the camera as long as the magnification is constant. Changes in magnification in the camera result in linearly proportional changes to the size of the pixels.

In order to determine the angular size of a pixel, frame 892 was used. (See Figure 1.) This frame displays a tank of known size. The tank is 108 feet in diameter based on satellite photos from Google Earth. The ground distance between the tank and the camera is calculated using the latitude and longitude of the tank and of the aircraft. The aircraft's location in this frame is 18º 31' 21” N and 67º 06' 42” W, while the tank is located at 18º 29' 02” N and 67º 08' 29” W. Using the haversine formula, the distance between the two points is calculated as 17,441 feet. The air to ground distance from the camera to the tank can be calculated since it is represented by the hypotenuse of a right triangle. The aircraft's altitude

is 1760 feet so the actual distance between the camera and the tank is 17,530 feet. Now that we have the size of the tank and its distance, we can calculate the tank's angular size based on the trigonometric properties of a right triangle. The tangent of the angle (angular size) is equal to the opposite side the angle (width or diameter of the tank) divided by the adjacent size (distance to the tank). Solving tan θ = 108 / 17441 gives an angle of 0.35299º. Image processing software developed at the National Institute of Health and known as ImageJ was used to analyze the image and calculate the diameter of the tank in pixels. The diameter of the tank was equal to 238 pixels. The angular size represented by each pixel is therefore equal to 0.35299 / 238 or .001483 degrees.

The angular size of the unknown object in the videos will vary with distance. But with the value of .001483º, we can determine the the object's angular size in any video frame, even if the zoom factor (focal length) changes since the pixel size will be proportional to the zoom factor.

Figure 1: Frame 0892. Known tank and unknown object.

2.0 Size of the object

As one watches the video at regular speed the object appears to tumble and if one watches carefully, it even appears to change shape. Viewing of the object frame by frame makes it much easier to see the sometimes rapid changes in shape and apparent size. Any change in apparent size of the object will add an error into the calculation of the object's distance when using a known angular size and a hopefully constant actual object size. Later in this appendix, an error factor will be used in calculating the object's actual locations during the video.

The size of the object can be determined when its distance is known. The angular size of the object is known based on the discussion in Section 1.0. The distance can be accurately calculated whenever the object is at very low altitude. This occurs towards the end of the video when the object passes behind a telephone pole, behind trees, and then finally enters the water. During these periods of time the crosshairs of the camera, via its laser range finder, are providing an accurate distance measurement because the object is at a very low altitude and there is no longer any error due to the crosshairs actually focusing on an object that is potentially far from the camera. For example, in the right triangle shown in Figure 2 the camera is at point 'C.' The crosshairs of the camera are pointing towards 'A'. Any object in the crosshairs (represented by point 'D') of the camera could be at any location along line 'AC'. However, when foreground objects such as trees or a telephone pole or the water surface itself interact with point 'D' then one knows that point 'D' is close enough to point 'A' (point 'A' is on the ground) to allow for a reasonably accurate determination of the distance from the object to the camera.

Figure 2: Right triangle

An example of the calculation will be discussed utilizing Table 1, which reflects information from Frame 5085 in Figure 3. In this frame the object is just above the water as three seconds previous to this frame the object was in the water. The distance to the object using the system's laser range finder is 5.2 nautical miles, which equates to 31,595 feet. This value is accurate to within 304 feet because the distance in nautical miles on the screen is rounded to the nearest .1 nautical miles. The use of the latitude/longitude coordinates that the thermal imager displays for the object and for the aircraft provides a distance that is accurate to

within 70 feet of the object's location and probably much closer. Using the haversine formula, the distance between the locations of the aircraft and the object is 31,469 feet. The object's angular size in video frame 5085 consists of six pixels, which at .000149° per pixel as described in Section 1.0. is an angular size of .00894°. With a known distance and a known angular size, the actual size of the object can be calculated. As described in Section 1.0, the tangent of the angle (angular size) is equal to the opposite side the angle (length of the unknown object) divided by the adjacent size (distance to the unknown object). In this frame, the calculated size of the object is 4.9 feet.

Time	1 24 57
Aircraft location	18:25:43N 67:07:45W
Aircraft altitude	3522'-645'=2877'
Cross hair's location	18:30:51N 67:08:08W
Object's location	18:30:51N 67:08:08W
Object's altitude	just above the water
FLIR distance	31595 feet
Object azimuth	356 degrees
Object's angular size	.00894 based on frames 5081-5089; 6 pixels
Gnd dist to cross hairs	31469'
Aircraft dist to cross hairs	31600'
Object's size	4.9 feet
Object's dist traveled	434 feet
Time since last frame	6.03 seconds
Object's speed	49mph
Aircraft dist traveled	1989 feet
Aircraft speed	225mph

Table 1: Information and calculations from Frame 5085

Figure 3: Frame 5085. Object in cross-hairs and just above the water.

Calculations of the object's size were done on multiple frames whenever the object was a known distance from the ground which allowed accurate values of the object's distance and its angular size. These values varied significantly from a minimum size of 3.0 feet to a maximum size of 5.2 feet. The variation in size is believed to be due to either varied angular sides of the object as it is tumbling or temperature variations that are reflected in the shape that the object presents to the IR camera. Calculations done on known objects in the video such as water tanks, aircraft, cows, and moving automobiles eliminate issues with the accuracy of the IR camera as a significant source of the variations in size. We can conclusively say that this object is between 3.0 feet to 5.2 feet in length.

3.0 Path of the object during the video

The path taken by this object during the video cannot be ascertained simply by plotting the latitude/longitude coordinates that are displayed by the thermal imager based on the cross-hairs. Those coordinates are driven by a laser range finder, which is not necessarily striking the object itself but the ground and other large objects in the background. As a result, when the object is at altitudes above about 40 feet there can be significant differences in the actual distance between the object and the camera. This was ascertained by careful observation of the latitude/longitude values displayed on the thermal video as the object moved and

sometimes the cross-hairs in the thermal video were stationary, which resulted in latitude/longitude values linked to the cross-hairs and not the object itself. It was clear that the latitude/longitude measurements correlated to the farthest ground-based location that was at the center of the cross-hairs. Referring back to Figure 2, the line AC represents the distance as measured by the thermal imaging system while line DC represents the true distance between the object and the camera.

The actual distance between the camera and the object can be determined using the angular size of the object and the object's true size. The one exception is when the thermal video system was at minimal magnification and the object consisted of only a 3-4 pixels in size. The errors in the calculated distance values using angular size were gross and did not match up with the quality of the system's information obtained at medium and high magnification. The exact cause of this error is not yet known but is suspected to be related to minimal pixel displays of object's in the infrared. Another method to determine the object's actual distance is with a known altitude of the object. Whenever the object is near the ground or passing between known objects then the actual distance can also be determined using the object's known altitude and the azimuth of the object relative to the camera and aircraft. This method is the most accurate because any errors in the object's size and angular size are eliminated.

The best determination that could be made of the object's actual path is shown by the brighter of the three light blue lines in Figure 4 of this appendix. This figure is a Google Earth image of the northwest coast of Puerto Rico. The airport that is seen in the image is the Raphael Hernandez Airport. It is a joint civil-military airport located in Aguadilla, Puerto Rico. This is the airport that is seen in the video. The top of the page faces west and the right hand side of the page faces north. The dark blue aircraft icons are the actual location of the aircraft with the camera as verified by both the thermal video system's latitude/longitude values and locations as supplied by radar from the Pico Del Este radar site. The numbers next to the aircraft represent the time in Zulu (aka Greenwich Mean Time) hours. A corresponding UFO (UFO represents the unidentified flying object and is not meant to indicate any other quality about the unknown craft.) location is on the map for the same time. The UFO locations marked in red are exact locations of the object at those times due to accurate altitude values being available. The UFO locations marked in orange represent approximate locations of the object to within about 500 feet. The UFO locations marked in yellow with a time value next to them and the darker light blue line connecting them represent a “best guess” of the object's location based on the previous path of the object and its known direction from the aircraft. This blue line ends at a question mark that represents that uncertainity and also is a possible point of origin of the object. The object's route does raise the question of the possibility that its origin could be the same as its final destination or its origin could be up to one mile farther to the west as is shown in the other two light blue lines. Those lines connect UFO locations that are also possible routes taken that are more westernly. The higher level of uncertainity in the yellow colored UFOs is believed to be due to the thermal video system being in operation at its lower magnification level.

The object's path is one that approaches the island of Aguadilla from the ocean. Its exact origin is unknown. It crosses the airport runway once it comes over land and then re-crosses the airport runway on its way back out to sea.

4.0 Speed of the Object

What is the energy source that propels the object in this video? The movements made by this object require some type of power source. The object transverses about four miles during the video and during that process changes direction from a southward direction to a northerly direction. No type of propulsion is evident from the infrared video yet some form of propulsion is required for the object to maintain and vary its speed, change directions multiple times, and move in and out of the water. The source that propels this object is not evident.

The speed of the object is most accurately determined during the latter half of the video when the object's location can be more accurately determined as discussed in Section 3.0. The calculation of the object's speed is straightforward as distance/time. The time between measurements is provided by the thermal video system's clock and the location of the object and its distance traveled is determined by the latitude/longitude locations provided by the video system. The speed of the object was measured every eight seconds. The main error is that the latitude/longitude values are in degrees, minutes, and seconds so that the location is rounded to the nearest second, therefore the accuracy is to within 0.5 seconds (maximum rounding error) of a degree. With eight seconds between speed measurements, the error due to rounding could equate to 51 feet from the object's true location which could result in an error in the object's speed of up to 4 mph.

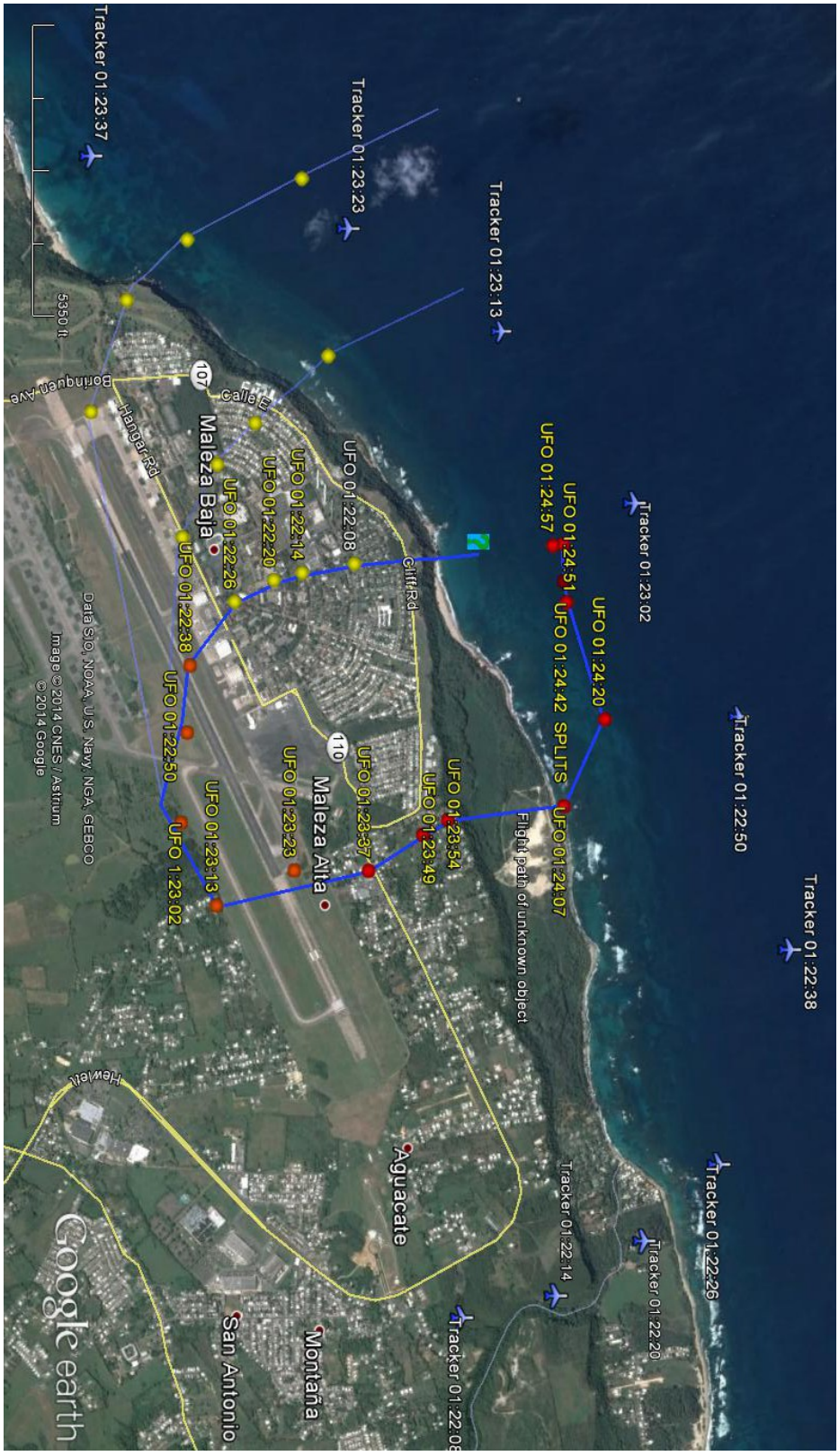

Figure 4: Possible Paths taken by Object

Table 2 shows the time of the latitude/longitude measurement, the distance traveled since the last measurement, and the calculated speed of the object. Although the speed of the object is fairly constant and normally varies from 70 mph to 110 mph, it is clear that the object slows and speeds up during this portion of the video, which again indicates some type of power source should be present. Some of the speeds shown in the table are noted as being through water.

ZULU TIME	DISTANCE TRAVELED	SPEED
01:23:21	.3753 km	105 mph
01:23:29	.3448 km	96 mph
01:23:37	.2735 km	76 mph
01:23:45	.2459 km	69 mph
01:23:53	.2623 km	73 mph
01:24:09	.3211 km	90 mph
01:24:17	.3409 km	95 mph *
01:24:25	.3179 km	89 mph*
01:24:33	.3072 km	86 mph*
01:24:45	.2141 km	60 mph**
01:24:53	.1784 km	50 mph**
01:25:01	.2459 km	69 mph

* Speed under water.

**Speed through water and air.

APPENDIX H

Modeling of Object

Introduction

The amount of data provided in the IR video this study is predicated upon is extensive. In most situations that is a desirable feature; however, when faced with a complete unknown it tends to hide aspects that may have been obvious if there was less data. Combining data by bundling multiple items into one is a feature provided by modeling. The data reduction obtained generating the model permits a more efficient utilization of the data and allows some aspects of the object to become obvious. Additionally, the thought that goes into determining a model tends to highlight aspects not otherwise noted. All aspects determined will be listed in the conclusion of the appendix.

Although it is philosophically possible to define a subjective[1] reality where anything dreamt of by the observer is equally real, scientists define existence as objective. Objective reality defines reality as that which does not require the participation of the observer. Effectively that means that science is the end result of observation and measurement.

In essence this appendix is attempting to define an object conforming to what is seen in the video while also obeying the laws of Physics; therefore, taking the physical world as real, the appendix is also asking if the object is real. One of the characteristics of a real "object" is its mass or more accurately its "invariant mass"[2]. As was stated in Appendix H, shape can be defined as the characteristic surface configuration of the invariant mass. Therefore a defined mass also implies an invariant shape. The difficulty in determining these objectives in the video supplied is, it does not show mass; it shows heat.

Another problem encountered when looking at unknown objects in an IR video is the difficulty in "seeing" all shades of the hot and cold areas of the object and in differentiating them from the background. The images provided are what is termed 8-bit grayscale. Grayscale indicates that the images are provided in various shades of gray. An 8 bit depth indicates that each pixel will have one value out of 256 (2^8) possible shades (intensities) of gray. More will be said about this later in this document. Although the shades are difficult to distinguish using only the eyes, the computer has no problem distinguishing them. That differentiation is provided by the "Surface Plot" function in the "ImageJ" program. That function will be used extensively in this document.

Various views of the object will be considered in the document. The most obvious way to see both hot and cold areas of the object is to look at the object in front of something else that was also warm but not hotter than the hot portions of the object. In that case an outline of the cold portions could be seen as a white shadow over the background heat while also seeing an outline of the hot portions. In a sense this is similar to seeing a shadow of the object, al la Lamont Cranston when he is in his Shadow identity. It is also possible to infer portions of an outline from its effect on its environment. Different views will be presented in an attempt to obtain clues to its shape.

It should be noted that the best this appendix can provide is a model of the object. It will be a model that fits the aspects seen; but it is a model and not the object. As such, it can only have validity in the subspace of reality that is described by the aspects used to create it. Expanding the model beyond that subspace would be highly speculative and wasteful of time and energy.

1.0 Reality of the Object

The first step in defining the shape of the object in the video is to determine if it is a real object or is it just some odd juxtaposition of heat rays. That is accomplished by determining if it has mass. Since the

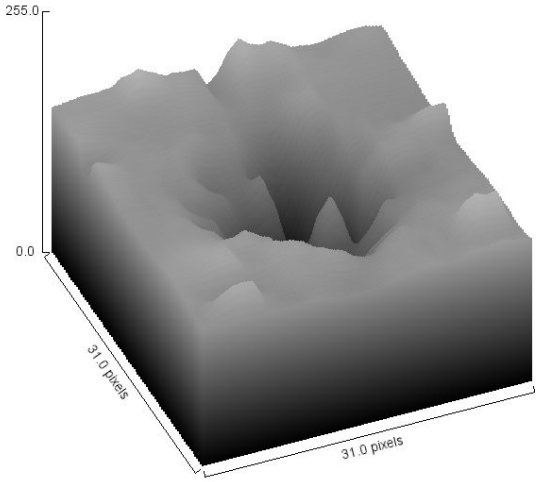

Figure 1 - 1: Frame 3769 - Surface Plot

object in the video can't be weighed to determine its mass, a less direct indication has to be used. Happily one such indication was described in Section 2 of the "Water Transit Appendix J". In that document it was shown that in Frame #3769 a splash can be observed when the object enters the water. That splash is the effect of an external mass displacing some of the water mass. It was also noted in that section that the video does not show a normal (to us rephrase?) picture of the world. It is IR and shows a heat picture. Therefore a determination had to be made as to what a splash would look like in terms of heat rather than mass. A splash is taking a volume of water and drastically increasing its surface area. Since both evaporative and radiative heat transfer are proportional to the volumes surface area, a splash provides a means to allow that volume of water to become a "little" cooler. Little is in quotes because the change is very small and is basically invisible to the viewers eyes but not to the FLIR system and to the computer.

The "Surface Plot" tool in "ImageJ" provides a three-dimensional view of the intensities of pixels. It therefore converts the heat variations in the IR frame to height variations with (in its default operation) the lighter (cooler) pixels being represented as hills and the darker pixels as valleys. Figure 1 - 1 is the surface plot of a small area around the object in Frame #3769. The cooler areas representing the splash are seen as raised areas around the upper right corner of the plot. Although only an indirect indication, this figure indicates the object in the video has mass and is therefore a real object with some constant characteristic shape or surface configuration seen from various angles in various frames. It is also known that the shape may not be possible to infer from the views seen in the video.

2.1 Initial View

Although not seen often in the video, in this view the object is seen to present itself in front of a building window in an oblong or slightly triangular shape in Frame #2616. This is shown in Figure 2.1 - 1. It is agreed that this figure is not particularly sharp but the general two dimensional shape can be seen. A red circle was placed around the object to outline its location.

A better view of the object can be seen in the Surface Plot view in Figure 2.1 - 2. It shows a much more detailed picture of this view of the object. In the IR pictures the object in both of the frames seems to be moving to the left with the hot area leading the colder area. In the surface plots it can be seen that although there is a hot area in lower right, there seems to be a cooler area behind it. Additionally, in terms of heat, the trailing cold area shows an almost cone shape getting cooler as it goes back but with circular warmer waves around the cone. There also looks like there may be a hot area above the cone to the front. Although the "cone" shape is interesting, there are two items that must not be forgotten: this is heat not mass; and this is only one view of the object.

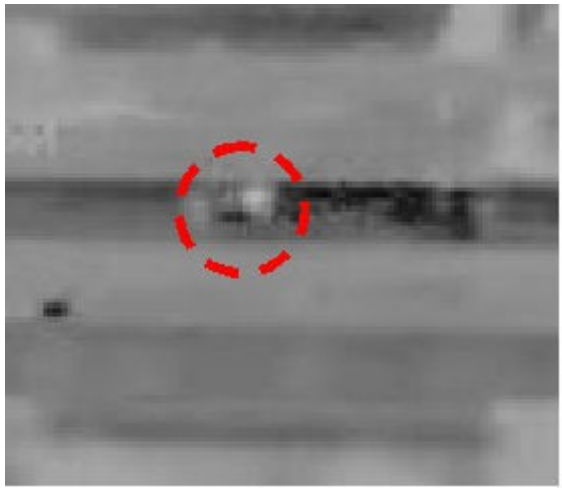

Figure 2.1 - 1: Frame 2616

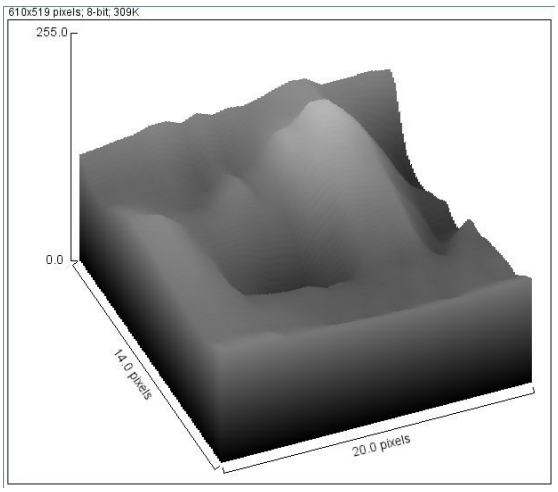

Figure 2.1 - 2: Frame 2616

There is an additional item of interest seen in Figure 2.1 - 2 that will have to be checked in later views. There does not seem to be any heat being transferred from the unknown object to the air surrounding it. That indicates a lack of turbulence surrounding and trailing the unknown object. It almost looks like the object is slipping through the air with minimal friction.

2.2 Second View

The most common view presented in the video is something that looks spherical. Frame #1240 was chosen to represent this shape. It and the corresponding surface plot can be seen in Figures 2.2 - 1 and 2.2 - 2. It should be noted the Figure 2.2 - 1 has been magnified to ~600% over the camera's basic magnification. Although this picture is a still, the hot (black) and (white) portions of the object can be clearly seen. As stated the figure shows a roughly

spherical shape surrounded by a colder spherical portion. Additionally, the object seems to have – spokes of heat radiating out from the center to the outer edge of the colder section. Although the object is unknown, when seen from this angle it almost looks like it is banking in a turn. A quick look a the surrounding frames shows the object seems to be moving to the left. It also should be noted that what looks like a dark outline around the object is an artifact resulting from the magnification and the video compression. Although it took a long time for this author to notice it, there is also a definite similarity between Figures 2.2 - 2 and 2.1 - 2. Basically Figure 2.2 - 2 is the inverse of Figure 2.1 - 2. This is easily seen in Figure 2.2 - 3 where the elevations of light and dark areas have been reversed.

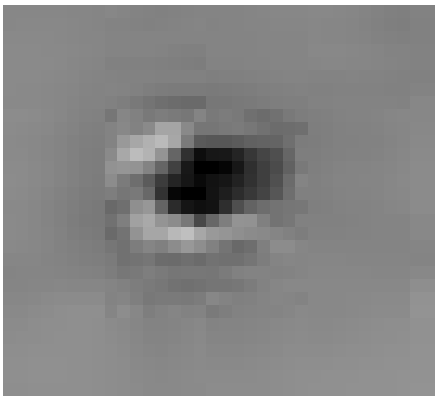

Figure 2.2 - 1: Frame #1240

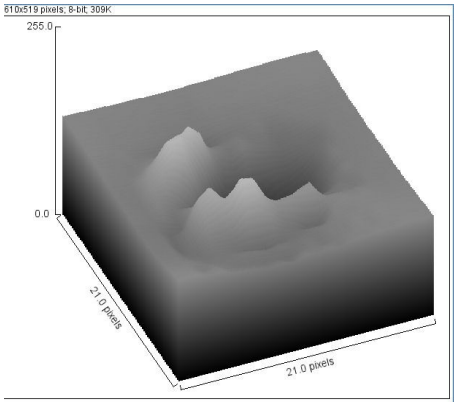

Figure 2.2 - 2: Frame #1240 Surface Plot

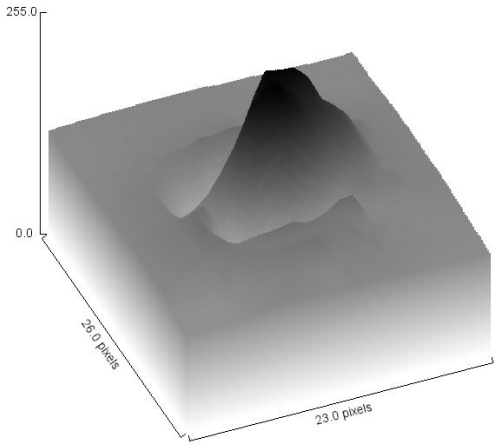

Figure 2.2 - 3: Frame #1240 Reversed Surface Plot

As in the previous section, there doesn't seem to be any heat being transferred to the air surrounding and trailing the object.

2.3 Third View

The third view to consider is one which is totally black. This can be an effect of a longer distance between the object and the camera or of the object itself. Frame #1194 is an example where the blackness of the object is not due to distance. It is observed in Figures 2.3 - 1 and 2.3 - 2. This view shows an almost dumbbell shaped object with very little (if any) cool

areas. The subject view also shows basically nothing outside of the black area. Unless there is a portion of the object that has almost exactly the same heat signature as the background, the shape shown is the outline of the object at this angle. Interestingly the object seems to be moving directly to the left and not in the direction of either its long or short axes. Also again no heat seems to be transferred from the object to the surrounding air.

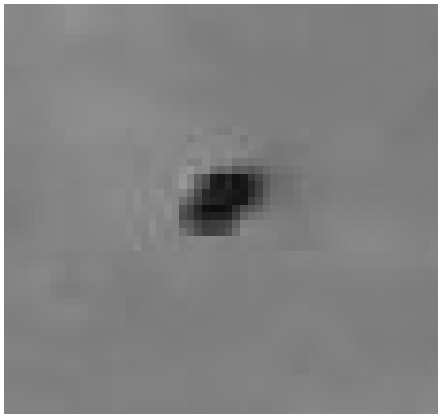

Figure 2.3 - 1: Frame #1194

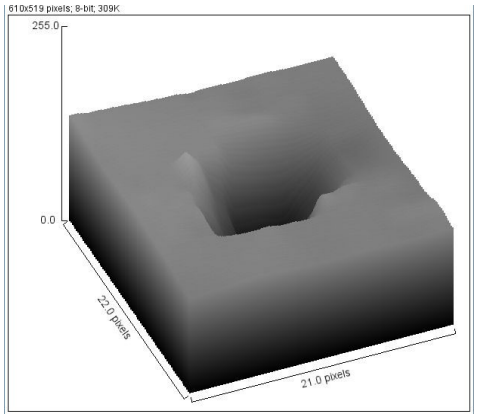

Figure 2.3 - 2: Frame #1195 Surface Plot

2.4 Possible Shape

Although not yet complete, it is possible to use the views in 2.1 through 2.3 as a start to determine a shape for the unknown object. Since it is hard to draw in three dimensions Figure 2.4 - 1 has been provided as a two dimensional view of the side of the object. The number at the base of the figure labels the location along the side in degrees. Additionally the label "Black" indicates a warmer area and the label "White" a cooler area. It is easily see that if one looks at the half labeled 0 - 180 degrees, the object will appear to be black in the middle with white at the bottom and going up the sides. Similarly, if one is provided with the half labeled 90 - 270, the object will appear as white in the middle with black across the top and going down the sides. Those 2 views therefore invert the object and reverse the colors. It should be noted that the size of the undulating curve is only meant as illustrative.

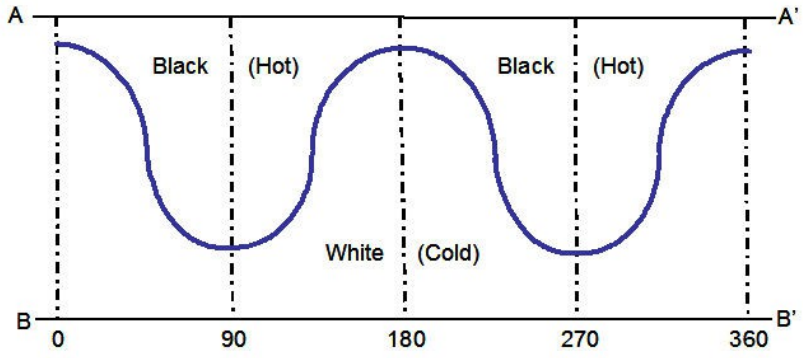

Figure 2.4 - 1: Expanded View of the Object Side

To obtain the object seen in Figures 2.1 - 2 and 2.2 - 2, requires shrinking line B-0, B-360 to almost a point and attaching the resulting sheet to the long side of an ovoid (acorn shape).

The result is illustrated in Figure 2.4 - 2. In this figure the dotted lines are only included to show the 3 dimensional nature of the object. Although this shape is indicative of some of the object's aspects, it is certainly not complete. At best this is a gross model of a completely unknown object.

Aside from the angles seen in many frames (particularly in Figure 2.3 - 1), the object shown in Figure 2.4 - 2 easily replicates the temperature outlines seen in Sections 2.1, 2.2 and 2.3. As indicated above, observed at an angle from the right replicates the temperature outline of Frame #1240. Rotate it a quarter turn around the B axis and it replicates the temperature outline of Frame #2616. Finally seen from the left it would replicate the temperature outline seen in Frame #1195. At this point the above is all that this model was created to do. The fact that it duplicates the temperature outlines is not sufficient to consider it the model desired in this appendix.

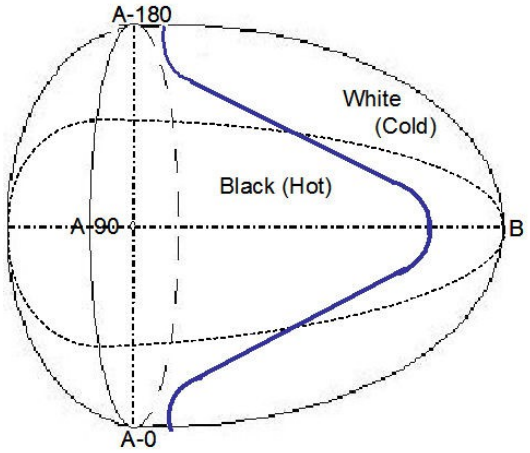

Figure 2.4 - 2: Ovoid

As many undergraduates have discovered, any attempt to fit a continuum to a finite number of points is very dangerous. That is basically due to the fact the mathematically there are an infinite number of solutions to any continuum when only discreet points are known. It also does not matter how many discreet points are used to fit the solution to. There always remain an infinite number of other solutions. Mathematicians call these problems, "ill-posed." Fortunately a Russian mathematician named Andrey Tikhonov provided a regularization procedure[3] that gave a iterative process for obtaining a particular solution. The fact that this appendix provides a pictorial model rather than writing an equation for it, does not eliminate the ill-posed nature of the problem. Unfortunately it does however eliminate the possibility of utilizing the above iteration procedure. Additionally there is no equivalent pictorial analog. The only available process is to demand that all transitions from solution to solution be accomplished by a continuous rotation of the object. Although that seems easy it necessitates a viewing consistency which due to reticule and background interference, is not completely provided in the video.

The lack of a viewing consistency is somewhat mitigated by the frame rate per second (approximately 29 - 33 fps) of the camera. That means each frame is approximately 30 m-sec in length. Although it is not known if the viewing angle of the object is changing due to a rotation of the object or the varying relative locations of the object and the camera, there seem to be long periods where the object presents views very similar to that seen in Frame #1240. Therefore the rotational speed is either intermittent, very close to zero, or

synchronous with the frame rate. The problem with accepting the coincidence of synchronicity is that there are areas where this view is seen to change quickly and the other views do not seem to have the same unchanging long stretches. It is therefore believed that the change is due to varying sighting angles possibly combined with transitory rotations of the object. This will be checked later in this section.

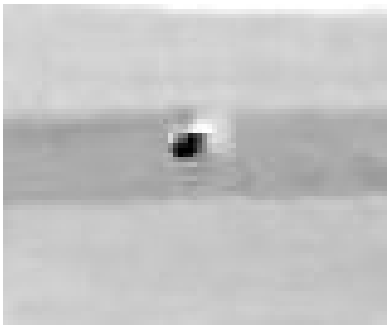

Figure 2.4 - 3: Frame #0775: Cropped & Lightened

Although Frame #2616 provides what is probably the best view seen of this angle of the object, it is not useful in looking for transitions to and from it. In this frame the object is viewed in front of a building window. The background in and around this frame is rapidly changing, making it very difficult to determine which effects are due to the object and which are due to the background. To solve this problem it was determined that Frame #0775 (Figure 2.4 - 3) is basically the same view as #2616 but with a more constant background

Looking backward in time from Frame #0775, Frame #0760 represents a time approximately 450 m-sec prior to that of Frame #0775. A cropped version of that frame is shown in the following Figure (2.4 - 4). Along with it, Figure 2.4 - 5 is a surface plot of the same view. As can be seen this view shows an object which is entirely black or hot. (This is similar to Frame #1194.) Therefore in 450 m-sec the object has transformed from one of the basic forms to another. Although not shown here there is no intervening frame that shows anything other than a continuous transformation.

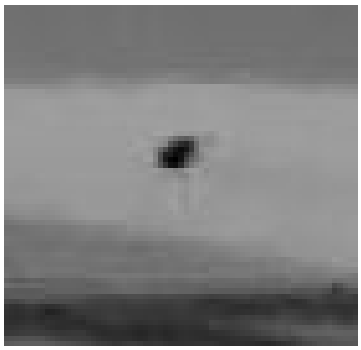

Figure 2.4 - 4: Frame #0760

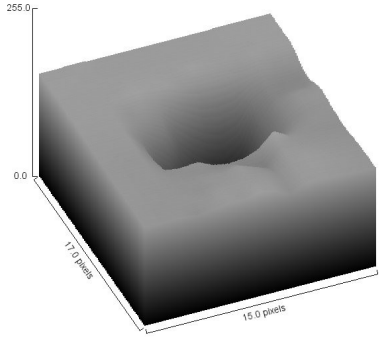

Figure 2.4 - 5: Surface Plot - 0760

Looking forward approximately 1 second from the time represented by Frame #0775 to Frame #0810 shows a second conversion to a view similar to that seen in Frame #1240. This

shows that the object seemed to rotate between the 3 basic views in approximately 1.5 seconds.

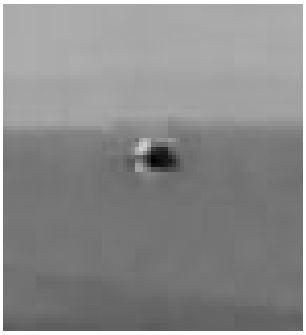

Figure 2.4 - 6: Frame #0810

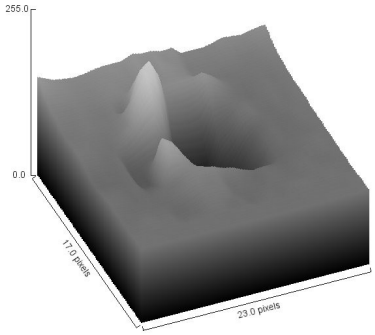

Figure 2.4 - 7: Surface Plot - #0810

Although it was determined above that that a rapid synchronous rotation cannot be occurring, that did not eliminate rotations entirely. It was left open that it is possible that in addition to varying sighting angles at least some of the changes could be attributed to slow and/or transitory rotations. Figure 2.4 - 8 has been provided to check the possible effect of sighting angles as the source of the above viewing changes. It shows the transformations discussed above in terms of the locations of the aircraft containing the camera and the target the camera is aimed at for Frames; #0810, #0775, and #0760. The lines connecting the targets and aircraft have been provided to show the approximate viewing angles for each frame. Although it is known the object is not located at the target location in any of these frames, it is believed the targets provide a reasonable approximation for checks such as this. It is easily observed that in this case the viewing change cannot be a attributed to variation of viewing angle. This therefore proves that the object does rotate.

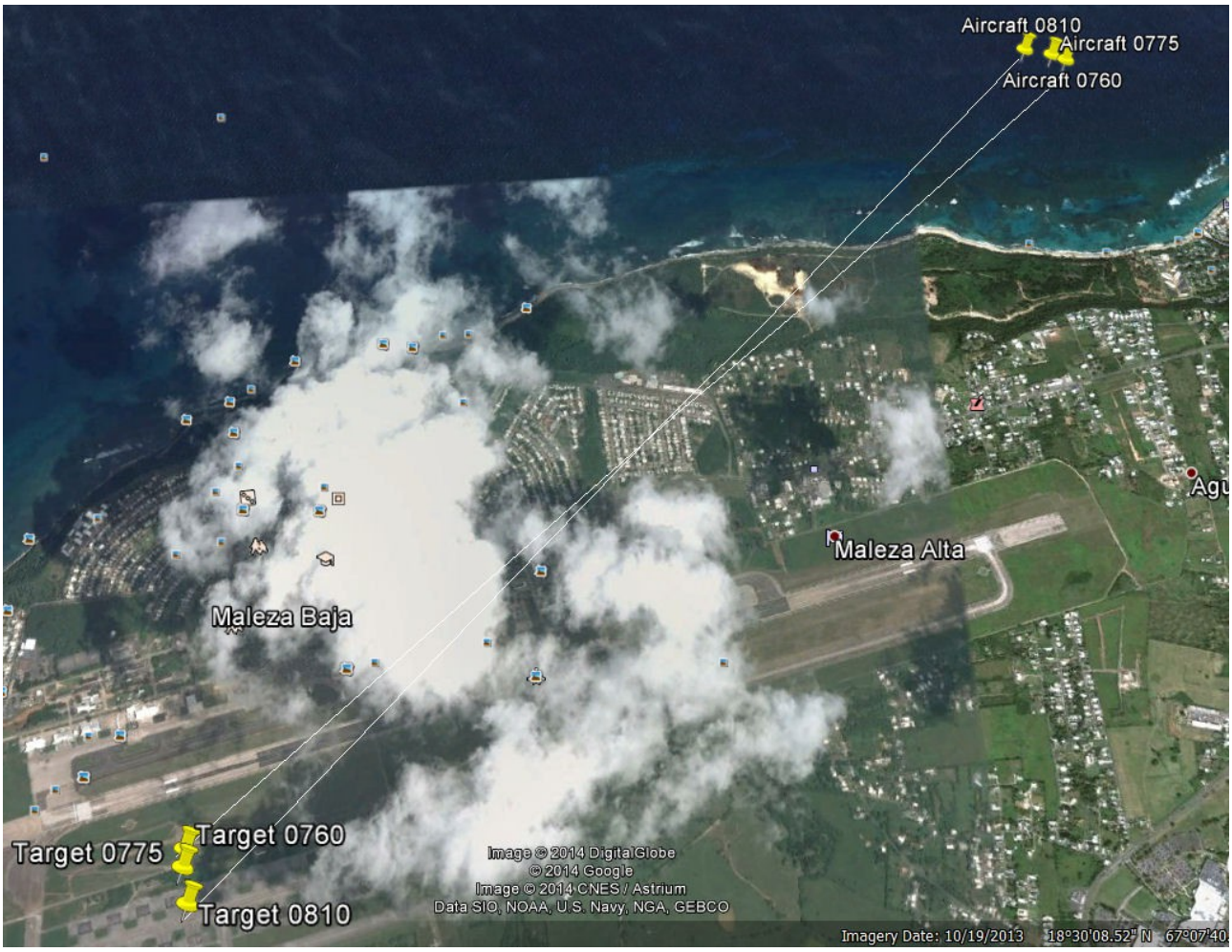

Figure 2.4 - 8: Relative locations of Aircraft and Target

2.5 Object Angularity

The problem with the shape discussed in Section 2.4 is that it assumes a completely smooth object. Since the video is entirely IR, that isn't a particularly surprising assumption. As has been emphasized, in IR one sees heat, not mass. Seeing an angle in an IR object does not necessarily indicate the object has an angle in that location. It indicates the heat source has an angle. In Section 2.4 a reference was made to angles seen in Figure 2.4 - 2 (the totally hot view of the object). It is seen in that figure that the hot area looks sort of like two offset overlapping squares. Even if there were no proof countering the assumption of a smooth object, it has to be questioned

There are, however, a few locations in this video where angularity can be seen directly. They are the times the object enters or exits the water. Concentrating on this entry period, each frame that shows that entry effectively provides a horizontal slice of the object. If the camera were looking directly downward, each of those slices would show the outline of the portion of the object which is located at the water level. However, since it is known than in all frames the aircraft is a distance off to the side of the object being viewed the camera never is looking

straight down at the object. It is aimed at an acute angle off of the horizon. Because of this, even the frames entering or leaving the water can only show an outline of the side of the object closest to the camera.

2.5.1 Entering the Water

Although Frame #3769 was used to illustrate the splash generated when the object entered the water, the last frame that didn't show any indication of a splash at all was #3758. Figure 2.5.1 - 1 is a cropped portion of that frame showing the object magnified to 400% over the camera's basic magnification. As can be seen, this view is similar to that seen in Figure 2.3 - 2. The object is almost all hot (black) and it shows a similar angularity. It remains to be seen if the angularity is real or an effect of the extreme magnification.

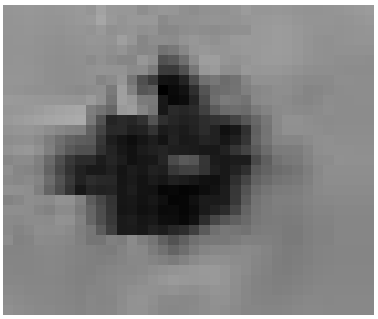

Figure 2.5.1 - 1: Frame #3758 Cropped and Magnified

Figure 2.5.1 - 2 provides a composite of Frames #3762 - #3768. It has been provided in an attempt to answer the above question. As previously stated, only the side closest to the camera in these plots should be considered as indicative of the object's shape. The back portion is heat from that portion of the object still above water. In these plots, the front of the object is found in the lower left corner and the back in the upper right. Since although the object may not be round, it has to be assumed that only the lower half of the left side can be seen directly. Additionally, in order to see the totally hot (black) area of the assumed ovoid, it has to be entering the water at an angle. In this case, the lower left should be entering the water first. Since the frame labels can be considered as labeling time the figure shows an object initially hitting the water in #3760 and sinking into the water as the numbers go up.

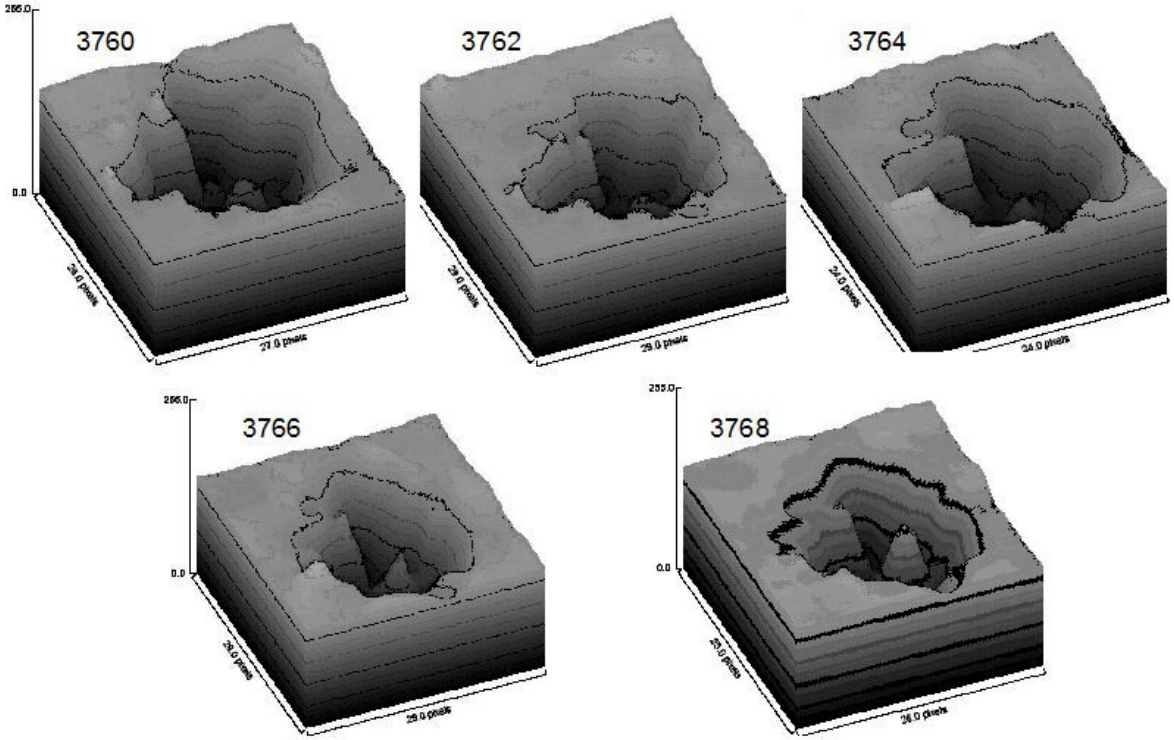

Figure 2.5.1 - 2: Surface Plots - Object Entering the Water

It is initially seen in #3760 that the lower left shows a sort of stair-step shape. Thus the angularity discussed above is the actual shape of the object and not an artifact of the magnification. Although there is no way to prove the following assertion, it will be assumed that the object is symmetric and that the stair-step shape also occurs in the back. It should not be forgotten that this is an assumption.

The second hint about the shape of the object is seen when looking at how the stair-step shape changes as the surface plots move forward. As time moves forward and the object sinks into the water, the edge moves in toward the middle and steps become less distinct. Basically this is exactly what would be expected if the general shape of this portion of the object was a dome.

Since the section of each frame shown in the surface plots was chosen by eye, the area covered by the plots is not constant. Due to this the writer checked the sizes by magnifying each object 4000x over the base magnification of the frames and counted the black pixels running along the center line. The result was that for each increase by 2 in the frame number there was a corresponding decease by 1 to 2 pixels in the pixel count.

2.5.2 Traveling through and Exiting the Water

There is a partial exit from the water in Frame #3912. There is very little information that can be obtained during this period. In addition to emerging under the frame reticle, due to molecular vibrational and rotational excitations, electromagnetic (EM) radiation is strongly attenuated by water. Although it is well known that visible light can penetrate water, the same is not true for the longer wavelengths in the EM spectrum. The attenuation of

electromagnetic radiation in water[4] for the longer wavelength portion of the IR spectrum is seen in log-log graph in Figure 2.5.2 - 1. Since the wavelengths used by FLIR lie in the ranges 3 - 5 and 8 - 12 micro-meters, it is easily seen that for any frequency in those ranges, the absorption coefficient is over 100 cm^{-1}. (A similar graph[5] specifically for seawater can be found in the Notes section of this paper.)

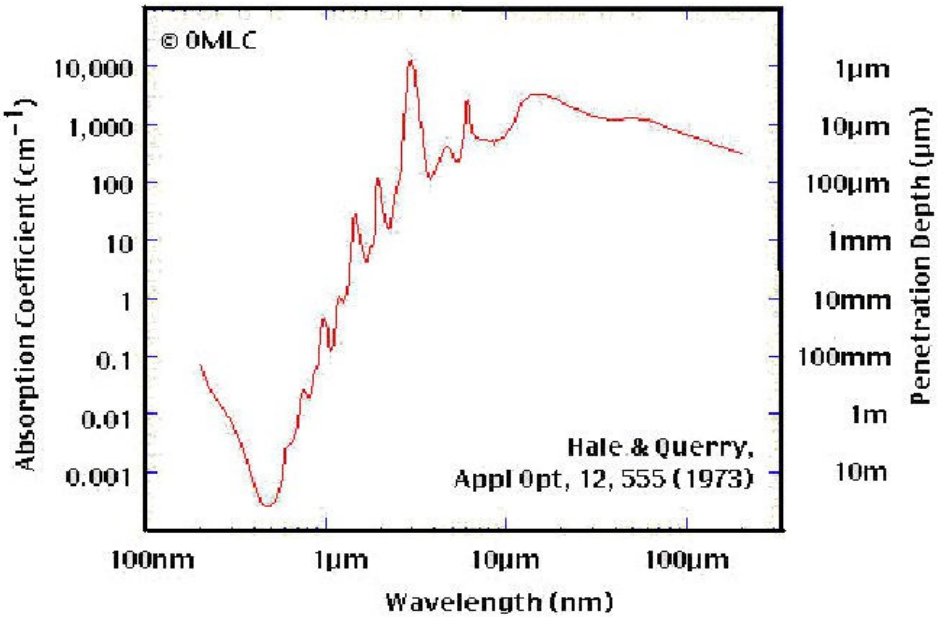

Figure 2.5.2 - 1

The usefulness of the absorption coefficient is seen in calculation the intensity[6] of the transmitted EM wave in water.

$$I(x) = I_0 e^{-\alpha x},$$

Where "x" is a distance in cm in the water, "α" is the absorption coefficient (assumed constant over the range), and I_0 is the initial intensity. With a coefficient of 100, the intensity drops by over 44 orders of magnitude in 1 cm and over 5 orders of magnitude in 1 mm). Essentially this means these frequencies do not penetrate water.

Although in essence, this means that a layer of at most a mm around the object will absorb virtually all of the IR generated, it doesn't answer the question of how it will affect what is seen in an IR video. Since the object is pumping heat into the surrounding water, it would seem reasonable to expect to see a sort of heat shadow of the object above the object and trailing it. Due to the depth of the top of the object while underwater and its speed that is not observed to occur. The speed obviously spreads out the heat but it is believed the depth is the larger reason. If the depth of the object were less than the wave size (peak to trough), it would break the surface as it moved and become visible as the water moved away from it. Therefore its minimum depth must be greater than the wave size.

While the object is underwater, there is additionally a competing thermal effect which can be seen in the video evidence as motion but not in the individual frames. It is a slightly cooler area which seems to remain over the object while it is underwater. It is believed by the writer that this is what is termed a Bernoulli Hump. It is basically a slight bulge in the surface due

to displaced water caused by the objects size and speed. The surface disturbance from a Bernoulli Hump is approximately given by[7]:

$$Y = W(d, v, h) \bullet S$$

where "W" is a scaling function and "S" is a shape function. In these equations: "d" is the objects diameter; "v" is the objects speed; and "h" is the objects depth. The shape function is a function of front to back location along the object and for this appendix will be assumed to have a value[8] of 0.8. The equation[7] for the scaling function is:

$$W = d^2 v^2/(8 g h^2) ,$$

where g is the acceleration due to gravity. Therefore the Bernoulli Hump increases with speed and cross sectional size and decreases with depth. Using a speed[9] of 82.812 mph and a diameter of 3 ft., the following graph for the surface disturbance (Y) was obtained.

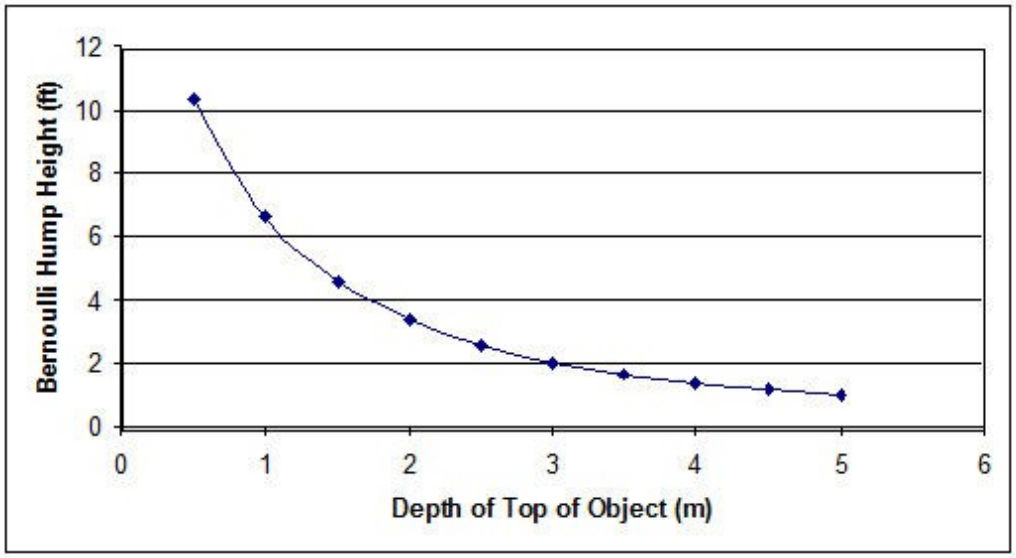

Figure 2.5.2 - 2: Bernoulli Hump Height as a function of Object Depth

The above figure shows that the Bernoulli Hump decreases with the depth of the object. Since we are assuming it is the expansion of the surface due to this bump in the water that is causing the decrease in temperature that we see in the video, the temperature change due to the surface expansion also decreases with the depth of the object. Additionally as has been said before, the temperature change is not visible in any single frame but its consistently coordinated movement is easily followed in the video evidence.

As per Weather Underground (www.weatherunderground.com), the average wave height (crest to trough) just off of the northern coast of Puerto Rico is 1-3 feet. Since it is possible to see some of the waves in the both the video and in single frames, the difference between the waves and the Bernoulli Hump provides a way to estimate the depth of the object. Specifically it indicates that the Bernoulli Hump height is less than 1-3 feet in height. Thus from Figure 2.5.2 - 2 for a height of <2 feet, the objects maximum depth is between 3 and 5 meters.

2.5.3 Second Entry

This water entry occurs after the initial object has divided into two objects. Figure 2.5.2 - 1 is a surface plot of Frame #4677 of the two objects prior to the water entry. The object on top is the one that will begin to enter the water 2 frames later. As indicated in this figure, the existence of the cooler (white) areas show that these objects bear a closer resemblance to a long end of the ovoide shown in Figure 3.4 - 2 than to the end view that was indicated in Section 2.5.1. Since the viewing angle is different this section may provide additional clues as to the objects shape.

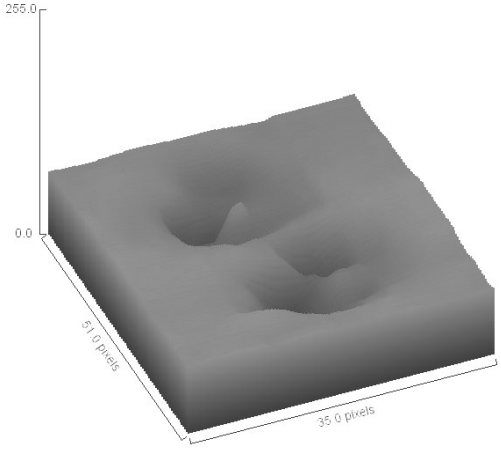

. **Figure 2.5.2 - 1: Surface Plot - Frame #4677**

As in Section 2.5.1, Figure 2.5.2 - 2 provides a composite of Frames 3762 - 3768. It has been provided in an attempt to answer the above question. As previously stated, only the side closest to the camera in these plots should be considered as indicative of shape information.

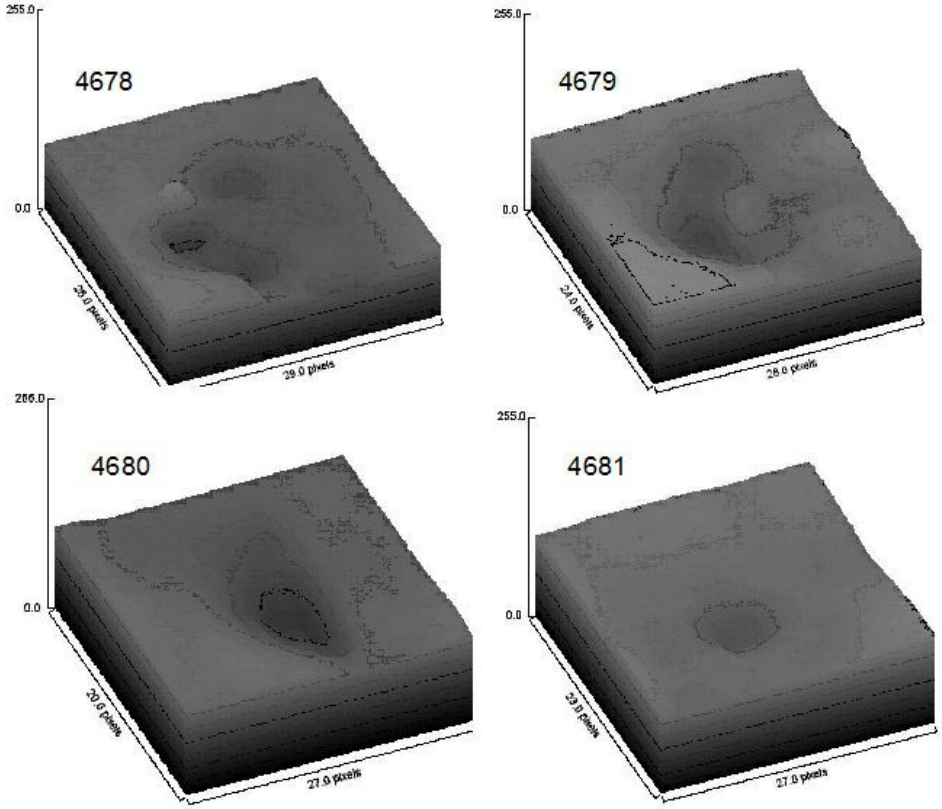

.

Figure 2.5.2 - 2: Surface Plots - Object Entering Water Second Time

The difference between this and that observed in Section 2.5.1 is easy to see. The most obvious difference is at this point there are 2 objects. Their shape is smooth with none of the angularity seen previously and they seems to be thinner in one of their lateral dimensions. Finally the last portion entering the water is offset from the middle. The sum of these statements seems to indicate that at this angle the objects looks very much like the side or end of the long side of the ovoid chosen in Section 3.4 but showing differing lateral dimensions.

2.6 Final Shape

It has been shown that the ovoid shape discussed in Section 2.4 was relatively close to what has been determined. The changes that occurred started at the increased temperature end of the object. Seen end-on (Figure 2.3 - 1) the object seems to be angular and have unequal lateral dimensions. The angularity was shown to be a result of the object's shape and not an artifact of the magnification in Section 3.5.1. The unequal lateral dimensions was then shown to carry through the entire ovoid in Section 3.5.3.

There is however a conundrum in what has been found. Seen from one side the shape or shadow of the object is an oval. At least when entering the water, the other side of the object is angular. Obviously these two sides cannot be along the same dimension. They also cannot be directly along either of the lateral directions the would be seen when the cooler or white sections are observed. This only leaves an angle including both the long axis and one of the lateral dimensions. From that angle, the angularity can be observed on one side with the far

side being smooth. This, of course, means the assumption near the end of Section 3.5.1 that the angularity would be symmetric is incorrect. It also means that when seeing the angularity, one is also seeing a small section of the right hand side (long portion) and that when seen directly from the left hand side, the object would be an oval. This is shown in Figure 2.6 - 1.

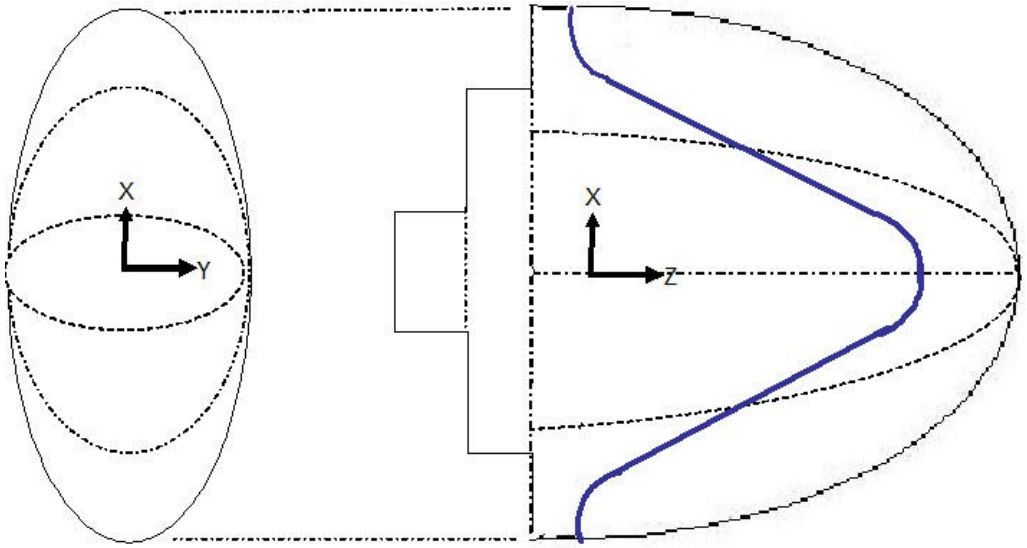

Figure 2.6 - 1

In this figure the back portion (possibly aside from the exact center) is black or warmer. The right hand image is being viewed in the negative y direction. The left hand image is being viewed in the positive z direction. A view at a 45 degree angle between the y axis and the positive z axis would angular on one side and round on the other.

3.0 Heat Transfer

It is obvious from the model that most of the object is hot or warmer then it's surroundings. That should raise the question of whether there is any heat being transferred to the surrounding air. Heat transfer essentially occurs via two different mechanisms; radiation and conduction. Normally a third mechanism, convection, is also stated. It however is just conductive heat transfer between two objects with a relative velocity between them.

In its simplest form convective heat transfer for a system where the wall temperature does not change is governed by Newton's law of cooling[10].

$$dQ/dt = H\ A\ \circlearrowright T\ .$$

In this equation: "Q" is the thermal energy transferred from the unknown object to the air; "H" is the heat transfer coefficient[11] (assumed independent of both temperatures); "A" is the unknown object heated surface area; and "↻T" is the difference in temperature between the unknown object and the surrounding air. Although this equation is easy to apply, we do not know the surface temperature of the unknown object or even its area, thus limiting the equation's usefulness.

In the present situation, since the fluid (the air) is forced to flow over the surface by the movement of the unknown object, the heat transfer is what is termed forced convection. The central concept used in forced convection is that of a boundary layer[12]. Any flow bounded by

a surface will develop a region adjacent to the surface, in which the flow properties are different from that seen an infinite distance from the surface. The primary cause of the boundary layer is friction.

The boundary layer is an important concept because it is the region in which heat transfer between the fluid (gas) and the surface takes place. It is known that the boundary layer will include both velocity and thermal layers. Since we have no knowledge of the surface conditions of the unknown object, this appendix will concentrate on its thermal properties. In a thermal layer, the temperature varies from a temperature T_o at the wall to the equilibrium temperature T_∞ at the outside edge of the layer.

The simplest type of convection is that which takes place in a laminar flow. Laminar flow is easy to predict and has very little fluctuation in it. Most situations begin as laminar flows and then later transition to turbulent flows. Laminar flow develops an insulating blanket around the object and restricts heat transfer. Conversely, due to the agitation factor, turbulent flow develops no insulating blanket and heat is transferred very rapidly. Also due to the same factor, turbulent flow is less structured and predictable than laminar flow. Structures called eddies dominate the flow. Since the driving force for heat transfer is the difference in temperature between the fluid and heat source, moving that fluid away from the source and replacing it with cooler fluid will carry off more heat. Turbulent flow therefore tends to carry off more heat than laminar flow.

It is noted in Appendix J that no wake was seen for the unknown object while it was traveling underwater. As in that appendix this lack of a wake was attributed to the unknown object being able to maintain laminar flow around it during that period. The effect being looked at in air is similar but not quite the same. In water turbulent flow produces pressure and shear waves that are termed wakes. Since the video in question is IR, those waves would have been seen as slight differences in heat. Neither they nor any convective heat transfer were seen during the water transit. While still looking for difference in heat when traveling in the air, the lower density eliminates the possibility that waves in the air could themselves produce heat that could be seen. Therefore the only heat to look for in air would be a trail following the unknown object and quickly dissipating into the bulk air temperature.

Since neither the unknown object surface composition nor the temperature are known, it is not possible to know if the air flow around it is laminar or turbulent. It is however known that due to expected conduction from the unknown object surface to the surrounding air molecules the air should carry off some heat and that heat should be noticeable in surface plots. Interestingly none is seen in any surface plots looked at. The reader is invited to inspect Figures 2.1 - 2, 2.2 - 2 and 3, and 2.3 - 2 in this appendix. It is therefore assumed that, although surprising, the air flow is probably laminar and that the temperature of the unknown object warmer areas is probably not exceptionally high. Thus any heat being carried away would dissipate so quickly as to not be noticeable in these plots. To check this, the writer used the "Transform Image to Results" function in Image J. The result of this function is a spreadsheet of the pixel values. Figure 3.0 - 1 is small portion of that spread sheet for Frame #0760.

154	155	156	156	157	152	154	156	157	156	157	158
156	158	160	160	160	165	163	161	159	158	158	157
159	160	159	155	152	153	146	139	141	148	152	150
156	154	149	141	134	109	100	94	105	126	140	140
153	150	139	122	88	62	37	33	51	115	134	141
153	136	102	77	52	31	18	31	53	105	131	151
157	128	68	33	13	6	11	47	76	108	134	161
161	135	74	35	12	4	20	70	104	113	131	150
148	125	79	45	16	13	31	79	119	124	144	158
155	158	152	150	134	137	137	149	168	153	155	150
147	145	140	145	138	134	129	126	148	144	148	142
155	152	143	152	152	155	149	137	160	156	154	140

Figure 3.0 - 1: Heat Trail - Frame #0760

In this figure heat is denoted by lower numbers. It shows the unknown object traveling to the right and the pink area is basically the outline of the unknown object. It should be noted that the author arbitrarily chose a cutoff value of 120 to distinguish the unknown object from the background. It is easily seen, there is no absolute outline for the unknown object. The numbers over 100 and below 120 and along the edge and represent areas which are partially unknown object and partially background. The interesting areas are those shown in orange. They are areas slightly warmer than the background and represent the heat trail of the unknown object as it moves through the air. It can be seen that there are also some areas around the unknown object that show a slight warming. The long axis of the object is contained in 8 pixels. Assuming the unknown object is 4 feet long, each pixel would represent about 6 inches and the heat trail only lasts 1 pixel length (about 6 inches) beyond the unknown object.

The reader is invited to compare Figure 3.0 - 1 with 2.4 - 4. In the latter figure it is seen the entire object is black with no specific area distinguishable. That isn't so in the above figure. In this figure it is easily seen the maximum heat (single digit values) is clustered near the center and falls off in all directions. It is believed that the smallness of the very hot area is the reason that overall the heat produced is relatively low.

4.0 Conclusion

This Appendix started by using various views of the unknown object to compile a model of it, During that process it was determined that:

- Since a splash was seen in Frame #3769, the object is physically present;
- In most of the frames the unknown object displays a smooth exterior shape;
- In some frames while entering the water some angularity was observed;
- In addition to its forward motion, the unknown object is observed to rotate;
- In relation to the forward motion, the rotation looked slow and variable;

- Assuming the hot and cold areas remain fixed on the unknown object, no relation was seen between the hot areas and the lead area (front) of the unknown object;
- The lack of a relation between heat and direction of motion eliminates most terrestrial propulsion systems;
- Only a minimal heat trail could be found following the unknown object.
- The air flow around the unknown object is likely laminar;
- With less than a mm of water covering the object, no IR radiation will escape;
- The wave size shows the object's minimum depth underwater to be between 1 to 3 feet.
- The Bernoulli Hump shows the object's maximum depth underwater to be between 3 and 5 meters; and
- The areas of the unknown object are not as hot as would be expected from a conventional aircraft or as cool as a balloon or plastic bag.

This is a surprising amount of information to be obtained from consideration of a simple model. Since these results are also all independent of the model, they could all have been (and some were) obtained without the model.

Notes and References

1. Subjective Realism is a world viewpoint in which the world is in the mind of the viewer.
2. Invariant mass is the portion of mass that is not a function of velocity. It is the portion of mass that defines shape. There are field quantizations which have mass but no invariant mass and there are mathematical constructs such as energy which is equivalent to mass. Those objects, however, do not define a shape.
3. Tikhonov, A; Arsenin, V; "Solutions of Ill-Posed Problems", John Wiley and Sons; 1977.
4. Hale, G.M., Querry, M.R.; " Optical Constants of Water in the 200 nm to 200μm Wavelength Region"; Applied Optics; **12**, Issue 3; 555-563 (1973): Plot obtained from data table provided in paper.
5. Wozniak, B,; Dera, J.; "Light Absorption in Sea Water"; Springer - Atmospheric and Oceanographic Sciences; (2007); Chapter 1; Page 4; Figure 1.2a
6. Electromagnetic rays interact with particles via discrete scattering. When energy is deposited onto the scattering material, the process is called absorption. The number of photons that experience an energy loss is proportional to the differential thickness of the scattering material and the number of photons incident on the material. The equation provided in this appendix is basically the number of photons left undisturbed after a distance x.
7. Stefanick, T.; "Strategic Antisubmarine Warfare and Naval Strategy"; Institute foe Defense and Disarmament Studies; (1987): Appendix 3; "Non-acoustic Means of Submarine Detection"; Equation A3-1. The assumptions used to create this equation were:
   - The ocean is infinite in depth and extent (the location of the object is far from the ocean's bottom and boundaries);
   - There is no surface tension at the oceans surface (the effect wavelength is large compared to surface tension wavelengths);
   - The ocean water has no viscosity (the boundary layer is small compared to the object's diameter);
   - The object can be approximates as an ovoid moving parallel to the ocean's surface.
8. ibid: Figure A3-2
9. Average underwater speed calculated in Table 3.2 of the Water Transit Appendix (Section 3).
10. Burmeister, LC; “Convective Heat Transfer”, 2nd ed.; Wiley-Interscience,; 1993; p 107
11. The heat transfer coefficient is normally defined by inverting Newton's law of cooling. Since that would result in a circular system, it is better to define it using the Nusselt number (Nu):

    $$H = k\,Nu / L$$

    In this equation "k" is the thermal conductivity of the fluid and "L" the characteristic length of the problem.
12. Anderson, J.D.; "Ludwig Prantl's Boundary layer"; Physics Today; **58;** No.12; pg42-48; (2005)

APPENDIX I

Alternate Speed Calculation Using Background Objects

OBJECT GROUND SPEED MEASURED WITHIN FRAMES 3769 THRU 3851

Abstract: During the specified frame range, the object was over the ocean and underwater for a subset of these frames. The speed was measured using the distance provided by the on screen video data, X (horizontal) pixel positions of the object in each frame and the X pixel positions of waves in the background which provided an angular rate of camera panning. These measures not only provide the ground speed but also evidence of object ground speed accelerations while underwater.

Method of Speed Measurement

First, the changes in the horizontal (the X) pixel positions from one frame to the next were derived by subtracting the current frame X position from the previous. Thus if the object moved to the left relative to, say the reticle, then the resulting difference would be positive. Consequently movement to the right would be negative. The background motion was always toward the right for all of these frames. To obtain the incremental change of the background, the X pixels of a selected background location were subtracted; previous frame minus the current frame – opposite to the objects incremental measure. This ensured that the background incremental measures were always positive since the background motion relative to the screen was always to the right.

Next, the incremental measures of both the object and the background can be converted to a horizontal angular rate by multiplying the degrees per pixel by each of those increments. If the object moved to left, relative to the screen, then its angular rate is faster than the angular rate of the background (i.e. a fixed location appearing to move to the right on the screen) – thus the angular rate of the object, relative to the fixed background, should be added to the angular rate of the background. This gives the angular rate of the object relative to a fixed background location which will enable a ground speed measure of the object. Figure 1 illustrates the method.

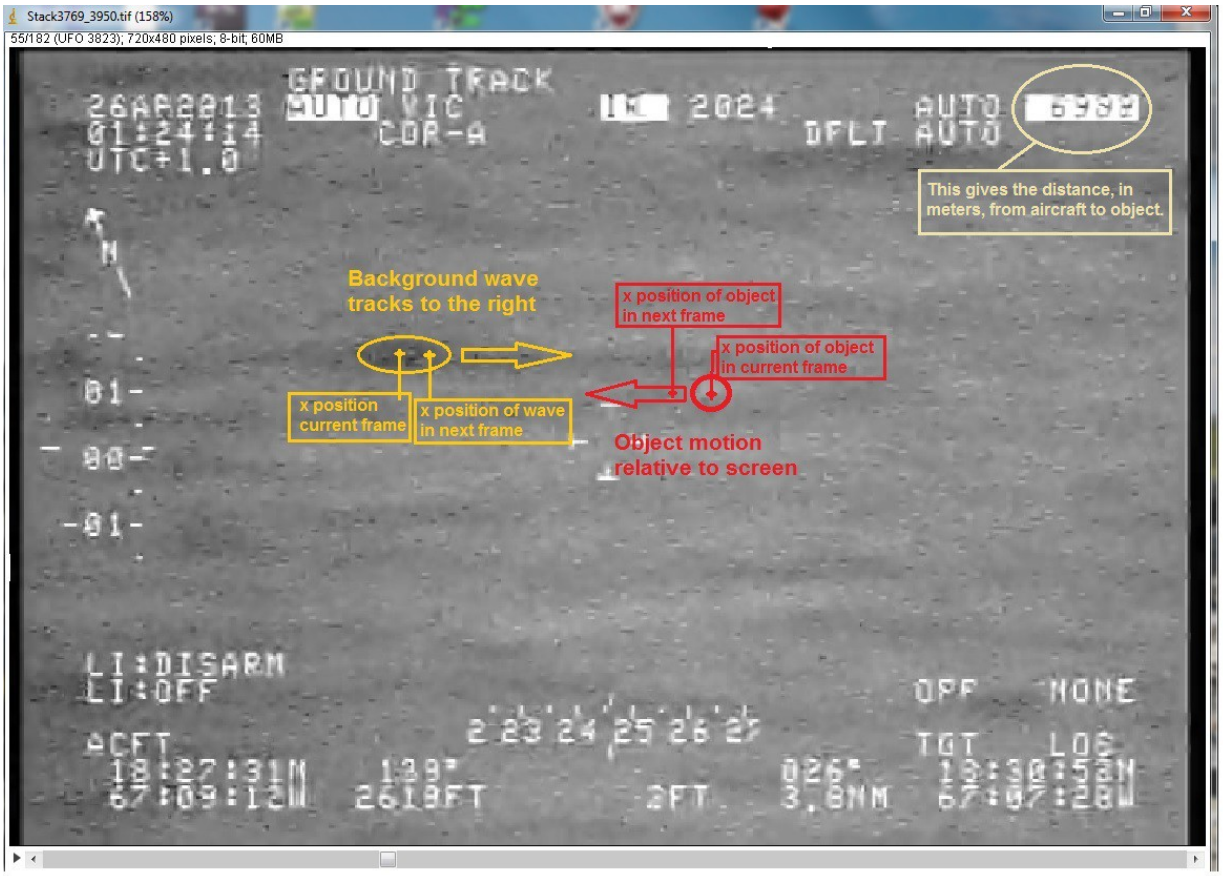

Figure 1 (Frame 3823)

Figure 1 is frame 3823 showing the object circled in red (difficult to see but present where indicated) and its relative direction of motion as the camera pans left. Waves, seen in the background, track right as the camera pans left. The full horizontal field of view at this magnification (2024) is about 0.3602 degrees. For 704 horizontal pixels, this gives about 0.000512 degrees per pixel. The background wave and the object can be seen in frames 3823 and 3824. The wave has moved about 16.33 pixels (an average) while the object has moved 5 pixels. Thus the angular increment for the wave is 16.33 pixels * 0.000512 deg/pix = .0084 deg change while the object angular increment is 5 pixels * 0.000512 deg/pix = 0.0026 deg change. What is the object's angular incremental change relative to the background? Since the object's relative motion to the left implies that the object is moving faster than the camera is panning to the left then we should add the angular changes; 0.0026 + 0.0084 = 0.011 degrees change relative to the fixed background.

Thirdly, we use the aircraft to target distance indicated at the upper right of Figure 1 to derive the ground speed of the object. This distance given in frame 3823 is 6938 meters (although not very legible in this frame, it is clear in immediately previous frames.) However, in frame 3824 the distance was updated to 6951. Under this circumstance, we took the average: (6938+6951)/2 = 6944.5 meters as the distance to the object from the camera. The object ground travel during frames 2823 to 3824 was 2*6944.5*tan(.011/2) = 1.33 meters or about 4.34 feet.

Fourth, we use the time increment from the start of one frame to the start of the next which is, essentially, the time increment for 1 frame. Because of the variation in frame rate, the on screen clock was used to count the number of frames in 1 second for specific sets of frames. In this case the frame rate was 32 frames per second. Thus the ground speed of the object based on movements measured from frame 3823 to 3824 was determined to be 4.339756 ft/0.031 sec or about 138.87 fps or about 94.69 mph.

Figure 2 depicts the moving average of object's ground speed, based on the above method, for frames 3769 thru 3851; 83 frames and 320 data points. That moving average includes sets of 5 frames.

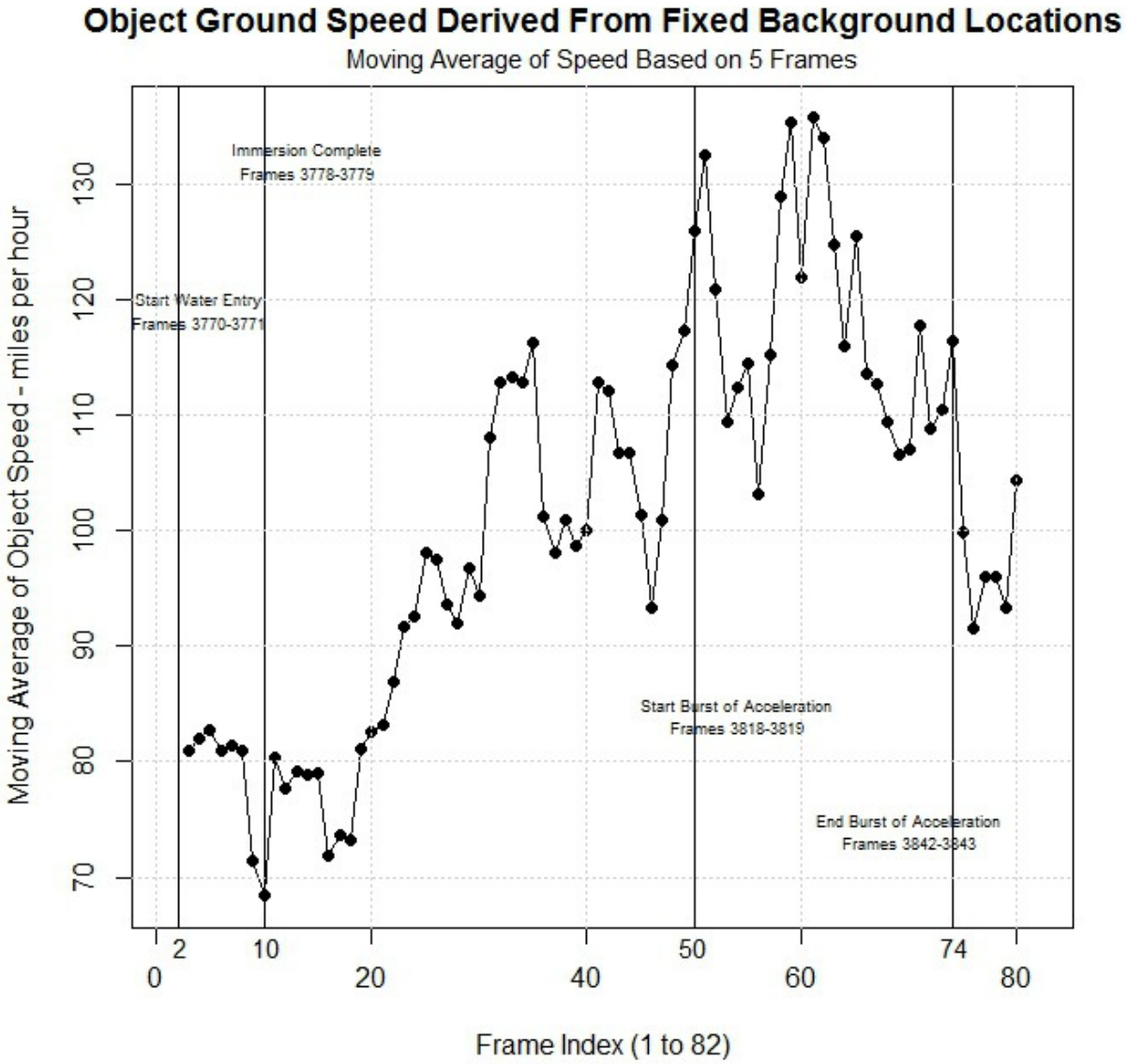

Figure 2 (Frame pairs 3769-3770 thru 3850-3851)

The difference between pixel locations for adjacent frames were used to determine incremental movement. Consequently pairs of frames are indicated instead of individual frames. Additionally, the frame index indicates the frame pair with less clutter across the base of the plot. The frame index represents frame pairs as follows; 1:3769-3770, 2:3770-3771 ... 82:3850-3851. Because each point represents an average of 5 frames, the plot does not start with 1 and end with 82. The methodology did have a fair amount of noise since tracking a wave across a sequence of frames did involve some estimates of location. Some frames had as many as 5 data points, tracking 5 different waves, while most others had 4, 3 and at least 2. The average standard deviation was 3.34 pixels per frame – an average noise level that is not too bad.

Viewing the specified frames of the video, the burst of acceleration has been determined to be real by this analysis even though the panning rate did slow which could have created the illusion of object acceleration.

APPENDIX J

Water Transit

Introduction

Although most of the video concerns the object moving through the air, there are portions where the object interacts with the ocean. These include approaching the ocean in preparation to enter it; entering the water; motion underwater; exiting the water; object division; and the transition period from water transit back to air transit. This appendix will examine each of these periods individually. After determining what is shown in the video for each portion and what is implied by each item, some discussion will be provided of the present level of Earthly science and engineering in these fields. A final section will also be provided continuing the results of each of the previous sections.

The basic difficulty in interpreting infrared (IR) pictures is our lack familiarity with them. We expect pictures to show the subjects mass and shape. IR pictures do not do that. They only show heat variations. Since we do not know what the nature of the object being filmed, we also cannot know how its heat would vary in any normal operation. However, although the object is unknown, its environment is not. The environment is a known; therefore, clues about the object can be derived from seeing how the environment reacts to it. Where possible this appendix examines the known to determine the unknown.

1.0 Preparation for Entering the Water

Since it is known that water is approximately 50 times more viscous[1] than air, a calculation of the speed in air before entering the water and its speed while in the water was made to see if there was any difference. It may be noted that, if the unknown object is piloted, it can expected that it may slow down some prior to entering the water to increase the time the reaction force from the water is applied thus reducing the instantaneous force. This calculation was done for a set of frames a short distance away (# 3700 - #3750) from that specific frame (#3769) in order to reduce any effect introduced by the period where the unknown object was actually entering the water. Since this 19 frame difference only translates to slightly more than 1/2 second, it is known that it can only be partially effective in eliminating any slowing down period.

The basic data for the frames chosen is shown in Table 1.1.

Frame	**3700**	**3750**
Latitude (DMS)	18 30 49	18 30 51
Longitude (DMS)	67 7 23	67 7 25
Time (H:M:S)	1:24:10	1:24:12

Table 1.1

The problem with the data given above is both coordinates and time are stated to within 1 second.

Since it is implicitly assumed that the unknown object will travel in a straight line during this period, the time and coordinates to use in calculating this speed are totals. Since any internal error between cells in this series will cancel, corrections have only been applied to the end cells. Those corrections were calculated using linear scaling. A check of the frames showed

that the first frame that showed the time of 1:24:12 was # 3734 and the last frame to show that time was # 3765. Therefore as shown below, frame # 3750 occurred at a seconds value of 12.52125 seconds.

$$X = 12 + (3750 - 3733) / (3765 - 3733) = 12.53125$$

Similarly the first frame that showed a time of 1:24:10 was # 3676 and the last frame was # 3701. This gives a seconds value of 10.96154. The total time is therefore 1.5597 seconds. The interesting result with this calculation is that if one had blithely used the 2 second difference determined by subtracting the given times the resulting velocity would have been approximately 28% lower than what will be calculated here.

Before considering a repeat of the above calculation for the coordinates, it is instructive to determine the possible maximum error that could have occurred due to their truncation. By truncating the coordinates of each frame the actual location is only known to a half second of degree for both Latitude and Longitude. Using 3963.191 miles for the equatorial radius of the Earth and 3949.903 miles as the polar radius, the radius of the Earth at latitude (L) of 18.5225 degrees is calculated as:

$R_1 = \{ R_E4 \cos2(L) + R_P4 \sin2(L) \} / \{ R_E2 \cos2(L) + R_P2 \sin2(L) \} = 3961.86$ miles .

Therefore the distance equivalent to a half second of latitude is

$$D(1/2 \text{ sec Latitude}) = \{(\pi/2) (R_1 / 90) (5280) / \{2 \times 3600\} = 50.71 \text{ feet} .$$

A similar equation exists for Longitude, but the radius used has to be (R_2), the perpendicular distance from a line connecting the poles to the specific Latitude location.

$$R_2 = R_1 \cos(L) = 3756.63 \text{ miles}$$

This results in the distance equivalent to a half second of longitude being

$$D(1/2 \text{ sec Longitude}) = \{(\pi/2) (R_2 / 90) (5280) / \{2 \times 3600\} = 48.08 \text{ feet}$$

Therefore every frame can be off by a maximum of 69.88 feet. Since the distance per frame is approximately 5 feet, the above possible maximum errors present the possibility of introducing spurious results. This could cause the distance between frames to vary from frame to frame. Therefore the velocity will also have to vary. In particular there will be instances where the object will stop for a few frames or even move backwards while instantly accelerating to high velocity values to account for other changes. Since it is known that with multiple frames internal errors always cancel twice the 69.88 feet is the maximum error introduced by the truncation of the seconds term in the coordinates regardless of how many frames are included. In the present case where the distance is 50 frames long, the total length is approximately 250 feet and the error bars would be plus and minus 140 feet. Therefore the correct values for the two ends must be calculated in this case.

The 49 second latitude seen on frame # 3700 runs from frame # 3690 to frame # 3706. The 23 second longitude value seen it runs from frame # 3685 to frame # 3700. Therefore by linear interpellation the coordinates of frame 3700 should be { 49.67, 23.94 }. Similarly the 51 second latitude seen on 3750 runs from frame # 3727 to frame # 3765. The 25 second longitude value seen on 3750 runs from frame # 3740 to frame # 3759. Therefore by linear interpellation the coordinates of frame 3700 should be { 51.62, 25.55 }.

Using the radius { R_1 } calculated above and denoting the coordinates of location 1 as { L_1 , Lo_1 } and location 2 as { L_2 , Lo_2 } the distance between 2 sets of coordinates is calculated from: $d = R_1 \cos\text{-}1 \{ \sin(L_1) \sin(L_2) + | \cos(Lo_1 - Lo_2) | \cos(L_1) \cos(L_2) \}$.

This equation with the above coordinates and radius of the Earth yields a total distance of 251.16 feet and results in an air-speed prior to entering the water of 109.72 miles per hour.

2.0 Entering the Water

In today's science, it is impossible to enter, leave and move through a fluid and not affect it. However, that seems to be the case in the video. Although the effect may be less than normally encountered, it is this author's opinion that the lack of a visual effect is basically due to our difficulty in translating a heat signature into the more normal mass picture.

Frame 3769 and those around it seem to show an object larger than 3 feet moving at over 100 miles per hour hitting and enter the ocean seemingly without creating a splash. Although present science knows ways to almost make the object almost invisible to the water and thus minimize the splash, eliminating it is not possible. Effectively a splash is taking a volume of water and drastically increasing its surface area. Since both evaporative and radiative heat transfer are proportional to the volumes surface area, a splash provides a means to allow that volume of water to become a "little" cooler. Little is in quotes because the change is very small and is basically invisible to the viewers eyes. This is seen in figure 2.1. In this figure, the red circle outlines the unknown object that has just hit the surface of the ocean and the red arrow indices the direction it is traveling in. As was stated above, even zoomed in no splash can be seen in this figure.

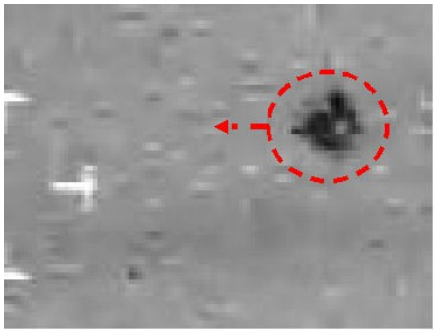

Figure 2.1: Frame 3769 - 300X zoom

The "Surface Plot" tool in "ImageJ" provides a three-dimensional view of the intensities of pixels of a non RGB or grayscale image. It therefore converts the heat variations in the IR frame to height variations with (in its default operation) the lighter (cooler) pixels being represented as hills and the darker pixels as valleys. The red outline in figure 2.1 was provided to allow a direct comparison of that picture with the surface plot shown in figure 2.2.

Although still small, the cooler areas representing the splash are seen as raised areas around the upper corner of the plot. It is believed these represent a splash rather than simply cooler areas of the unknown object since they do only show up in these plots where the unknown object is entering the water. By comparing the 2 figures it can be observed that the object in figure 2.1 is moving to the right and slightly down. This raises an interesting observation.

Rather than the splash being in front of the unknown object, it is trailing it and to the right. Since a front located splash cannot be found in this plot or any of the later frames, it is believed the splash has been caused by a portion of the unknown object more to the middle or back and the front of the unknown object is angled such that it sliced into the water with little or no splash.

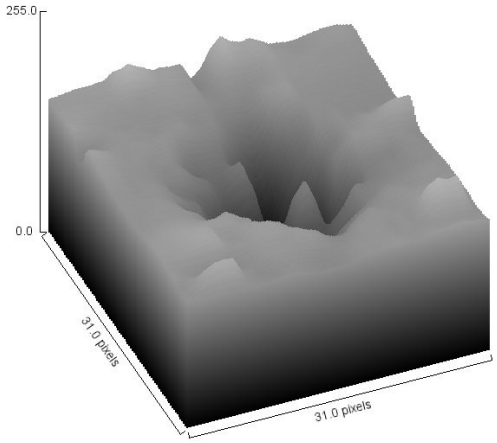

Figure 2.2: Frame 3769 Surface Plot

Although the discussion of the entry portion is almost complete, there is an additional piece of information that can be gleaned from the above surface plot. While it is understood that this plot is not showing a real hole in the water, it does allow a view of 1 slice of the unknown object. Since the slice isn't exactly flat, it isn't quite the same as the 3-d printer slices but given many slices it would be possible to reconstruct the top portion of the unknown object's warm sections outline. In particular the above slice show that in the unknown object contains a warm section shaped vaguely like a dumbbell. It also shows the forward portion of the warm area is not rounded but has some sharp corners. It may also be possible to outline cold portion of the top since they would rise up higher than the water. It is difficult to distinguish them from splashes. The end of the splash can be seen in Figure 2.3. At this point, only a very small remnant of the unknown object heat signature remains along with four low remnants of the splash.

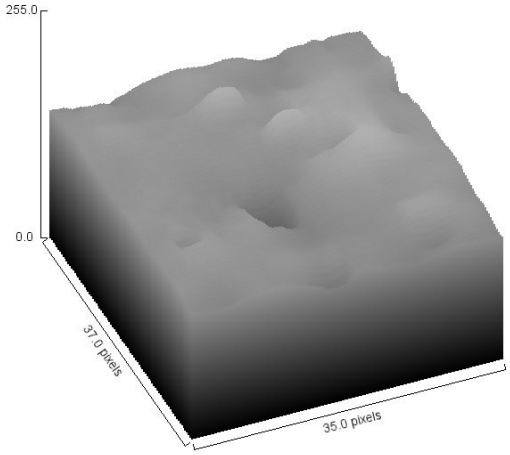

Figure 2.3: Frame 3777 - Surface Plot

3.0 Transiting the Water

During the underwater journey there are a couple of places where a dot can be seen indicating the unknown object is quite near the surface. Additionally, although the video does not show the object for most of its underwater period each time the object appears, the camera is found to be pointed almost directly at it. Since one of the witnesses specifically rejected the idea that the camera was locked onto the object, this implies that the object has remained visible to either the camera operator or the pilot or both. It further implies that while traveling underwater the unknown object has remained relatively close to the surface throughout. Since these assumptions essentially mean the unknown object is at an altitude of sea level and is placed at the target location printed on each frame, we can assume the target location as the unknown object location throughout this period.

If close to the surface it is possible to determine the object's speed while underwater. Since frame lengths are measured in the tens of milliseconds, it is understood that arguments can be made as to the exact frame number to use for the start and end of the underwater period. Frame 3769 was chosen as the start frame where the object can be seen entering the water and the end frame to be Frame 4560 where it starts to emerge. Although other choices would change the central results given below, any difference would be relatively small. The basic data from these 2 frames is provided in Table 3.1.

Frame	**3769**	**4560**
Latitude (DMS)	18 30 52	18 30 53
Longitude (DMS)	67 7 26	67 7 56
Time (H:M:S)	1:24:13	1:24:39

Table 3.1: Underwater Frame Span

Although it would be possible to correct these coordinates the same as was done in section 1, the frame span here (791 frames) is a lot longer than the 50 frames previously considered. As in that section the maximum error introduced by the truncation of the seconds portion of the coordinates is twice 69.88 feet over the entire span. Where that error was approximately plus or minus 56% of the total length, this error is only plus and minus approximately 3.5% of the total length. It is therefore not reasonable to search for the exact start and end coordinates. However, the time is a smaller number and has more of an effect on the result and should be determined exactly.

A check of the frames showed that there were 26 frames that showed the time of 1:24:13 with the first frame being # 3766. Linear scaling therefore indicates that frame 3769 occurred at a seconds value of 13.15385. Similarly there were 32 frames that showed a time of 1:24:39 with the first frame being # 4544. Linear scaling therefore indicates that frame 3769 occurred at a seconds value of 39.84375. The total time underwater is therefore 26.6899 seconds.

Since reality is most likely to be a constant underwater speed but not necessarily a constant direction, the most reasonable method is to calculate the total distance by adding calculated

sections of frames and determining the velocity from it with the time calculated above. The sections used were each 50 frames long except at the start and end. The initial section had 31 frames and the final section had 60 frames.

The error bars were determined first assuming the coordinate for those frames were each shortened and then elongated by a half second. The results for the above calculations are shown in Table 3.2.

Start Frame	End Frame	Distance (feet)	Dis. per Frame	Shortened End Frames	Elongated End Frames
3769	3800	96.170	3.10	152.904	69.881
3800	3850	217.43	4.35	217.43	217.43
3850	3900	279.52	5.59	279.52	279.52
3900	3950	217.43	4.35	217.43	217.43
3950	4000	217.43	4.35	217.43	217.43
4000	4050	192.33	3.85	192.33	192.33
4050	4100	192.33	3.85	192.33	192.33
4100	4150	217.43	4.35	217.43	217.43
4150	4200	192.33	3.85	192.33	192.33
4200	4250	217.43	4.35	217.43	217.43
4250	4300	217.43	4.35	217.43	217.43
4300	4350	217.43	4.35	217.43	217.43
4350	4400	192.33	3.85	192.33	192.33
4400	4450	217.43	4.35	217.43	217.43
4450	4500	217.43	4.35	217.43	217.43
4500	4560	139.76	2.33	209.543	69.880
Total		3241.69	<4.10>	3368,21	3145.39
Speed (mph)		82.812		86.044	80.352

Table 3.2: Speed in Water

As has been, it is believed that while underwater, the unknown object travels close to the surface. In our science, when an object travels on or close to the surface of water, it produces a wake trailing it. Although the wake equations will not have to be solved in this document, a small discussion of the mathematics of wakes should be included. Wakes are three-dimensional. They include the scalar problem of pressure waves and the two-dimensional shear problem. Shear refers to a material deformation that occurs due to movement of internal surfaces parallel to each other. Basically, water shear refers to the extra water being dragged along as an object moves through it. Effectively what is actually being moved is much more massive than the object itself. The equation used to describe this situation is the vector Helmholtz[2] equation.

As described above shear is basically a friction and like all friction it opposes motion and generates heat. In an IR image, the effect of the shear portion of a wake would be a dark "V" whose apex originates at the object. Additionally the pressure wave would add lighter lines following the same path to the wake.

The "stack" tool in the program ImageJ was used to look for any sign of a wake from the unknown object as it moved underwater. This stack included all images from frame 3757 through frame 4272. By animating them and going backwards and forwards it was possible to follow the unknown object's path while it was underwater. Figure 3.1 is one such still image during this period. The unknown object is the slightly whiter circle within the red circle. Although exceptionally hard to see in a still picture, it is easy to follow this whitish circle when the frames are animated. Since the object shows as slightly whiter than the ocean around it, it is actually cooler than the surrounding water but does not show any sign of a wake. It is, however, interesting since the unknown object showed itself as hot when entering the water and it is now located by a slight cooling effect on the water. This seems to indicate that not only is it not creating heat via friction with the water, it is also not transferring heat to the water via contact.

Figure 3.1: Frame 3781

The relative coolness shown is assumed to be a slight "hump" in the water at the location of the unknown object. This is similar to the same effect that occurs over submarines. The lack of any wake indicates that once the unknown object is inside the water, it is essentially invisible to it. As the object moves, water directly in its path flows smoothly around it in a shell and exits at the same point with the same energy as it had before the object arrived. The cool area observed would be the top of the shell where the "hump" slightly increases the surface area. Additionally, all water outside that shell would remain still. The word

"invisible" to describe this was chosen for a reason. Although this description considers particles of water rather than photons, it is completely equivalent to the problem of normal invisibility (if invisibility can be considered normal). Since the water outside the shell remains still, there is effectively no shearing force, and since the water at the shell returns to the location it was prior to the arrival of the object and has the same energy, there is no pressure wave. Hence, there is no wake generated. This movement does however take energy that would not normally be expended in movement through the air. That use of energy would be shown as a reduction in speed of the unknown object while in the water.

4.0 Exiting the Water

As has been discussed, the unknown object exits the water in or around frame 4560. Normally it would be expected that the act of exiting would bring water up with the object thus increasing its surface area and showing in the video as a white area surrounding the unknown objects hot section. However due to interference by the reticule none of this was visible.

Although it was impossible to "see" the unknown object exiting the water, it is possible to replicate the work done when investigating the preparation undergone before entering the water. As in that section an effort was made to reduce the effect of the period where the unknown object was actually emerging from the water, the calculations were done for a set of frames a short distance away from the exit frame. The results from these calculation are shown in Table 4.1.

Start Frame	End Frame	Distance (feet)	Time (Sec)	Speed (mph)
4570	4620	53.99	1.781	36.81
4620	4660	187.83	1.169	109.55

Table 4.1: Speed in Air upon Exiting

As was expected, near the exit location, the speed is significantly less than its normal air value. It was rather surprising to find the speed immediately upon exiting the water to also be less than that in the water. If this effect is real, it would seem the object has altered its path at this point to be almost completely upwards while exiting the water. Additionally, since the calculations occurred approximately 10 frames following the start of that period, the period must have extended for over the approximately 0.3 seconds it took for the 10 frames to complete. Although a specific acceleration value cannot be determined due to the lack of knowledge about the initial velocity or time, the expected strong acceleration between the initial section leaving the water and the section immediately following it is apparent.

5.0 Object Division

Following its exit from the water the unknown object appears to divide into 2 separate sections. Since this is confusing and difficult to understand this section will begin with a

description of what is seen in the video and the attempt to discuss the possibilities that are occurring.

The division seems to begin in frame 4627. The word "seems" was specifically chosen since at the point of division the camera operator has the camera at the long range zoom factor of 625. At that setting the unknown object is essentially a dot over the water. In frame 4627 the dot is starting to become elongated but two distinct dots cannot be seen. Additionally there is a period where the reticule hides the unknown object but the first frame in which this viewer can make out 2 separate dots is 4740. Interestingly in frame 4758, the upper dot (unknown object) seems to go back underwater and then re-emerges 6 frames later (4764). This apparently interested the camera operator since he then changed the zoom factor to 2625 two frames later. It should be noted that when the camera changes zoom factors there is a set of frames that are completely black.

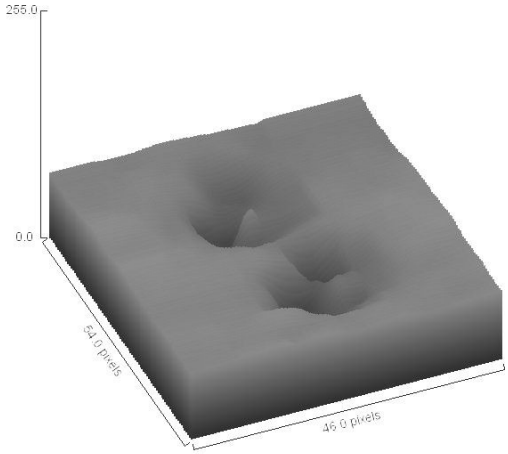

Figure 5.1: Frame 4677

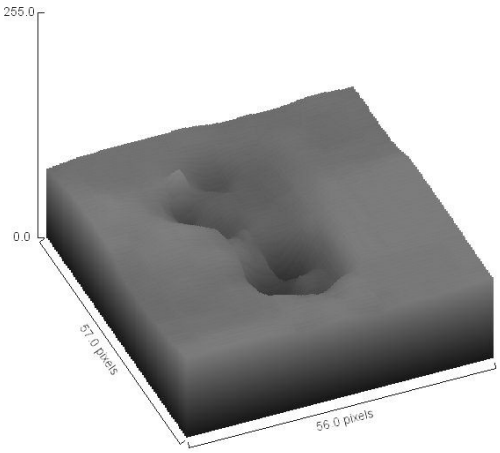

Figure 5.2: Frame 4678

It isn't until frame 4676 that an image of the unknown objects and the water begins to reappear. Interestingly the top unknown object appears to enter the water again starting at frame 4678. Figures 5.1 and 5.2 are surface plots for just before the top unknown object hits the water (5a) and just after it hits the water (5b). A slight splash in front of the object can be seen in 5b. The next 20 frames of the video shows the upper unknown object to be skimming along the top of the water; disappearing and reappearing a couple of times. The lower unknown object then evidently goes a little lower and begins to copy the first unknown object starting around frame 4788. Although the 2 objects can be seen to move together for many more frames, this discussion will be concluded at that frame.

The problem we have with discussing this section of the video is that it is not known if the unknown object actually divided or if there were simply 2 unknown objects that appeared from beneath the water and the emergence of the second had been hidden by the first. Although the second possibility makes more sense both possibilities will be considered.

The first item to look at is speed. We know there is something driving these objects. We do not know what is providing this motive power but it must exist. If a single object divided into 2 objects it has to be assumed that the "engine" driving the object also divided. That would seem to imply that after a division both object would travel slower than the single object did

prior to the division. A quick calculation was made between frames 4679 and 4990. The results can be found in table 5.1.

Title	Distance (feet)	Speed (ft/sec)	Speed (mph)
Average	680.77	68.08	46.42
Top Error Loc	795.63	79.56	54.25
Btm. Error Loc	577.00	57.70	39.34

Table 5.1: Speed of both unknown object between frames 4679 & 4990

Remembering that the final speed of a single unknown object after leaving the water was determined to be 109.55 mph, it is seen these results are significantly lower and seem to indicate that the objects have indeed divided their engines. It should be noted, however, that this is only an indication. It is possible but very unlikely that two independent unknown objects with exactly the same initial speed, decided to reduce that speed to this value at almost exactly the same time.

An interesting but unexplained oddity occurs during this period. Even though there is a period of time where one of the 2 objects was moving through both the air and water while the other was totally in the air, there was no difference in speed between the two seen. It would be expected that the object partially traveling through the water would be slightly slower than the object traveling totally in the air. However, the unknown object in the air is not seen to pull away during that period.

6.0 Comparison to Terrestrial Science

Although most of what has been described above could have been done as individual effects, We have not yet replicated all of them in a single object. The following two paragraphs discuss two such terrestrial objects. In each it is seen that in addition to their presenting an IR signature at odds with the what is seen in the video, neither can duplicate the ability to travel through the water without producing a wake. The section concludes with a statement of the present level of terrestrial science in the field of wakes.

Submarine missiles provide an example of objects that can leave the water, fly in the air and split into multiple flying objects. The Lockheed-Martin Trident II D5 missile[3] has this capability. It is launched underwater, pops up through the surface, accelerates off and divides into up to 14 independently targetable warheads. It, however, cannot first dive down into the water and after traveling a distance underwater re-emerge for the remaining portion of its travel. It is also much bigger than the unknown object seen and since it is a rocket, would produce a markedly different IR signature. It also doesn't really "swim" up through the water as a powered object. It is shot upward 30 to 40 feet through the water by compressed gas with the rocket essentially creating a "hole" in the water initially filled by the compressed gas. The movement of the "hole" and the water rushing back into it would easily be seen as a

wake behind the rocket. Finally at the surface, the movement of the holes and water rushing back combine to form a plume of water that follows the missile upward. The plume would be seen as a splash. At that point, the missile's rockets ignite.

Figure 6.1: Trident II Missile exiting the water

Since they have been in existence for over 20 years, a rocket driven supercavitating torpedo[4] should be considered. Although to the author's knowledge it hasn't been done to date, there is absolutely no scientific or engineering reason to rule out the possibility of building one that could be launched and as was seen in the video, fly in air prior to entering the water. Travel in the water and then reemerge into the air. In both the air and the water this object is simply a rocket. Supercavitation is only an effect that exists while in the water. It is an effect that occurs when the water pressure around the rocket is lowered below its vapor pressure[5] thus creating a bubble of air around the rocket. That allows the torpedo to essentially fly in the bubble while underwater. There are, however, some major problems with attempting to equate this concept with the unknown object in the video. The first is all supercavitating bodies produce compression waves at the front and strong two-phase wakes at the trailing end. The second is they also require very high speeds to maintain the cavitation bubble. The second is they are simply rockets that can fly underwater. They are bigger than the unknown object observed and as rockets, would produce a markedly different IR signature.

In both of these examples it was mentioned that the object under consideration produced a wake. That is not particularly surprising. It is simply a statement that the water reacts to an object moving through it. Although that seems like an obvious requirement, recent physics papers[6,7] have begun to question its validity.

Figure 6.2: Russia's Shkval Rocket Torpedo

Those papers and others employ the Transformation Optics (TO) procedure initially proposed at Duke University for electro-magnetic cloaks. That procedure makes use of the fact that both Maxwell's equations of electromagnetic (EM) theory and the Helmholtz equation are invariant under a coordinate transformation. Although not as exact as electromagnetic cloaks, these papers of a part of a flurry of theoretical papers recently published on acoustic and fluidic (water) invisibility cloaks. The above two referenced papers form a complimentary pair of views of invisibility cloaks in water. In the first one, by Farhat et. al., the water is invisible to the object[6] (the water doesn't affect the object - protection against Tsunamis, etc.). In the second, the object is invisible to the water[7] (the object doesn't affect the water). The latter paper envisioned using a meta-material[8] shell composed of parallel rows of fiberglass slats etched with copper to transport the water in a laminar fashion around the object

Although the paper by Farhat[6] et. al. was published first, in relation to this appendix the second paper[7] by Urzhumov and Smith is the most important in. Similar to the EM cloak, it "warps" the water around the object such that it attempts to preserve the streamlines of flow and the pressure distribution that would have existed in the absence of the object. Since it was known that simply steering the water around an object would tend to slow down the water thus causing a frothy wake, it was proposed that small piezoelectric pumps be placed in the shell to offset the energy loss. Consequently, the structure cancels the viscous drag force and prevents the onset of turbulence. However, the paper was published in 2010 and only shows that scientifically the shell is possible. Although it is believed that such a shell would be exceptionally interesting to the navy, as far as this author knows, to date there hasn't even been a proof of principle engineering design.

An additional advantage of the cloak envisioned by Urzhumov and Smith is that it makes the object essentially hydrophilic[9] It was experimentally shown by Truscott, Aristo, and Techet[10] that since there is no void (bubble) produced when a hydrophilic ball is dropped into water, it makes a much smaller splash than the more normal hydrophobic ball. There is, however, a relatively large vortex wave that spreads out from the ball. The splash for the hydrophobic object is a result of the bubble collapsing due to hydrostatic pressure and forming an upwards jet or water.

7.0 Conclusion

This appendix began with a short discussion of the difference between infrared pictures and visible light pictures in air and water. Specifically it was shown that in water, it can be very instructive to look at how the environment (the water) reacts to the external objects and how its heat may change due to that interaction.

It was determined that the first frame that showed the unknown object entering the water was # 3769. To provide a base or point of departure, the air speed prior to that frame was calculated using frames 3700 through 3750. The speed calculated was 109.72 mph.

Following that, the period of entering the water was investigated. It was seen in figure 2.1 that no splash can be seen by eye the figure. However as is seen in figure 2.2, the computer was able to see the difference in heat between the ocean and a splash as the unknown object hit the water.

The period of moving underwater was covered in section 3.0. It was shown in that section that the unknown object traveled at about 82.812 mph or approximately 75% as fast as it had traveled in air prior to entering the water. It was also seen in this section (figure 3.1) that the unknown object produced no visible wake as it moved through the water. The unknown object however did seem to slightly raise the water level immediately above it.

The exit of the unknown object from the water (frame 4560) was discussed in section 4. Interestingly immediately upon exiting (frames 4570 - 4620), the unknown object moved at a speed of 36.81 mph which is less than half of its speed underwater. This may, however be due more to direction of motion than an actual loss of speed. The speed then increases to 109.55 mph in frames 4620 - 4660.

Section 5 then discusses a division of the single unknown object into 2 unknown objects starting at frame 4627. After the division, the speed of each was calculated to be 46.42 mph indicating a true division of one object into two rather than the emergence of a hidden object from behinds the first object.

The following table shows the speed variation though the entire period covered by this appendix.

	Frames	Distance (feet)	Time (Sec.)	Speed (mph)
1. Speed in air	3700 - 3750	251.16	1.560	109.72
2. Speed underwater	3769 - 4560	3241.69	26.690	82.81
3. Initial Speed in air	4570 - 4620	53.99	1.781	36.81
4. Later Speed in air	4620 - 4660	187.83	1.169	109.55
5. Speed after division	4679 - 4990	680.77	14.665	46.42

Table 7.1: Speed Table

The interesting result of this appendix is as previously stated, although most of what has been described could be done as individual effects, a capability of doing all of them has not yet been demonstrated.

Notes and References

1. The dynamic or shear viscosity of a fluid is a measure of its resistance to shearing flows. In relative units, the dynamic viscosity of air at 20° C is 0.0198. The dynamic viscosity of 20° C sea-water is 1.08. Therefore sea-water is 50.46 more viscous than air at 20° C.
2. The vector Helmholtz equation is: $\nabla^2 \mathbf{F} + k^2 \mathbf{F} = 0$, where F is a vector function, Del-squared is the vector Laplacian and k is a scalar constant.
3. http://www.naval-technology.com/projects/trident-ii-d5-fleet-ballistic-missile/
4. The first super-cavitating torpedo was the Russian **Shkval** torpedo. Work began on that torpedo in 1960 and it was deployed in 1990s. It is reported to travel over 200 knots That means even if fired from ~3.5 miles away, the target has less than 1 minute to employ counter-measures. Recently there have also been (unconfirmed) reports of a new German super-cavitating torpedo capable of ~500 mph.
5. When the water pressure is less than the vapor pressure the water vapor remains in gaseous form.
6. Farhat, M;, Guenneau, S; et. al.; "Analytical and numerical analysis of lensing effect for linear surface water waves"; Physical Review E 77, 946308; 2008; 11 pages
7. Urzhumov, YA; Smith, DR; " Fluid Flow Control with Transformation Media"; Phys. Rev. Lett. 107, 074501; 2011
8. Meta-materials are artificial materials engineered to have properties not found in nature. They are assemblies of multiple individual elements arranged in repeating patterns fashioned from conventional microscopic materials such as metals or plastics. Unlike natural materials, meta-materials are able to reduce the "index of refraction" to less than one or less than zero.
9. A hydrophilic object is an object with a strong affinity for water. They seem to attract water Examples are objects with dissolve in water such as sugar cubes. A hydrophobic object is one which tends to reject water.
10. Truscott, T.T.; Aristo, J.M.; Techet, A.H.; "Dynamics of Water Entry"; arXiv:0810.1888 [physics.flu-dyn]; http://arxiv.org/pdf/0810.1888v2.pdf

APPENDIX K

Estimated UAP Temperature

Introduction

Since we do not actually have possession of the object seen in the video, determination of the principles employed to create its motion remain a mystery. That, however, does not mean we can ignore this subject. The object is seen to move making multiple direction, altitude, and speed changes. Some source is supplying the energy needed to do that. There should be waste heat produced. This appendix provides an approximate calculation of the waste heat seen in the video. In this appendix:

- Section 1 provides a pixel based approximation to the objects temperature; and
- Section 2 provides a determination of the appropriate heat equations for the object and integrates them with the results of Section 1.

Section 1.0

Temperature measurements were approximated to estimate the heat distribution of the unknown object. The range of temperatures of the object, found by the methods detailed here, were from 10^{o} F below ambient air, 69^{o} F to 70^{o} F, thru 105^{o} F or higher. A single frame, 1251, was used for all the pixel value measurements to avoid frame to frame temperature range adjustments that may occur with the infrared (IR) or thermal imaging equipment. It should be noted that among the 5,000+ frames of video containing the unknown object, the temperature distribution appears to change. A complete study has not been done to include a determination of any correlation of the presence of cooler areas of the unknown object to the higher temperatures – this could be IR artifacts.

1.1 Pixel Value to Temperature Relationship

In an ideal world, we would have access to an equation such that given a pixel value, 0 to 255, the equation would produce a limited temperature range represented by that pixel value produced by the IR hardware and software. However, analysis of the various frames indicates that the temperatures associated with the 256 different gray shades of pixels is periodically recalibrated to the temperature range in each frame. Without the software algorithms used in the thermal video processor, the temperature of the 256 different gray shades must be determined by using objects of known temperatures in a given frame. Frames were selected where known objects such as roads, pasture and animals, were used to associate pixel values to their estimated temperatures.

Frame 1251 was used because there were three known temperatures that could be used to establish the temperature of the unknown object based on the relationship of temperature to the 256 pixel shades. An assumption was made that there is a linear relationship between pixel values and object temperatures within a given frame.This is represented in Figure 1-1.

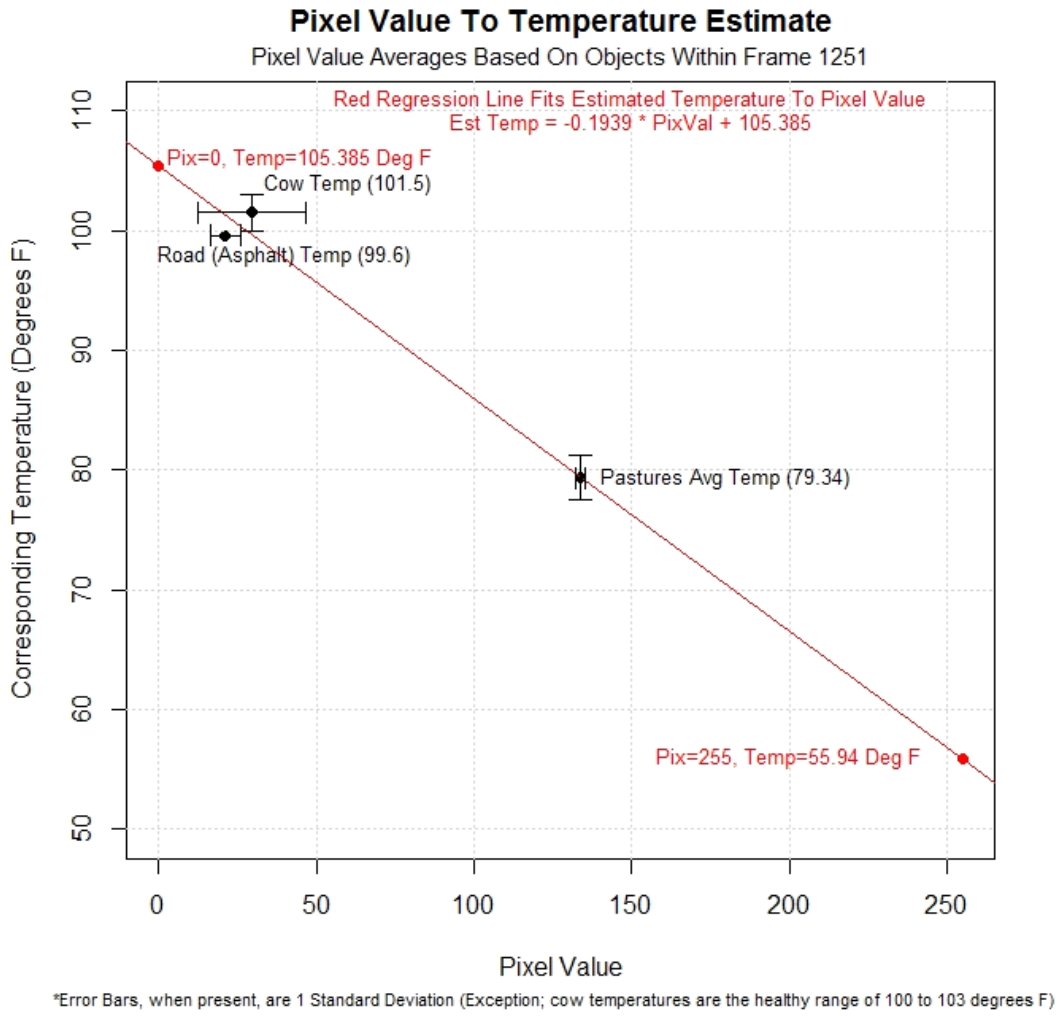

Figure 1-1

The average temperatures for asphalt roads, cows and pastures were found to be 99.6° F[1], 101.5° F[2] and 79.34° F[3] respectively. These temperatures were plotted against the average pixel value for the road, cows and an area of pasture seen in Frame 1251 (see Figure 1.5). A regression line, seen in red in Figure 1-1, is the best fit for all three points. Although regression is not usually used for extrapolation, a linear relationship between the endpoints of the temperature range is reasonably assumed here for estimation purposes. We can see, apparently for this frame using a linear assumption, the IR equipment used a temperature range of 56° F to 105° F to adjust the pixel values to temperature. All temperatures colder than 56 are mapped into pixel 255 while all temperatures hotter than 105 are mapped into pixel 0. The equation for the regression line provides an approximation of temperature with t being the temperature in degrees F, p the pixel value used to obtain the temperature estimate t:

$$t = -0.1939\ p + 105.385$$

It can be seen that each pixel represents an incremental change of 0.1939 degrees F given our stated assumptions.

1.2 Unknown object Temperature Distribution

Using Equation 1-1 we can take every pixel value seen to comprise the unknown object and convert them to temperatures. Figure 1-2 is a 3D false color representation of the unknown object temperature.

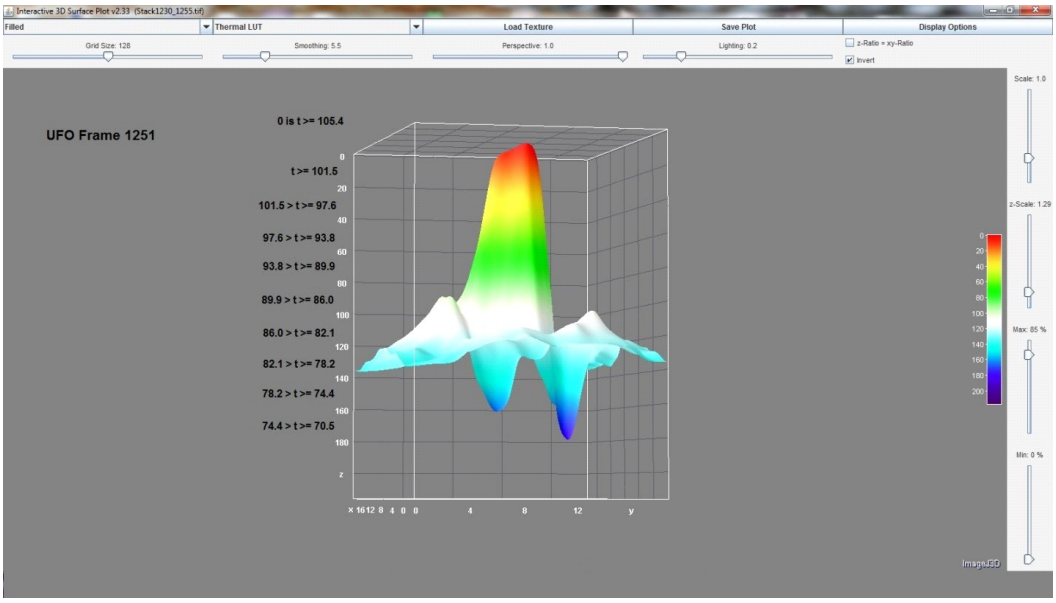

Figure 1-2

This 3D image was produced using the ImageJ (version 1.45 S) Interactive 3D Surface Plot. The temperature ranges are given in between each z axis pixel value. Red represents the hottest, temperatures 101° F and up, and blue the coldest at 74° F and below. Note the smoothing is set fairly high to remove pixelization.

Figure 1-3 depicts the hottest and coldest locations of the unknown object.

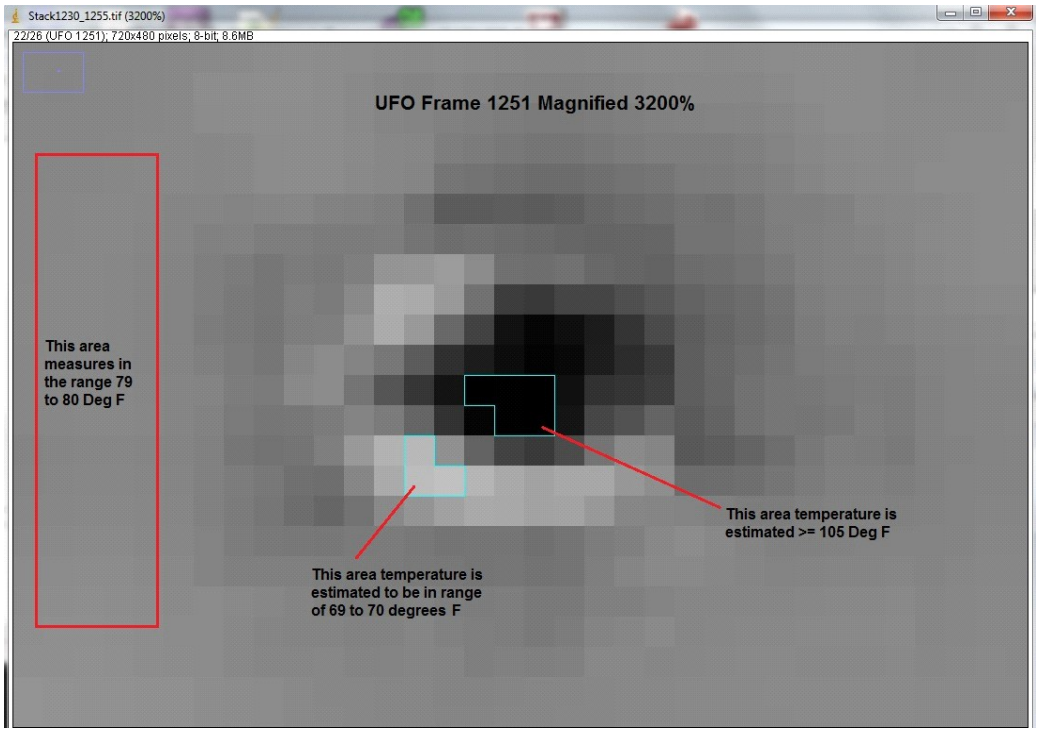

Figure 1-3

It is usually the case that the hottest (blackest) locations are in and about the center of the unknown object while the coldest are usually around the edges. It has not yet been determined whether the cooler (white) pixels are possibly thermal imager artifacts due to high differential temperatures. The red rectangle, non unknown object pixels, are in the 79 to 80 degree range and corresponds to the pasture in the background.

Figure 1-4 is profile of temperatures along the pink line seen in the figure that cuts through the center of the object. This graph demonstrates how the hotter part of the object is usually in its center zone although not completely symmetrical. It also shows how the infrared system detects the heat of the object as a contrast against the ambient temperature.

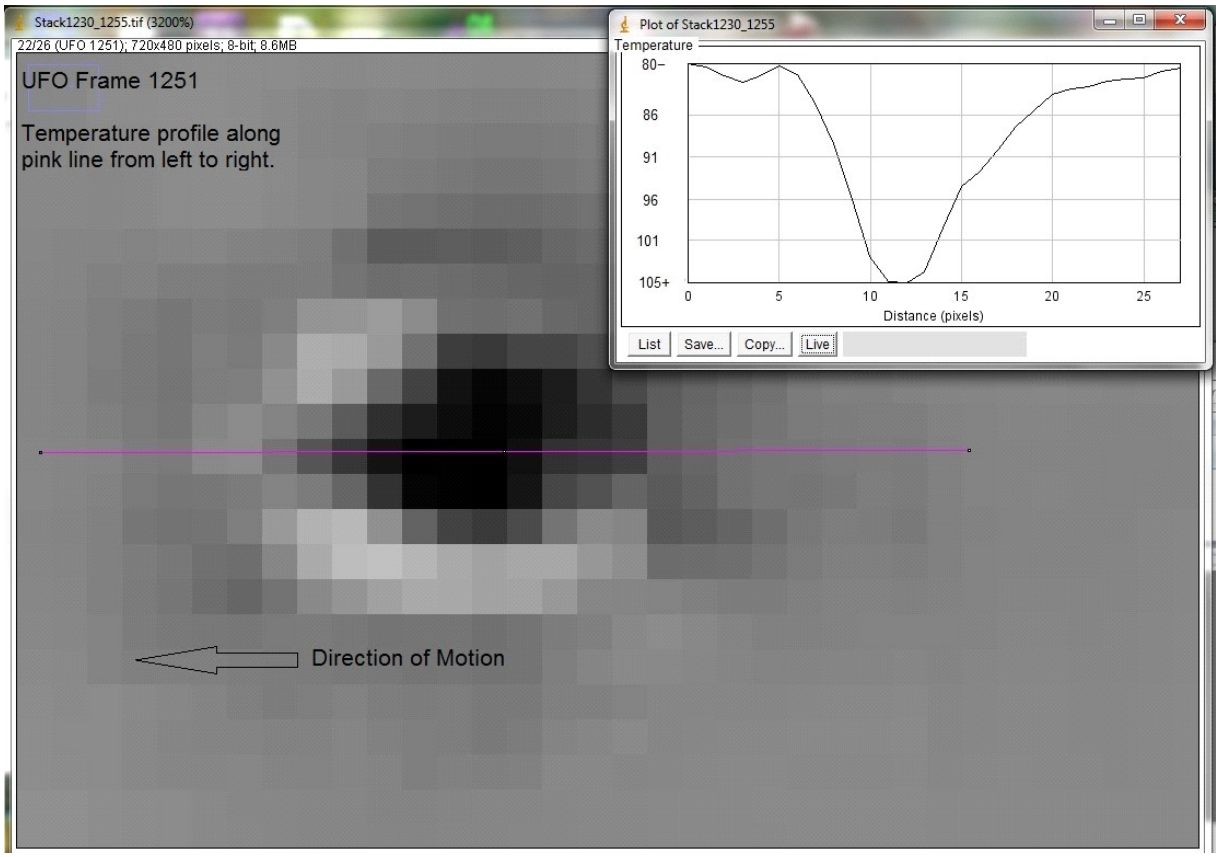
Stack1230_1255.tif (3200%)
22/26 (UFO 1251); 720x480 pixels; 8-bit; 8.6MB
UFO Frame 1251
Temperature profile along
pink line from left to right.
Direction of Motion
Plot of Stack1230_1255
Temperature
80–
86
91
96
101
105+
0
5
10
15
20
25
Distance (pixels)
List
Save...
Copy...
Live

Figure 1-4

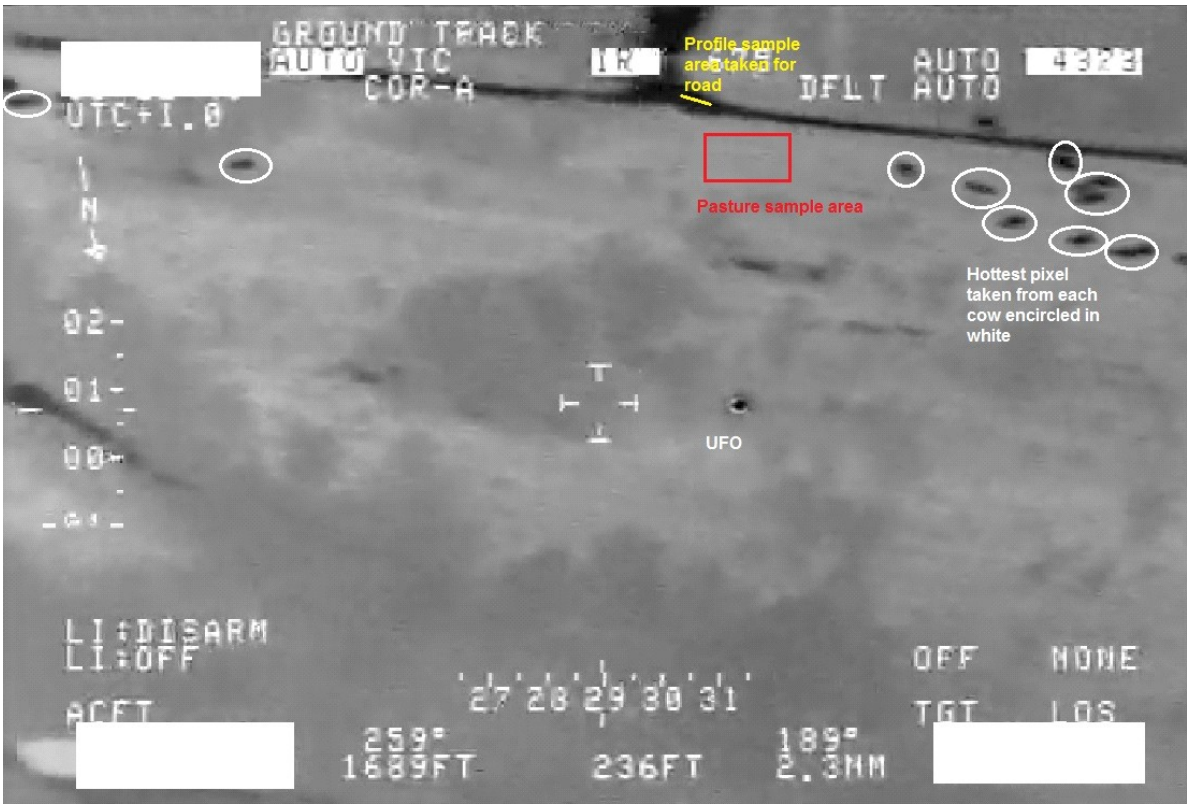

Figure 1-5

Figure 1-5 was created from Frame 1251. Within this IR frame is the object labeled as UFO, cows in the upper right and upper left quadrants, trees/grass throughout the frame, and a road that runs along the upper part of the frame.

The average (21.07 on a scale of 0 to 255) and standard deviation (4.73) of pixel values of the road was obtained from all 24 pixels along the yellow line seen on the road. ImageJ provides the average and standard deviation of all selected pixels in a profile selection. A Google Earth view of the area pictured above, shows what appears to be an asphalt road – so asphalt temperatures were assumed for the given time of day. These temperatures can be determined based on the maximum temperature during the day, the amount of cloudiness, and the length of time since sunset.[1]

Each of ten cows, as indicated, were selected within a rectangle and the lowest valued pixel was chosen to be representative of the temperature. An average (29.5) and standard deviation (16.94) of the pixel values were then derived.

All pixels within the red rectangle were selected to be representative of pasture. The average(133.59) and standard deviation(1.49) of the 242 pixel values within the rectangle was provided by ImageJ as a matter of course.

The unknown object seen in Figure 1-5 was magnified in Figures 1-2, 1-3 and 1-4.

1.3 Sources

1. American Concrete Pavement Association; http://www.pavements4life.com/qds/environment_1heatisland.asp; last accessed 11/10/2014
2. "Animal Heat." Encyclopedia Britannica. Chicago: Encyclopedia Britannica, 1965:A 965.
3. Remote Sensing of Environment 89 (2004) 467–483

Section 2.0

Forced convection is the heat transfer mechanism occurring when a fluid is forced to flow over a hot surface. Although it sounds different, there is actually no difference between the above definition and the heat loss of the object seen in the video. In this case the motion used to transfer the heat is motion of the object itself through a quiescent volume of air.

In this case, the heat transfer will be a function of many variables. The only information source available for this investigation is the video itself. Therefore everything is predicated on that video. It should be stated at the outset that convective heat loss depends greatly on source shape. The object's shape is believed to be spherical. It is possible that this assumption may not be correct, but a shape has to be used.

As stated the information source is a video. That means we are seeing individual static snapshots at different times. There are a couple bits of information that are immediately obvious in this video. The first is, the object does not seem to be getting any hotter as it flies around. Therefore if the object is generating heat, it must also be expelling it as it moves. As the object moves we can see a heat trail following it.

2.1 Pixels and Distance

Since the frames are basically showing the same picture (albeit at slightly different locations) over and over again, we really have only one picture. Since the video runs at 30 frames per second, each frames is approximately 33 milliseconds long. It has been estimated that the object is approximately 4 feet long (See Appendix G). Since it has been shown that it is also 8 pixels long on the average, we can say that each pixel covers approximately 6 inches. If the object is traveling at X mph, in one frame, at any point in the frame it will travel a distance in feet shown by the following forumla:

$$(D / Frame)_{obj} \approx 0.033\ (5280\ X / 3600)\ .$$

Therefore the approximate number of pixels moved by any point on the object per frame is:

$$N \approx (D / Frame)_{obj} / 0.5\ .$$

2.2 Heat Equation

The heat equation describing the diffusion of heat through the air is:

$$\dot{T} = \alpha \nabla^2 T .$$

Although we are assuming a sphere, we are also seeing a tail directly following the object. Therefore the above equation can be simplified to one spatial dimension.

$$T_t - \alpha T_{xx} = 0 .$$

In the above equation, the subscripts are denoting partial derivatives with respect to the subscript. The initial and boundary conditions for this equation are:

IC: $T (t=0) = T_0$

BC1: $-k T_x|_{x=L} = h (T - T_1)$ (The vert. line is for "evaluated at")

BC2: $T (x=0) = T_0 \quad \forall t$ ($\forall$ means "for all")

There is also a boundary condition at infinity but it would be superfluous.

This equation can be solved by separation of variables, but it is easier to just use a source[4,5] that has already solved it. (For any interested reader the complete solution methodology can be seen in reference 5.) These references use an electrical analogy to obtain the following thermal response function:

$$T_0 - T_{air} = (T - T_{air}) \exp \{ - h 6 t / (\rho D Cp) .$$

In this equation:

D is the diameter of the sphere;
V is the flow velocity of the air;
Cp is the specific heat of the air at constant pressure;
ρ is the density of the air;
h is the Heat Transfer Coefficient

2-3 Application to Video Frame

Solving Equation 2-4 for "t" yields an expression that gives the time needed to reduce the temperature in the trail to some set value (higher than the air value).

$$t = \{ \rho D Cp / (6 h) \} \ln \{ (T_0 - T_{air}) / (T - T_{air}) \}$$

$$t = \{\text{Time Coef}\} \ln \{ \Delta T_{init} / \Delta T_{final} \}$$

Interestingly this result is not simply dependent on the bulk air temperature and the source temperature. It has a has a third temperature. This is a result of the resulting temperature being an exponential starting at the source temperature and falling to the bulk air temperature "**at infinity**". Therefore a solution ending at a finite distance is defined as a value that is close enough to be considered correct. That is the variable T with no subscripts in the equation.

To determine numeric results, the density and specific heat are treated as constants. The Engineering Toolbox values[6] at 300 °K is used.

It is obvious that the convective heat transfer must be dependent on the fluid removing the heat. Since convective heat transfer is governed by Newton's law of cooling:

$$dQ/dt = h A (T_{obj} - T_{fluid}) ,$$

That functionality must be found in the heat transfer coefficient (h). An approximate relation for it if found in the Engineering Toolbox[7] pages and is shown in Figure 2-1.

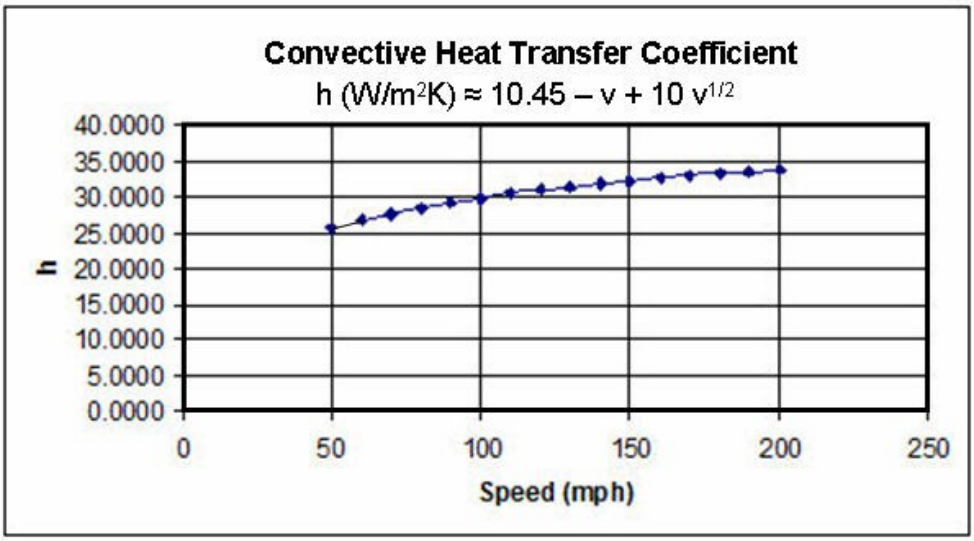

Figure 2-1

As stated above, the heat equation (eq. 2-5) requires a definition of an intermediate temperature close enough to be considered acceptable. Stated in this manner, that definition would be a complete guess. However in the present case, there is another way to look at this definition. It is how many pixels show the trail following the object. That distance was discussed in section 2-1. The results are shown in Figure 2-2 and Table 2-1.

V(mph)	h	Time Coef	Dis in 1 frame (ft)	Ln(X) 1 Cell	1/X (%) 1 Cell	Ln(X) 2 Cells	1/X (%) 2 Cells
50	25.5988	0.0098	2.4444	3.4002	3.3368	6.8003	0.1113
60	26.6824	0.0094	2.9333	3.5441	2.8895	7.0882	0.0835
70	27.6232	0.0091	3.4222	3.6691	2.5500	7.3381	0.0650
80	28.4509	0.0088	3.9111	3.7790	2.2846	7.5580	0.0522
90	29.1862	0.0086	4.4000	3.8767	2.0720	7.7533	0.0429
100	29.8441	0.0084	4.8889	3.9640	1.8986	7.9281	0.0360
110	30.4360	0.0082	5.3778	4.0427	1.7551	8.0853	0.0308
120	30.9707	0.0081	5.8667	4.1137	1.6347	8.2274	0.0267
130	31.4552	0.0080	6.3556	4.1780	1.5328	8.3561	0.0235
140	31.8953	0.0079	6.8444	4.2365	1.4458	8.4730	0.0209
150	32.2956	0.0078	7.3333	4.2897	1.3710	8.5793	0.0188
160	32.6600	0.0077	7.8222	4.3381	1.3062	8.6761	0.0171
170	32.9918	0.0076	8.3111	4.3821	1.2499	8.7643	0.0156
180	33.2939	0.0075	8.8000	4.4223	1.2007	8.8445	0.0144
190	33.5687	0.0075	9.2889	4.4588	1.1577	8.9175	0.0134
200	33.8184	0.0074	9.7778	4.4919	1.1199	8.9839	0.0125

Table 2-1

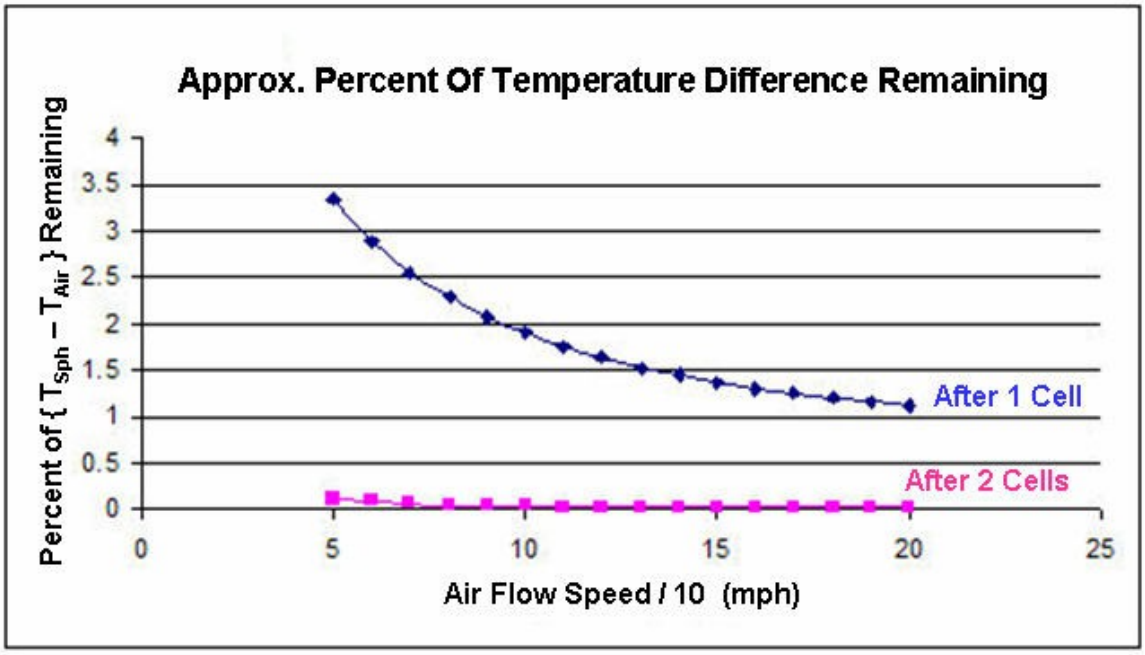

Figure 2-2

It is obvious from the above that the result for two cells is very close to zero. However the result for one cell is also quite good if the average temperature of the object is not greatly different from the bulk air temperature. Since it is possible to look at pixel values in each frame there is a means of obtaining an approximation to these temperatures.

The "Transform Image to Results" function in ImageJ allows the investigator to see the pixel values throughout any picture. Figure 2-3 is small portion of Frame #0785. The numbers depict the relative heat of each pixel. The higher the number the cooler the area represented by the pixel and the lower the hotter. Although the object is hotter than its surroundings, it is easily seen that the large distance between the object and the camera makes the heat outline difficult to determine. To help the reader, color was used to provide an approximation of the object. The cells with backgrounds that are various shade of blue are the colder areas of the object (lighter blue areas are warmer); those with a violet background are the hot area of the object; and the cells with yellow backgrounds are the heat trail being discussed in this document.

112	107	107	107	108	109	111	112	113	112	112	112	113	113	114	114	114	114
111	106	104	106	100	115	113	119	121	117	118	117	120	114	114	113	117	115
113	105	106	110	108	115	120	123	125	130	136	127	121	121	124	116	117	116
114	115	107	104	111	121	139	143	143	153	145	141	141	130	128	123	117	116
113	116	112	107	118	141	154	154	149	136	142	140	136	129	130	124	120	116
112	122	170	173	144	148	125	95	74	80	102	122	134	130	129	124	121	117
111	127	195	201	136	107	53	16	22	43	63	103	134	127	124	123	121	117
111	135	191	194	100	52	30	1	12	64	87	111	127	124	121	116	118	118
111	138	133	124	45	2	19	14	46	65	73	100	126	121	119	121	122	118
112	136	112	87	34	0	16	13	57	76	75	95	116	118	119	122	116	118
115	146	147	128	68	26	47	60	102	120	118	118	115	112	113	115	112	117
115	132	147	139	110	94	113	109	114	101	101	105	111	113	112	113	113	117
111	107	120	118	118	120	127	116	103	100	96	104	113	112	112	115	113	117
117	112	115	112	114	115	115	117	116	110	114	113	112	115	116	115	116	116

Figure 2-3

The outside box of numbers represents the background at the location of the object in this frame. Although many frames show a background value of approximately 150, this frame has the object within a warmer rectangle (average pixel value pf 113.58).

One of the problems with Figure 2-3 is it is difficult to see the shape of the object. Figure 2-4 is provided to help with that problem. This figure was generated using the "Surface Plot" functionality in ImageJ. In this figure colder areas are higher and hotter ones lower.

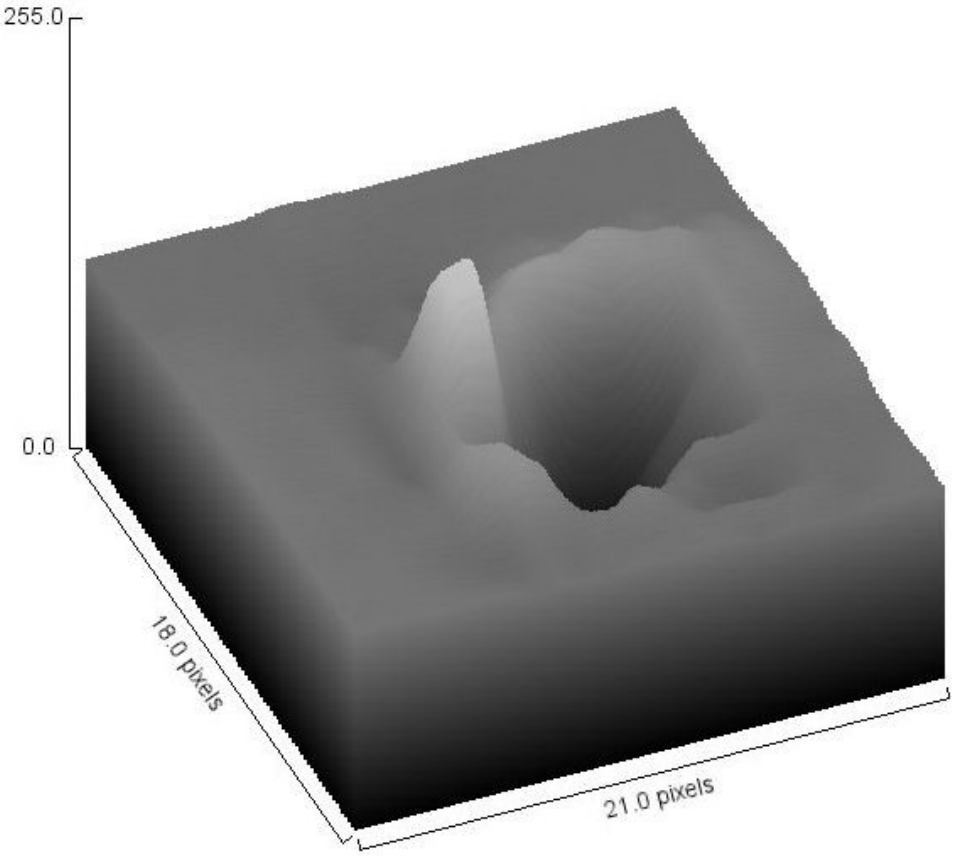

Figure 2-4

It is easy to see the coldest area of the object is in the front; it is a little cooler on the sides; and the hot area of the object is in the center. There is a small heat trail immediately to the right and a larger one near the bottom. This correspond to the yellow colors in Figure 2-3.

2.4 Temperature distribution

Most IR systems use some equalization variant to overcome the problem of distinguishing low contrast targets in dynamic scenes. The most common methods used are variants of histogram equalization. The problem faced in this investigation is that these equalization systems are inherently non-linear. They provide enhancement by increasing contrast in the dominating temperature range in a scene and decreasing it in the non dominating range. Additionally the histograms used to describe the scene in 256 levels of gray are functions which are unlikely to be straight lines. Therefore Equation 1-1 is at best a rough estimate of

the pixel-temperature function. It does however provide a realistic approximation. Applying it to Figure 2-3 yields Figure 3-1.

83.67	84.64	84.64	84.64	84.44	84.25	83.86	83.67	83.47	83.67	83.67	83.67	83.47	83.47	83.28	83.28	83.28	83.28
83.86	84.83	85.22	84.83	86.00	83.09	83.47	82.31	81.92	82.70	82.50	82.70	82.12	83.28	83.28	83.47	82.70	83.09
83.47	85.03	84.83	84.06	84.44	83.09	82.12	81.54	81.15	80.18	79.01	80.76	81.92	81.92	81.34	82.89	82.70	82.89
83.28	83.09	84.64	85.22	83.86	81.92	78.43	77.66	77.66	75.72	77.27	78.05	78.05	80.18	80.57	81.54	82.70	82.89
83.47	82.89	83.67	84.64	82.50	78.05	75.52	75.52	76.49	79.01	77.85	78.24	79.01	80.37	80.18	81.34	82.12	82.89
83.67	81.73	72.42	71.84	77.46	76.69	81.15	86.96	91.04	89.87	85.61	81.73	79.40	80.18	80.37	81.34	81.92	82.70
83.86	80.76	67.57	66.41	79.01	84.64	95.11	102.28	101.12	97.05	93.17	85.41	79.40	80.76	81.34	81.54	81.92	82.70
83.86	79.21	68.35	67.77	86.00	95.30	99.57	105.19	103.06	92.98	88.52	83.86	80.76	81.34	81.92	82.89	82.50	82.50
83.86	78.63	79.60	81.34	96.66	105.00	101.70	102.67	96.47	92.78	91.23	86.00	80.95	81.92	82.31	81.92	81.73	82.50
83.67	79.01	83.67	88.52	98.79	105.39	102.28	102.86	94.33	90.65	90.84	86.96	82.89	82.50	82.31	81.73	82.89	82.50
83.09	77.08	76.88	80.57	92.20	100.34	96.27	93.75	85.61	82.12	82.50	82.50	83.09	83.67	83.47	83.09	83.67	82.70
83.09	79.79	76.88	78.43	84.06	87.16	83.47	84.25	83.28	85.80	85.80	85.03	83.86	83.47	83.67	83.47	83.47	82.70
83.86	84.64	82.12	82.50	82.50	82.12	80.76	82.89	85.41	86.00	86.77	85.22	83.47	83.67	83.67	83.09	83.47	82.70
82.70	83.67	83.09	83.67	83.28	83.09	83.09	82.70	82.89	84.06	83.28	83.47	83.67	83.09	82.89	83.09	82.89	82.89

Figure 3-1

Although this figure is identical to the previous one, it now gives the results in terms of degrees Fahrenheit. Using the temperatures around the outside of this figure the average temperature of the background air is found to be 83.37 and the standard deviation is 0.55 degrees. Additionally the hottest point in the object is 105.39 degrees. The figure therefore shows an average maximum temperature differential between air and object of 22.02 degrees.

It was noticed in Figure 3-1 that there are locations in the air (pixel values of <80) where the temperature is less than the background air. It was initially thought that these cooler pockets may be examples of low pressure zones that always follow objects moving in fluids. The size of these zones are a function of the relative velocity of the object and the fluid, and the shape of the object. If the object is moving slowly and has a streamlined shape (canoes etc), the zone will be small but it will still exist. In the present situation although we do not know the object's shape, we do know the speed is relatively high. We therefore can expect that this zone may be sizeable enough to have an effect on the results found. Rather than make a molecular argument for the temperature-pressure relationship it is simpler to just state the Gay-Lussac gas law:

$$\text{Pressure} = k * \text{Temperature}$$

where k is a constant. Therefore a region of lower pressure is also a region of lower temperature. With very short heat trails this effect would be a slight cooling below ambient just before returning to the ambient air temperature. It could then also be the cause of some of the cooler pixels trailing the object.

2.5 Conclusion

The problem with assigning the temperature variation to low pressure zones is that variations with the same order of magnitude are seen to be occurring at areas away from the unknown object. This was particularly noticeable when the author looked at an area twice the size of the matrix shown in Figure 3-1 (28x36 verses 14x18). With the larger matrix the average

ambient temperature (outside rectangle) was calculated to be 82.99° F and the standard deviation is 0.5° F. Both values are slightly cooler than the ones calculated using the smaller matrix. That is to be expected since exponentials never actually reach zero. The interesting result is that around the large matrix, the maximum temperature value was fond to be 83.86° F and the minimum value to be 81.73° F. That results in a delta temperature of 2.13° F at a distance where it cannot be attributed to the unknown object. Additionally there is nothing at all seen in the picture outside of the unknown object (see Figure 3-2).

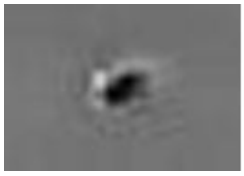

Figure 3-2

Since it is known that the maximum and minimum temperatures and related pixel values are:

	Temperature	Pixel Value
Maximum	105.39	0
Minimum	66.41	201 .

each integer pixel value equates to:

$$\delta T / \delta p = | (105.39 - 66.41) / (0 - 201) | = 0.198 \{ ^\circ F \text{ per pixel} \} .$$

Therefore the temperature variation occurring along the periphery (2.13° F) is equivalent to 10.76 pixels and no source for this variation is known. Since the 2 degree variation with unknown source in the "ambient temperature" is approximately four times larger than the assumed low pressure zone delta temperatures, that assumption cannot be defended and must be discarded. Since the delta temperatures in the tail are approximately 3 degrees the assumption of a heat tail falling off exponentially remains.

A statement has to be made concerning the long heat trail that occurs at the bottom back of the object. Initially this looks like a much longer tail than what has been suggested. Since this tail begins approximately 2/3s to 3/4s back from the start of the object and not directly at the rear of the object, it is assumed the heat is not a single pixel location. It is believed heat is being exhausted along the object. Therefore although heat at any particular location is falling off backwards exponentially, that loss is being made up for by more heat being exhausted.

2-5 Notes and References

4. Bahrami, Majid; "Forced convection Heat Transfer"; Simon Fraser University; ENSC 388 (F09)
5. John H. Lienhard IV & John H. Lienhard V; "A Heat Transfer Textbook"; Cambridge TJ260.1.445 2000, 3rd Edition; Chapter 5, "Transient and Multidimensional Heat Conduction"
6. "Dry-Air Properties"; http://www.engineeringtoolbox.com/dry-air-properties-d_973.html
7. "Convective Heat Transfer"; http://www.engineeringtoolbox.com/convective-heat-transfer-d_430.html
8. The result is a value of 6.8054 for "c". This would indicate a very rapid heat dissipation.

APPENDIX L

Line-of-Sight Evaluation

Introduction

Some arguments have been advanced that the object could be a balloon and that the motion of the balloon relative to the background is an illusion created by the motion of the plane circling the balloon. This is incorrect. There are some frames of video having no background motion at all and the UAP can be seen changing locations relative to the background. Consider Frames 711 and 712 of Figure 1:

Figure 1

Figure 1 clearly demonstrates the intrinsic motion of the UAP and that the motion of the plane from one frame to the next contributes nothing to the difference in the location of the UAP. This, in itself, does not eliminate the possibility of a balloon since a balloon could have drifted into the frames due to its own motion.

The wind was out of the east at 8-13 mph.[1] Upper wind speeds were measured out of San Juan, which is 50 miles to the east of Aguadilla. At 8 pm local time the upper wind speeds from 400 feet to 3200 feet were similar and were out of the east northeast at 12 to 18 mph.[2] Given that eighteen miles per hour was likely the fastest speed of a balloon in Frames 711 and 712 then the distance from the plane could be no more than 1,250 feet considering the angular distance the object traveled within these two frames. (The calculation of this distance is detailed later in this appendix.) This 1,250 feet from the plane creates serious discrepancies with the aircraft-to-target azimuth readings[3] given by the on screen data. The discrepancy is illustrated in Figure 2.

[1] http://www.wunderground.com/about/data.asp

[2] University of Wyoming, Department of Atmospheric Science. http://weather.uwyo.edu/upperair/sounding.html

[3] This would be the compass direction in which the IR camera was pointed.

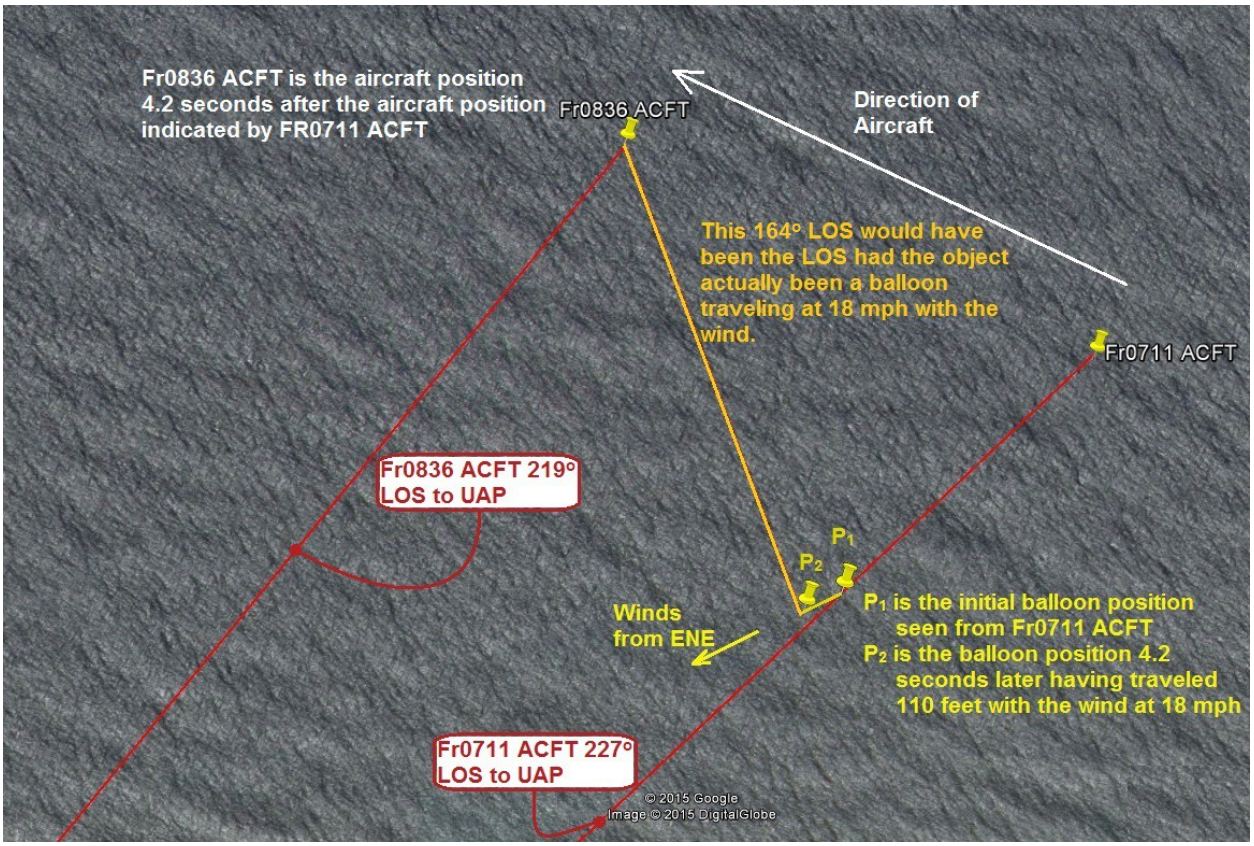

Figure 2

The first position (P_1) of a possible balloon is established along the line oriented at 227° azimuth given by the aircraft-to-target screen data seen within Frame 0711 (See Figure 3) and established at a distance from the aircraft position of 1,250 feet. The Frame 0711 on screen data indicated the plane position (Fr0711 ACFT in Figure 2) to be 18° 31' 13" N and 67° 06' 22" W. The second balloon position (P_2) was given by the distance a balloon would have covered in 4.2 seconds at 18 mph; 110.88 feet. The next frame, 0836, was arbitrarily chosen to allow comparison of aircraft and balloon travel distances. The 2nd plane position, specified by the yellow pin annotated (Fr0836 ACFT), is the plane location 4.2 seconds after the Fr0711 ACFT plane location. During this time the aircraft traveled a distance of 1504 feet along a WNW (295° azimuth) path which subsequently created a line of sight (LOS), from plane to balloon, of 164°. The actual azimuth to the target (UAP) for Frame 0836 can be seen as 219° (See Figure 4). This is a discrepancy of 55° (219° – 164°) between the actual target azimuth and the one calculated for a balloon.

Figure 3

The 227° bounded in red is the plane-to-target azimuth; the compass direction in which the infrared (IR) camera was pointed within Frame 0711.

Figure 4

The 219° bounded in red is the plane-to-target azimuth; the compass direction in which the IR camera was pointed within Frame 0836. There is a time difference of 4.2 seconds between Frames 0711 and 0836 (1/30th of a second per frame). Over that time, the plane tracked the UAP over an 8° degree azimuth change (227 ° – 219 °). The plane would have passed an object as slow a balloon creating the much greater azimuth change of 68 °.

How it was established that the balloon was 1,250 feet from the plane in Frame 0711 does need some attention. See Figure 5.

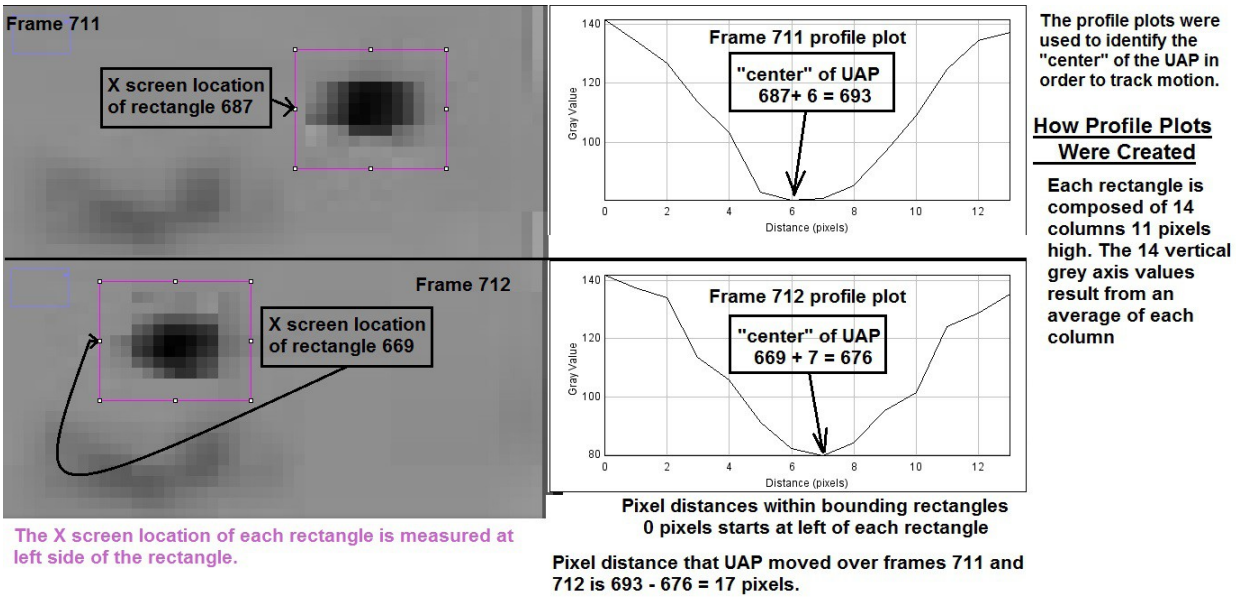

Figure 5

Figure 5 establishes that the UAP seen in the video moved about 17 pixels from Frame 0711 to 0712. The Field Of View (FOV) of the IR Camera was determined to be about 1.07 degrees at magnification 675 which amounts to 0.001483 degrees per pixel (see Appendix G for details on degrees per pixel). The UAP having moved 17 pixels implies that the UAP traversed 0.025211 degrees in 1/30th of a second. It was noted earlier the weather at the time had maximum winds of 18 mph winds thus inferring that a balloon, going with the winds out of the ENE, would have moved 26.4 fps * 1/30 = 0.88 feet. However, the trajectory of the UAP over Frames 0711 to 0836 was almost due south (188^{o} azimuth). The fact that the image is a two-dimensional projection of a three-dimensional area changes the path length of 0.88 feet as seen from the IR camera perspective. The angular change of 0.025211 degrees is not over 0.88 feet but rather 0.55 feet. See Figure 6.

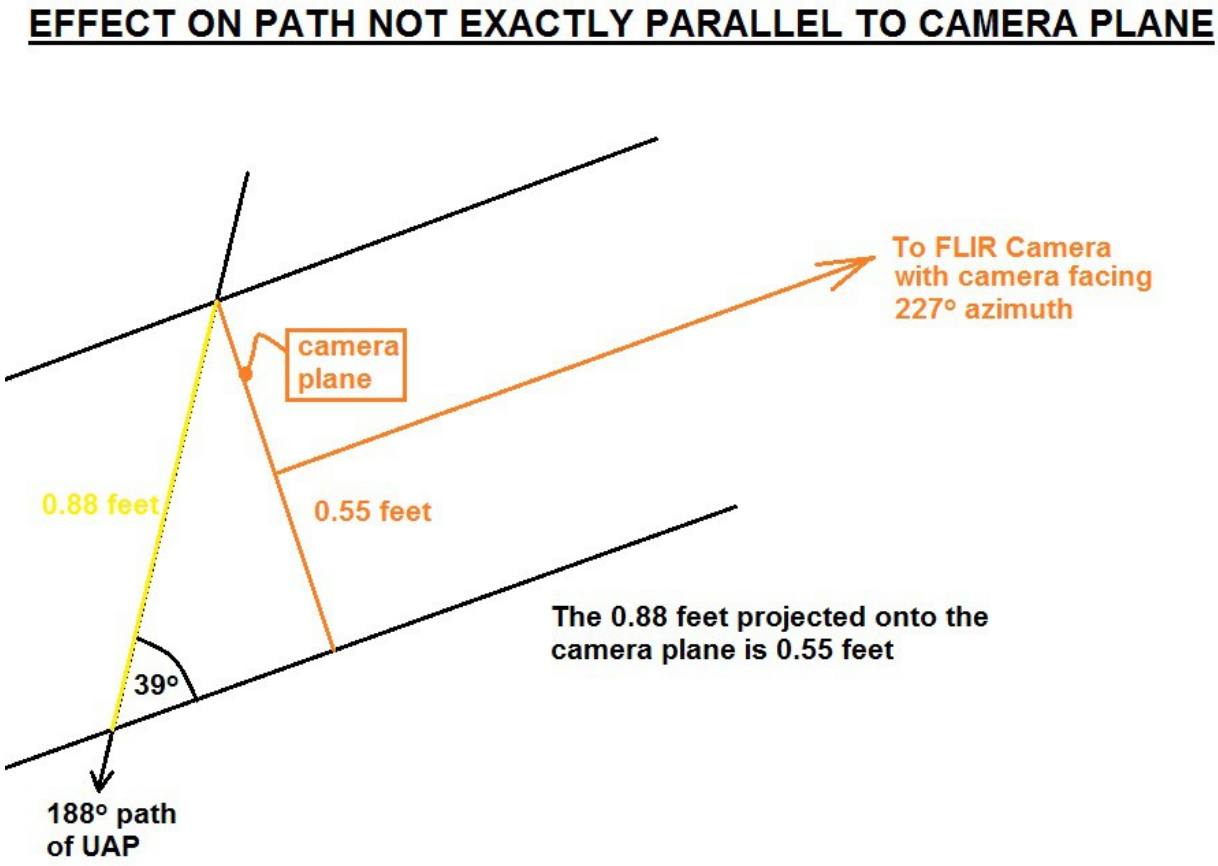

Figure 6

The angular change of 0.025211 degrees, from the IR camera perspective, must be applied using 0.55 feet. Consequently the distance a balloon, traveling at 18 mph, from the aircraft would have been 0.55/(2*tan(0.025211/2)) = 1250 feet.

Line-of-Sight measurements, angular size, and speed preclude a balloon from being a possible explanation.